

Silesian University of Technology
Faculty of Mechanical Engineering
Department of Fundamentals of Machinery Design

Doctoral Dissertation

**MANUFACTURING PROCESS
DIAGNOSTICS AND DAMAGE
ASSESSMENT OF HSLA STEEL
BUTT-WELDED PIPELINES**

MSc., Eng., Massimiliano Pedot

Supervisor

Dr hab. inż. Prof. PŚ Anna Timofiejczuk

Gliwice, 2022

TABLE OF CONTENTS

1	Introduction	5
1.1	Resilience engineering concepts	5
1.2	Background and motivation	7
1.3	Scope.....	11
1.4	Description of the research	13
2	Petrochemical plants layout.....	18
2.1	Main elements of a petrochemical plant	18
2.2	Typical configurations of petrochemical plants.....	22
2.3	Case study piping system.....	26
3	Welding processes and diagnostic methods	29
3.1	Welding technologies	29
3.2	Welding imperfections.....	31
3.1	Non-destructive methods of welding process assessment	35
4	Preparation of case study butt-welded joint pipe specimens	38
4.1	Specimens with induced imperfections	38
4.2	Specimens with optimal quality acceptance level	56
5	Quality assessment of defective samples.....	65
5.1	Defects detected on GMA2 pipe specimen.....	67
5.2	Defects detected on GMA3 pipe specimen.....	68
5.3	Defects detected on MMA1 pipe specimen	70
6	Destructive test of the pipe samples	73
6.1	Destructive test of defective welded joints	74
6.2	Impact load test on optimal quality pipe samples.....	80
7	Monitoring of welding process.....	88
7.1	Critical conditions in GMA2 pipe specimen	88
7.2	Critical conditions in GMA3 pipe specimen	91
7.3	Critical conditions in MMA1 pipe specimen.....	96
8	Conclusions	99
8.1	Manufacturing process.....	99
8.2	Analysis of defective samples.....	102
8.3	Analysis of non-defective samples	105
8.4	Final considerations	106
	Bibliography.....	108

A Appendix 113

A.1 Welding Technologies 113

A.2 Defects detected in the pipe samples 119

A.3 Destructive test on defective samples 132

1 INTRODUCTION

1.1 RESILIENCE ENGINEERING CONCEPTS

Resilience is a term that recently has a widespread use in different contexts, defining the ability of a system to face challenging events and phenomena, for example shocks, and recover the original condition [1]. It is used in different scientific fields, e.g., in medicine, material science, environmental science and economy, and describes the ability of the system, subjected to an external perturbation, to withstand it and return to the initial state or a state which is considered as the correct one. From another perspective, considering for example a complex system, it could be defined as the capability to cope with unexpected and unplanned situations and respond rapidly to events, with excellent communication and mobilisation of resources to intervene at the critical points [2]. However, especially in case of technical systems these definitions do not consider all aspects of this characteristics. It would be also desirable to have the opportunity, if possible, to predict incoming events and thus try to minimize their impact on the system. In addition, it is essential to consider not only the capability of minimize the consequences and recover the original conditions, but it is important to take into account the speed at which the recovery process takes place after the accident. As a general example two different systems have different levels of resilience if one of them can recover the original functionality quicker than the other. Summarizing, resilience is:

- prevention of the loss of control over risk, which can be seen as the capability of a system to minimize risk through the implementation of advanced prediction models that allows to better understand the mechanisms generating the hazardous events.
- recovery from that loss of control over risk, which can be defined as the capability of a system to minimize adverse consequences adopting proper countermeasures.
- the capability of a system to quickly recover from a damage to the original or acceptable condition.

These concepts are depicted in Figure 1 [2], [3] that represents a bowtie model for accidental scenarios. In the centre an undesirable event striking the object of the study is placed, e.g. a disruption on a natural system in environmental science, a failure of infrastructures [4] or machines in the engineering field, a crisis of a community in social/economic science, while at its sides are placed what could be defined as the main aspects of resilience. On the left-hand side the potential threats to the system are placed, i.e., a pollutant substance in the environment, an explosion on a structure, an economic crisis on a population. Then all these measures that are possible to be adopted in order to

minimize these threats are defined. On the right-hand side, there are possible outcomes of the undesirable event, e.g., the death of some species in a polluted environment, the interruption of the serviceability for a structure or a machine, the increase of crime rate in a poorer community and at the same time the countermeasures that allow us to reduce these outcomes and restore original conditions of the system.

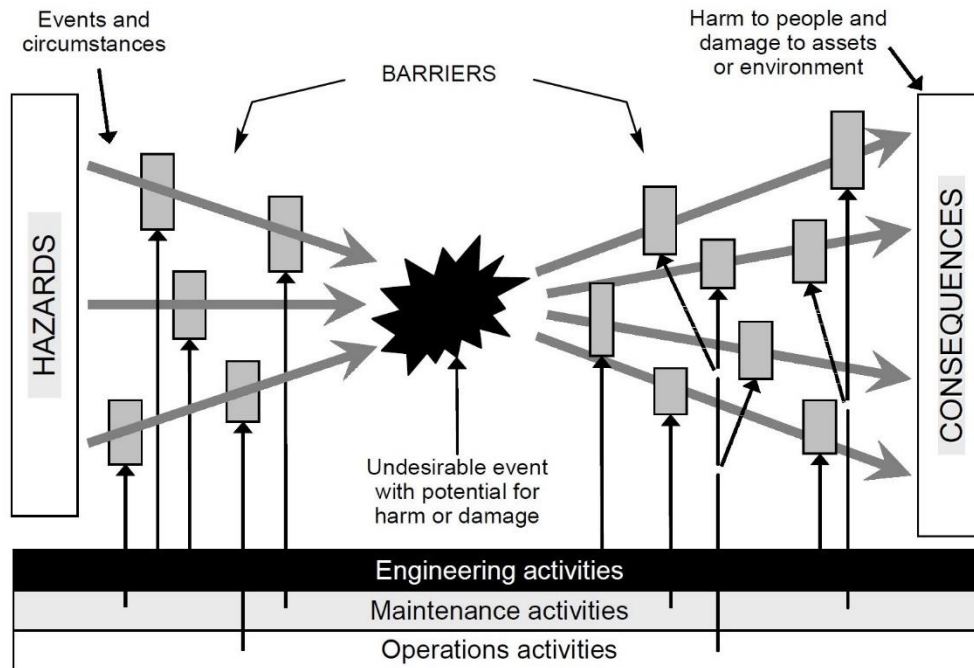


FIGURE 1: BOWTIE MODEL FOR ACCIDENTAL SCENARIOS [2]

In the previous paragraph, general concepts defining resilience was introduced. The main purpose of this thesis is to apply these general concepts to specific cases with practical applications in the engineering research field. Of a particular interest are so called “Natech” accidents, that are secondary effects resulting from natural hazards [5] on infrastructures and complex industrial systems, causing i.e. fires, explosions and toxic or radioactive releases. Major examples of Natech accidents are the nuclear meltdown at Fukushima Dai-ichi nuclear power plant hit by a tsunami in 2011 [6], hydrocarbon spills from off-shore platforms in the Gulf of Mexico caused by Rita and Katrina hurricanes in 2005 [7] or fires and multiple hazardous-materials releases at the Izmit refinery in Turkey in 1999 caused by the earthquake [8]. Increasing awareness of Natech risk led to new research activities and new national regulations aimed at prevention of these accidents. In fact various research activities have applied resilience concepts described before to practical cases: some of them are aimed at risk minimization suggesting an enhanced model for hazardous events like earthquakes [9], gas release and explosions [10] or floods. Other studies and research projects, i.e. [11], are focused on the performances of single components of a plant, i.e. storage tanks and piping systems (Figure 2)

[12], in order to predict their behaviour during Natech accidents and consequently minimize the catastrophic effects of these extreme events.



FIGURE 2: ELEPHANT FOOT BUCKLING OF A STEEL STORAGE TANK (LEFT) AND LOCAL BUCKLING OF A PIPE (RIGHT) [12]

The problems and the research described in the thesis are particularly focused on high strength steel butt-welded joint pipes. Such structures are used for transporting oil, gas and other flammable substances. This situation requires continuous and careful evaluation of the health of the piping systems through all their service life because leakage of the content could lead to explosions. One possible source of risk could be the result of poor manufacturing quality of the connections. In the next two paragraphs are described the use of carbon steel in oil and gas industry and the motivation for the possible adoption of high strength steel pipes. The behaviour of these components manufactured using different welding technologies was studied. The experiments and observations were made to assess their mechanical properties and their resistance during catastrophic events.

1.2 BACKGROUND AND MOTIVATION

Primary energy demand has faced an increase in the last decades, from 6101 Million Tonnes of Oil Equivalent (MTOE) registered in 1973 to 13650 MTOE registered in 2015 as depicted in Figure 3 [13].

World¹ TPES from 1971 to 2015 by fuel (Mtoe)

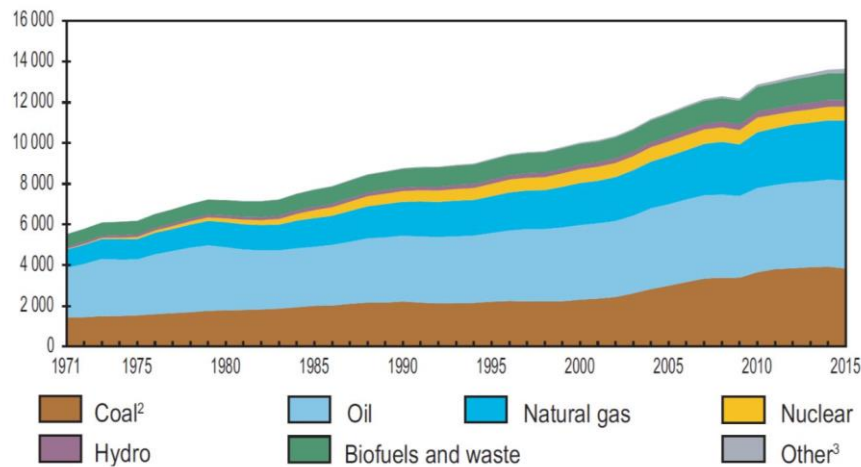


FIGURE 3: PRIMARY ENERGY DEMAND 1971-2015 [13]

Moreover, future predictions suggest the same trend for the next years. According to [13] the energy demand is going to raise until 2040 at the rate reported in Table 1. Values refer to One Thousand Barrels of Oil Equivalents per day MBOE/d.

Year	2015	2020	2030	2040
Energy demand [MBOE/d]	276	298	339	372

TABLE 1: ENERGY DEMAND TREND [13]

In details, all the energy resources are facing a demand increase with the proportions showed in Table 2. Oil and gas demands are supposed to have a growth of 0.6% and 1.8% per year until 2040.

Resource [MBOE/d]	2015	2020	2030	2040	Var [% yr.]
Oil	86.5	92.3	97.9	100.7	+0.6
Coal	78.0	80.7	85.8	86.2	+0.4
Gas	59.2	65.2	79.9	93.2	+1.8
Nuclear	13.5	15.8	20.1	23.8	+2.3
Hydro	6.8	7.5	9.0	10.3	1.7
Biomass	28.0	30.1	34.0	37.3	+1.2
Other Renewables	3.8	6.6	12.9	20.0	+6.8

TABLE 2: ENERGY DEMAND BY FUEL TYPE [13]

The energy demand increase causes the necessity of building not only new infrastructures and terminals for oil and gas extraction but also requires application of proper treatment, distribution, and energy production.

Piping systems are key elements of petrochemical and refinery plants. A typical installation includes storage tanks and a complete interconnection of linear pipes, elbows, pipe fittings and auxiliary elements like pumps, heat exchangers and valves. All these elements are connected to each other through bolted flanged or butt-welded joints (Figure 4). The most used pipe material in the oil and gas industry is carbon steel. The manufacturing of steel pipes is exposed in Paragraph 2.1.2.



FIGURE 4: PIPING INSTALLATIONS IN JAMNAGAR INDIA REFINERY - THE WORLD'S LARGEST OIL REFINERY WITH AN AGGREGATE CAPACITY OF 1.24 MILLION BARRELS [14]

The initial design and material properties of the piping system are established by the functional requirements characteristic for transmitting fluid from one point to another. The detailed design is set by criteria such as type of fluid being transported, allowable pressure drops or energy losses, desired velocity, space limitations and process requirements like free drain or requirement of straight run, stress analysis, temperature of the fluid, etc.

The piping systems are also essential components in terms of efficiency and safe service of the plants. Among other parts and aspects of these structures the joints are critical elements that require attentions towards hazardous events. In complex piping systems it is necessary to connect each other multiple pipe sections, branches and fitting allowing to fit service and safety requirements of the plant. There are mainly two possibilities to connect two elements of a piping system: butt-welded joints and bolted flanged joints. The first method (Figure 5) is a permanent connection directly between the ending faces that are properly prepared and then bonded together using an external heat source that melts a portion of the material. Adopting the proper welding manufacturing process, the connection completely avoids leakages. On the other side, bolted flanged joints (Figure 6) are non-permanent connections made coupling by mean of variable number of bolts the plain faces of two flanges. The back part of each flange is in general butt-welded with the pipe end. The sealing properties of the joint is then demanded to the gasket placed between the two adjacent faces of the flanges. The quality

of the gasket, its installation and the appropriate bolts torque are the key elements to avoid the leakage of pipe content. Another drawback of these kind of joints is the additional quantity of steel for flanges manufacture resulting in increased weight of the connection.

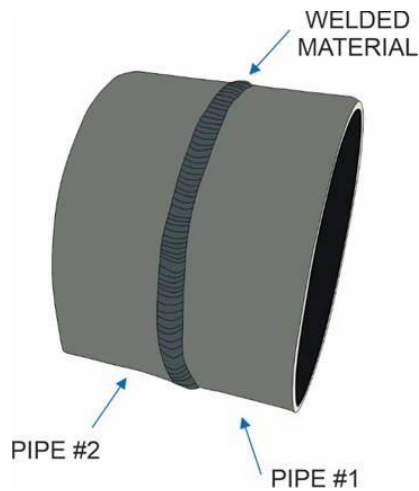


FIGURE 5: BUTT-WELDED JOINT

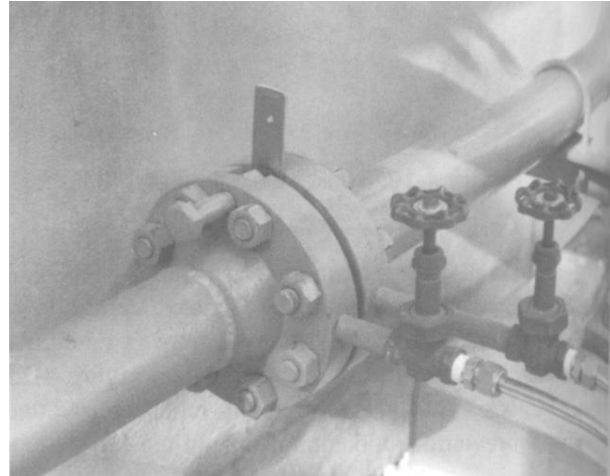


FIGURE 6: BOLTED FLANGE JOINT [15]

The structural integrity and fitness for service of refinery piping installations and welded joints particularly, require complete knowledge of specific threats, mainly unexpected catastrophic impact loads due to e.g., collapse of nearby structures like walkways, steel or concrete support structures, vessels, towers, etc. The designing and manufacturing process of piping systems must ensure a high level of structural integrity to prevent and avoid adverse consequences leading to structural failures. Severe structural failures of piping systems could cause an interruption of serviceability of the plant with remarkable economic losses and in the worst cases, leakage of internal content. In case of flammable contents, loss of containment could generate explosions causing not only economic losses but also risk for personnel and nearby communities. An example of explosion due to leakage of flammable substances is depicted in Figure 7: on August 2012 the rupture of a 52-inch pipe component being extremely thin due to a damage mechanism known as sulfidation corrosion caused an explosion inside Chevron Richmond Refinery #4 Crude Unit [16].



FIGURE 7: EXPLOSION AT CHEVRON REFINERY PLANT AND RUPTURE OF 52'' COMPONENT [16]

Combining the increase in energy demand and the necessity of modern piping solutions able to withstand catastrophic loads during extreme events, the piping industry put effort in the development of new cost-effective solutions with increased performances.

1.3 SCOPE

Modern design approaches of complex structures involve the concept of resilience which, according to [2] is the ability to avert the disaster or major upset, anticipate and circumvent threats and if necessary rapid recovery from a disastrous event. In this sense, the adoption of special manufacturing processes and also selection of proper material is essential. HSLA steel pipes for petrochemical plants can be seen as the application of the concepts abovementioned to a real scenario. Two approaches can be adopted to the study of these structural elements: the first one is typical of mechanical engineering with the focus on new methods for the manufacture of steel products with enhanced performances. Preliminary literature review showed a fair number of studies regarding manufacturing technology and methods for the optimization of production processes of this category of materials. Examples are [17], [18], [19] or [20] that focus on the improvement of aspects like chemical composition, cooling temperature and thermomechanical treatment process in order to enhance mechanical properties and satisfy current quality acceptance levels. Other research in mechanical engineering field are for example these involving study of corrosion process of high strength steel piping systems to understand better their performances under maintenance conditions. Works like [21] and [22], try to replicate these conditions, i.e. simulate pipe-soil interaction in case of buried pipelines or wet/dry conditions for open air piping systems and then assess pipe response.

The other perspective, which is adopted in this research, is typical for mechanical and structural engineering field with the assessment of the mechanical behaviour of piping systems, both during manufacturing and installation process as well as during service conditions.

In this context, high strength low alloy (HSLA) steels for pipeline applications are a noteworthy research field. The concept behind the introduction of this kind of steel is essentially to increase strain resistance capability and reduce thus thickness and consequently weight. Moreover, reduction in thickness allows reduction of welding consumables and better control of welding process. There is not a precise definition of High strength low alloy steels, but commonly they might be appropriately defined as low carbon steels having yield strength over 275 MPa [12] and a composition with small amounts of alloying elements (as Ti, Cu, V, Nb, etc.) to obtain a good combination of strength, toughness and weldability [13].

In this research the attention was particularly put on the welded connections between two HSLA pipes. Although significant aspects of piping systems installations, e.g., layout, materials, joining solutions are discussed in a following specific paragraph it is necessary here to motivate the reason behind this choice. For complex piping systems there are several connections between the various elements e.g., pipes, elbows, fittings. These connections are sensitive parts that could trigger failure mechanisms in case of extreme loads. In fact, joints are discontinuities regarding material and/or geometry and therefore they can constitute a possible weakness to the integrity of the system. Regarding butt-welded joints, which were shown in Figure 5, the discontinuity is the results of the interactions between three different interfaces. The first one is represented by the parent material, which is the original metal constituting the pipe. The second one is the heat affected zone (HAZ), which is a region of the original material that is affected by the thermal input typical of the welding process. The last one is the welded metal, which is the external molten material that solidifying creates the bonding between the two pipes. A section of a butt-welded joint with the indication of the three areas just described is depicted in Figure 8.

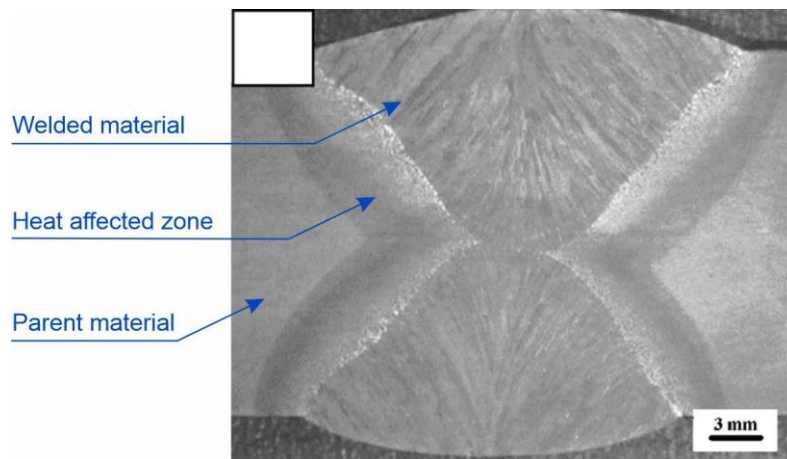


FIGURE 8: TRANSVERSAL SECTION OF A BUTT-WELDED JOINT [23]

Given these aspects, welded joints could include a possible source of failure of the piping system and a threat to the integrity and safety of the whole plant. The focus of this thesis is not directly connected to the study of the microstructure of welded joint but on the assessment of its the mechanical properties. Particularly, sets of different welded joints, manufactured with various welding technologies, were tested against extreme loads to simulate limit state conditions. In addition, the manufacturing process were monitored to understand critical condition for the development of defects inside the welded joint that could undermine the resilience of the whole system.

The study of high-strength steel butt-welded joint pipes followed four distinct directions as it is summarized in Figure 9.

- study of the manufacturing process and conditions of butt-welded joints
- assessment of the influence of imperfections on the mechanical behaviour of the piping structure and joints
- behaviour of the real scale pipes under impact load test
- detection methods of defects inside butt-welded joints of piping structure

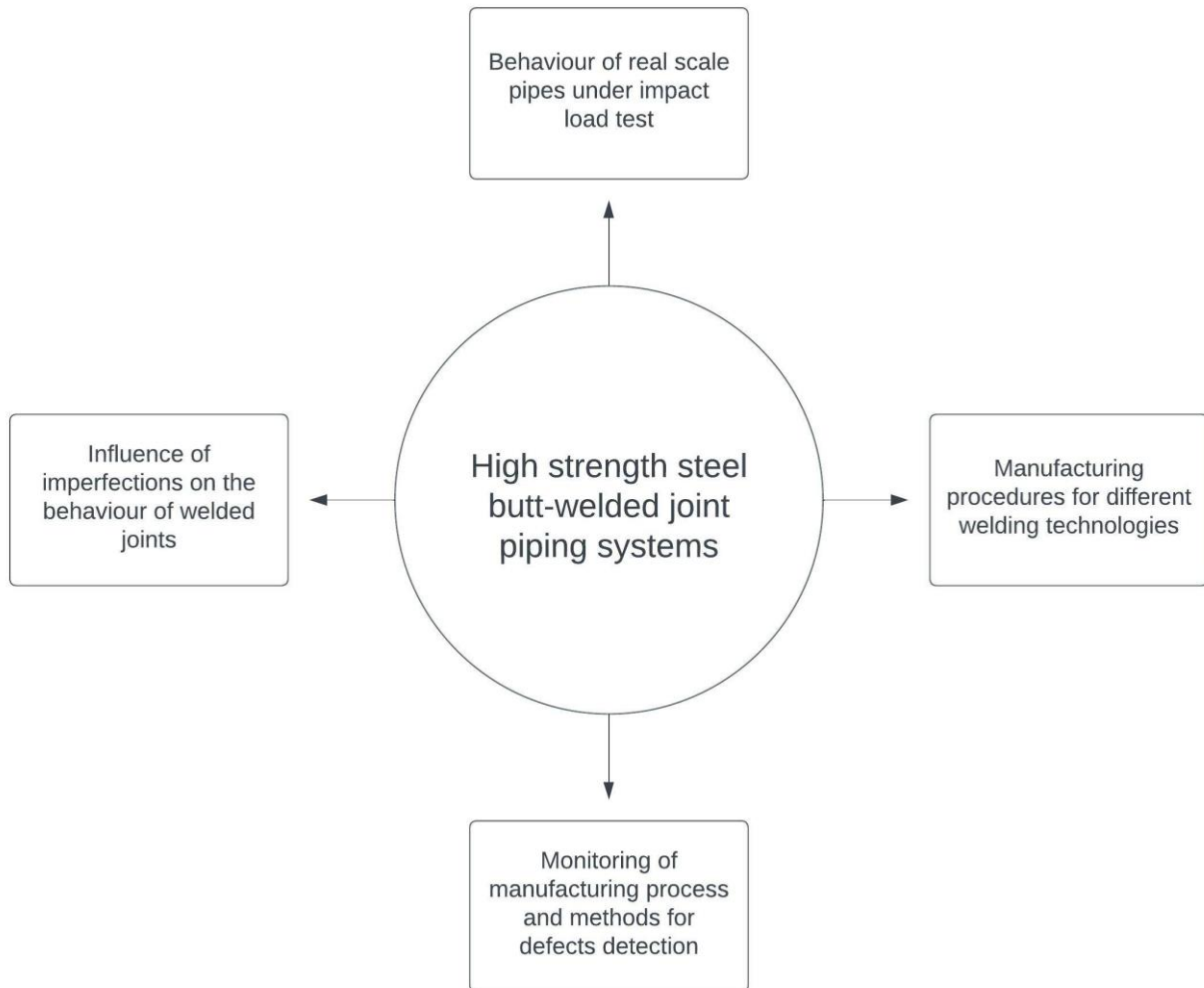


FIGURE 9: SCOPE OF THE ACTIVITIES

1.4 DESCRIPTION OF THE RESEARCH

During this research activity a special attention was put on butt-welded high strength steel pipes for petrochemical plants. Hereafter is described the content of each chapter based on different steps performed during the experimental activity, which is represented in Figure 10.

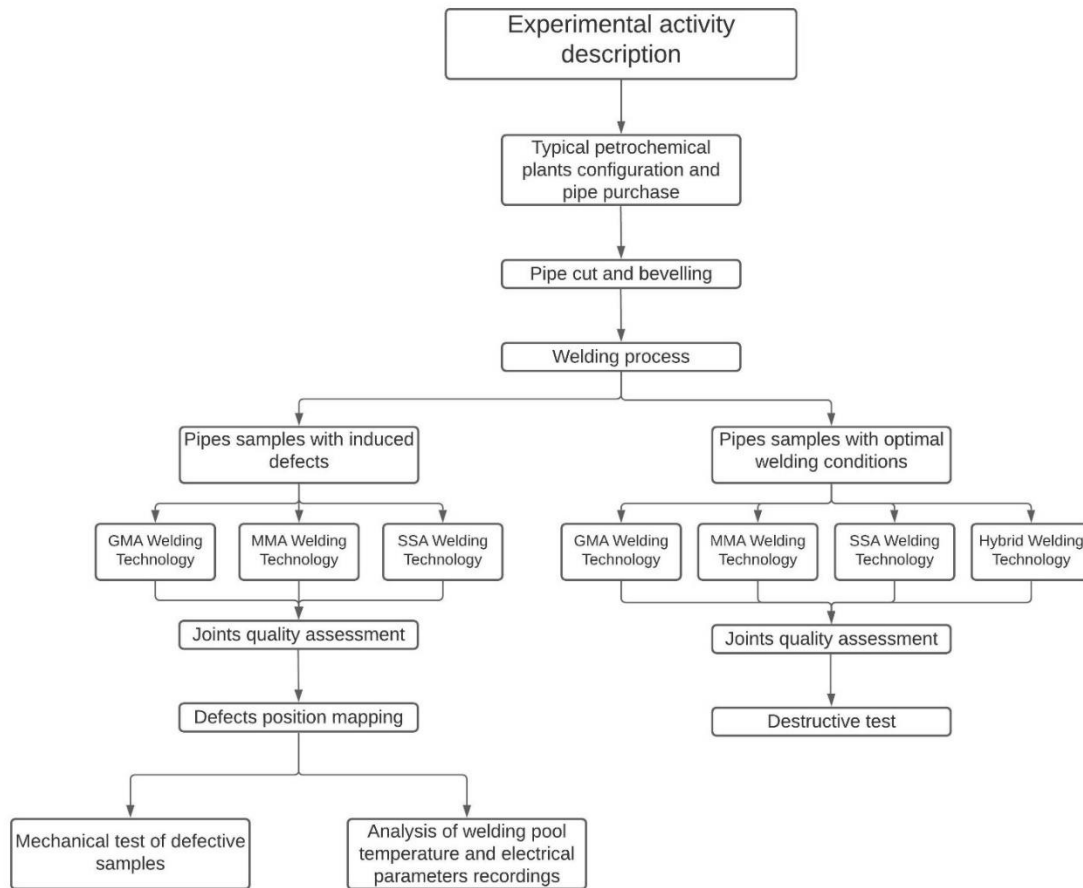


FIGURE 10: DIAGRAM DESCRIBING ALL THE STEPS OF THE EXPERIMENTAL ACTIVITY

In the second chapter typical petrochemical plants, and especially piping systems, are characterized. Following this assessment and according to the list of products available from a local supplier [24], a 12’’3/4 API-5L X80 pipe were selected as suitable elements for the experimental activity. The geometrical and mechanical properties of the pipe selected are also described in this chapter.

In the third chapter welding technologies commonly used for pipe manufacturing processes are characterized. Their advantages and disadvantages are pointed out and discussed. At this stage traditional and modern welding technologies were used. The first group includes Gas Metal Arc Welding (GMA) and Manual Metal Arc Welding (MMA), while the latter Self Shielded Flux Core Wire technology (SSA) and an “hybrid” welding technology consisting in laser welding technology coupled with Gas Metal Arc Welding. After presenting welding technologies a brief description of typical weld defects is also characterized. This is necessary because defects in welded joints are the primary source of failure of the connection. In addition, the manufacturing process are often held directly on the construction site under difficult atmospheric conditions that heavily affect the final result.

In the fourth chapter the process regarding the manufacturing of butt-welded joint pipes is introduced. A part of the pipe samples was produced with induced imperfections in the welded joint, while the second set of pipe samples was manufactured with optimal acceptance quality level of the welded joints. The first group consisted of twelve pipes specimens: four of them were manufactured using GMA welding technology, four using MMA welding technology and the last four using SSA welding technology. For each welding technology two welding positions were adopted, horizontal and vertical, and imperfections were artificially introduced alternatively on the root layer and on the fill pass to simulate the possible adverse conditions occurring during welding process. A resume of all these samples manufactured is depicted in Figure 11. During this stage, the parameters of welding process were recorded: in particular, welding pool temperatures with a thermal camera as well as the electrical parameters, welding current and arc voltage.

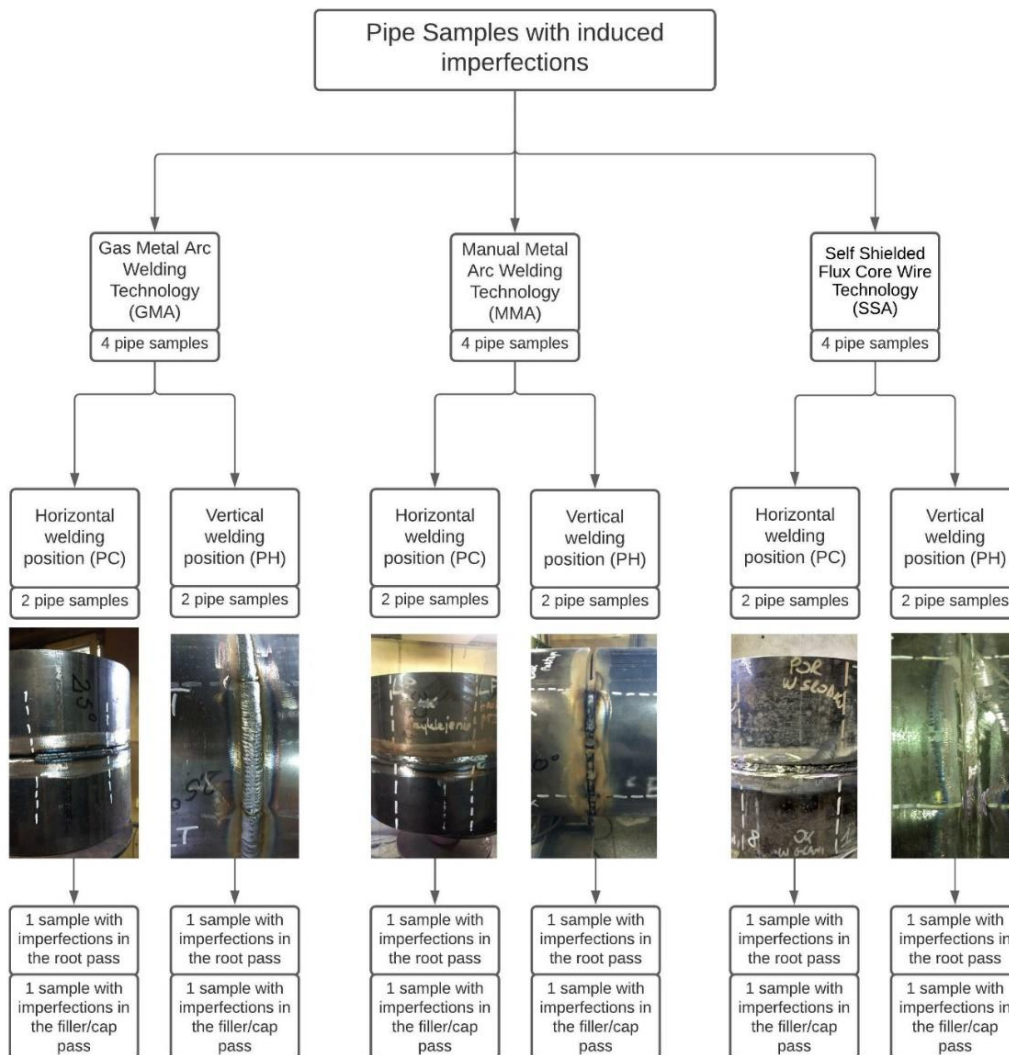


FIGURE 11: PIPE SAMPLES MANUFACTURED WITH DEFECTIVE WELDED JOINTS

The second group of pipe specimens were manufactured to obtain optimal quality of the welded joints in accordance with accepted standards and regulations. It was produced using the same welding technologies (GMA, MMA and SSA) in addition with hybrid welding technology where the root pass is manufactured with the use of laser technology and the filler/cap pass with GMA technology. These pipe samples were later tested with impact load test. A total number of seven pipe specimens were manufactured at Mostostal Zabrze laboratories as reported in Figure 12

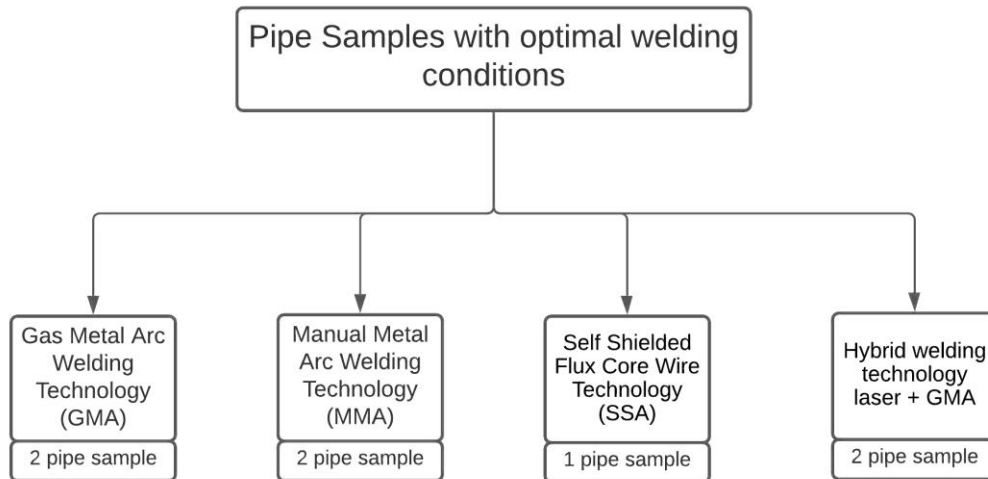


FIGURE 12: PIPE SAMPLES MANUFACTURED WITH OPTIMAL JOINTS

The fifth chapter describes the non-destructive evaluation methods for the assessment of the quality of defective pipe samples. All twelve pipes of the first group mentioned above were subjected to quality control process necessary to assess, according to actual standards, the exact magnitude and position of induced imperfections. They were subjected to visual inspection and radiographic tests allowing to define a map of the defects for each pipe specimen. Knowing the accurate position of weld defects, it was possible to cut the pipes and then prepare samples containing the defects.

These samples were mechanically tested using tensile and bending methods to evaluate the influence of defects on joints resistance. The procedure is described in the sixth chapter. This chapter also contains the results of the impact load test that was performed with the use of the second group of pipes that are of optimal quality.

In the seventh chapter the concept of a monitoring system that allows to assess welding quality using the information retrieved during the manufacturing of defective pipe specimens it is described. The exact position of welding defects obtained with radiographic and ultrasonic tests was correlated with thermal records and welding parameters variation. Critical conditions for typical defects outbreak were obtained. This information could be compared with any future welding process to characterize

a weld quality control method based on such parameters like welding pool temperature, welding current and arc voltage.

The last chapter includes the summary of all results achieved during the experimental activity and the validation used for pipes for petrochemical applications.

2 PETROCHEMICAL PLANTS LAYOUT

2.1 MAIN ELEMENTS OF A PETROCHEMICAL PLANT

In typical oil and gas plants the substances are processed or stored in tanks and vessel of different sizes connected each other with complex piping systems. Bolted flanged joints and butt-welded joints connect the storage tanks to the piping system or two different sections of the piping system. The main components of a petrochemical plants are:

- storage tanks which are steel or concrete elevated structures used to store fluids or gases.
- piping systems which are formed connecting tubular elements one another and used to move the fluid or gas between the various part of the plant.
- fittings e.g., pumps and valves which are elements placed along the piping system and used to regulate the flux of the material processed.
- connectors between the different elements above-mentioned. They are components used to join two or more parts of the plant e.g., two or more pipes, piping system and storage tank.

Storage tanks, piping systems and connectors are the primary interest of this thesis and are therefore described in the next paragraphs.

2.1.1 STORAGE TANKS

Tanks are being used in innumerable ways both to store liquid, vapor or even solid and in a number of interesting processing applications [25]. For example, they perform various unit operations in processing such as settling, mixing, crystallization, phase separation, heat exchange, and as reactors. Tanks can be classified based upon whether they are above- or belowground and upon the external or internal pressure to which they are subjected. Three class of tanks are defined:

- atmospheric tanks, which operate at internal pressure usually slightly above the atmospheric pressure.
- low-pressure tanks, which are designed to operate between atmospheric pressure and 15 atm
- pressure vessels, which are also be characterized as high-pressure tanks, operating above 15 atm.

In general, storage tanks are cylindrical shells, made of different materials based on their serviceability conditions, with a vertical axis of symmetry. The bottom is usually flat while the top is made in different shapes and has different constraint conditions with the cylindrical shell below.

Regarding the top, it can be made in a shallow cone, umbrella or dome shape. The roof can also be fixed or floating on the cylindrical structure below. In the first case the roof is completely connected with the vertical walls of the tank, while in the second solution it raises and lowers to automatically adjust to the level of the commodity in the tank [15]. The material is selected based upon its cost, ease of fabrication, resistance to corrosion, compatibility with stored fluid and its availability. Most common materials are carbon steel, stainless steel, used for storage of corrosive liquid tanks and concrete. In Figure 13 it is depicted the section of a fixed roof concrete storage tank (left) and a section of a floating roof steel storage tank (right).

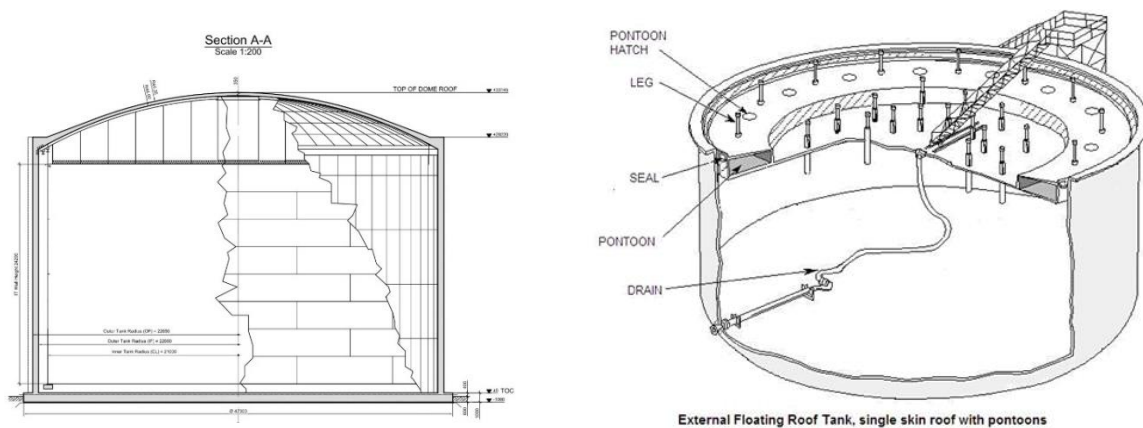


FIGURE 13: FIXED ROOF STORAGE TANK (LEFT) [26] AND FLOATING STORAGE TANK (RIGHT) [27]

2.1.2 PIPING SYSTEMS

A pipe is a term used to designate a hollow, tubular body used to transport any commodity of flow characteristics such as liquids, gases, vapours, liquefied solids and fine powders [28]. Pipes are manufactured using different technologies and materials including e.g., carbon steel and steel alloys, lead, plastic, aluminium and concrete. The properties of the material must be considered during design process. It should be stressed that each of the enumerated materials has limitations that may make it inappropriate for a given application. In the thesis particular attention was paid to carbon steel pipes especially suitable for petrochemical applications. Generally, there are three manufacturing methods: seamless, butt-welded and spiral welded. Seamless pipes are formed from near-molten steel rod that are pierced with a mandrel. The result of this procedure is a pipe that has no seams or joints. In Figure 14 is depicted the manufacturing process and the final result of seamless production method.

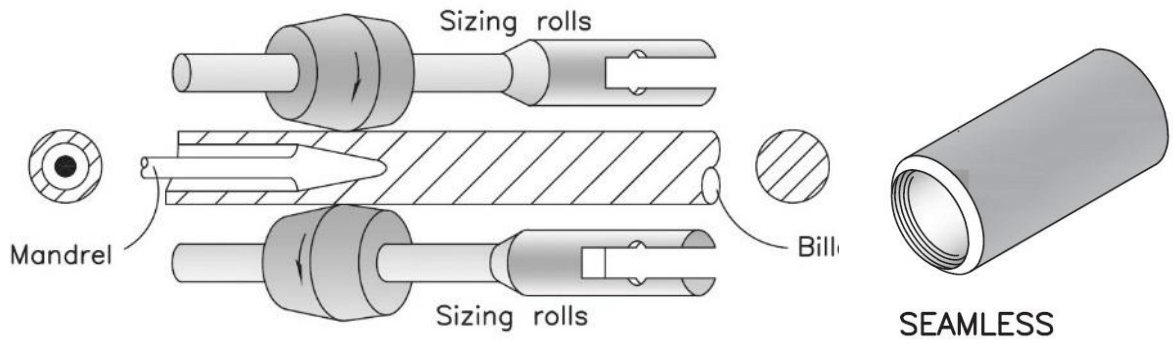


FIGURE 14: SEAMLESS PIPE [28]

Butt-welded pipes are manufactured starting from a steel plate that is then processed through shapers that roll it into a hollow circular shape. If the pipe is manufactured from a hot steel plate the two ends of the plate, squeezed together, produce a fused joint or seam. If instead the initial element is a cold steel plate the joint of the two ends is performed with automatic welding process. Figure 15 shows the manufacturing process of butt-welded pipes.

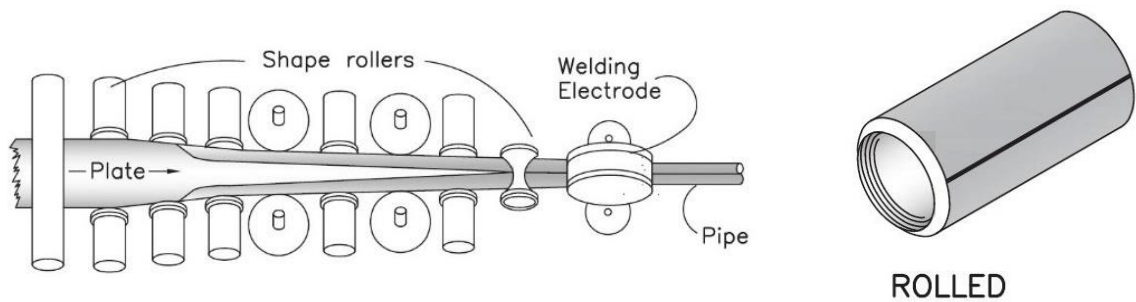


FIGURE 15: BUTT-WELDED PIPE [28]

Spiral-welded pipes are formed by twisting strips of metal into a spiral shape and then welding the edges one another to form a seam (Figure 16).

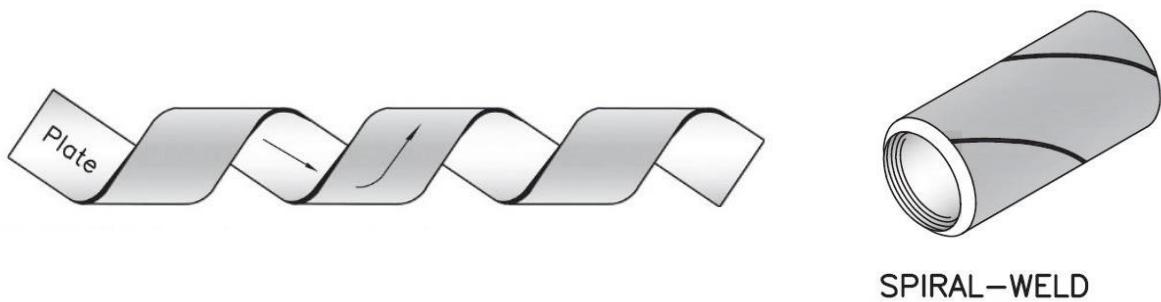


FIGURE 16: SPIRAL WELDED PIPE [28]

During the experimental activity, which is described in the next chapters, were used rolled butt-welded steel pipes.

2.1.3 CONNECTORS AND JOINTS

There are two main methods of connecting pipe sections to storage tanks and fittings: mechanical fastening and physical bonding [29]. The first one approach includes bolted joints while the latter includes welded joints. The bolted flanged joint is a mechanical, non-permanent method of joining together pipe to pipe, pipe to fitting and pipe to valve [30]. The components that allows the coupling of two different pipe sections are flanges. Each of them has two distinct areas:

- the flange blade with the bolt holes and the sealing face.
- the flange hub with the pipe connection ends.

The flange blade is the circular area through which there is a standard bolting pattern, based on the outside diameter of the pipe and the design pressure rating. It has a seal face accurately machined to a predetermined finish, on which the gasket sits and a back face on which the nut sits. The hub is located on the back of the blade and it receives the pipe. An example of a typical bolted flange joint is depicted in Figure 17.

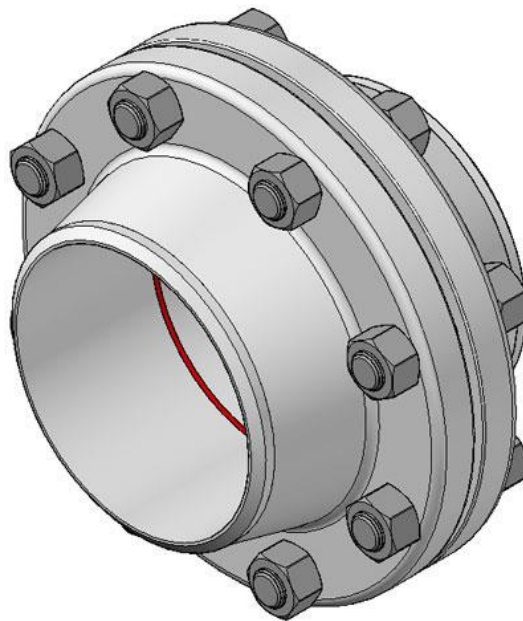


FIGURE 17: PIPE BOLTED FLANGE JOINT [31]

Bolted flanged joints in pipes for oil and gas industry are potential sources of leakage of toxic or flammable liquids. Thus, the joint must be assembled and tightened with an extra measure of knowledge. Furthermore, a gasket is usually placed between two blades sealing the joint and this adds

major uncertainties to the behaviour of the joint. Different research activities (i.e. [32]) try to assess the behaviour of bolted flange joints under ultimate limit state or serviceability limit state.

A butt-weld joint is made by welding the bevelled ends of pipe together. The ends of two pipes are prepared by forming a 25-30° bevel on the full thickness of the pipe wall except for a portion of the inner section. This preparation process allows to create a V-groove between the pipes then filled with weld metal using different welding technologies (Figure 18).

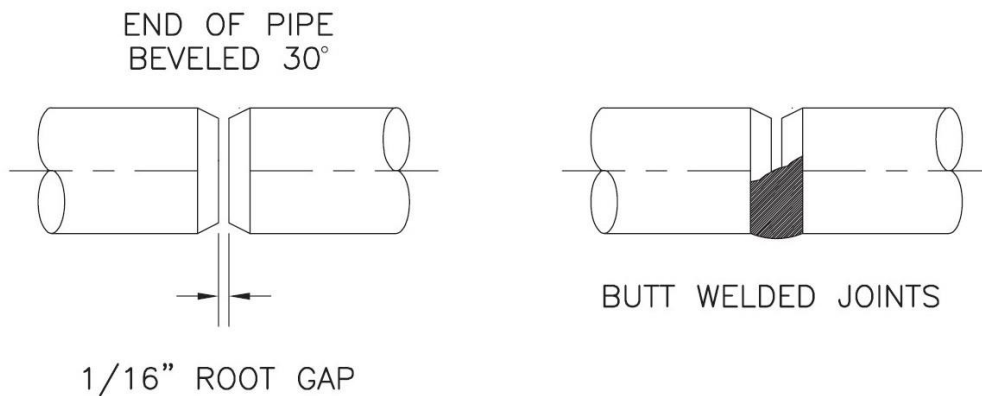


FIGURE 18: BUTT-WELDED JOINT [28]

Bolted flanged joints, butt-welded joints and elbows are critical elements in case of Natech accidents. Numerous issues involving the safety of bolted flanged joints and elbow elements is broadly discussed in the literature. Examples in [32]–[34]: authors try to assess the behaviour of these components during extreme events.

The approach described in the thesis is based on the similar idea. The investigation was aimed at observation of behaviour of butt-welded joints of high strength steel pipes.

2.2 TYPICAL CONFIGURATIONS OF PETROCHEMICAL PLANTS

The first step of this research was to perform a review of typical configurations of petrochemical plants that allows to study common piping systems installations. Considering a generic configuration, like the one depicted in Figure 19, typical configurations of piping systems consist of a combination of different elements:

- linear pipe elements
- elbow elements connecting linear pipes placed on different levels or directions
- tee-joint elements that allow to diverge the flux into two directions
- reducer elements that connect two elements having different section diameter

In the case of oil and gas or industrial plants the enumerated elements are made of steel and are usually of circular section. Linear pipes are characterized by means of their nominal diameter and wall thickness while, in addition to these parameters, elbows elements are defined also for their angle. All these elements abovementioned are connected each other by butt-welded joints.

It is clearly visible that pipe elements of various sizes laying on different levels and planes impose different welding positions, i.e., vertical and horizontal, during manufacturing process. The positions are defined in proper regulations. They are depicted in Figure 20 [35].

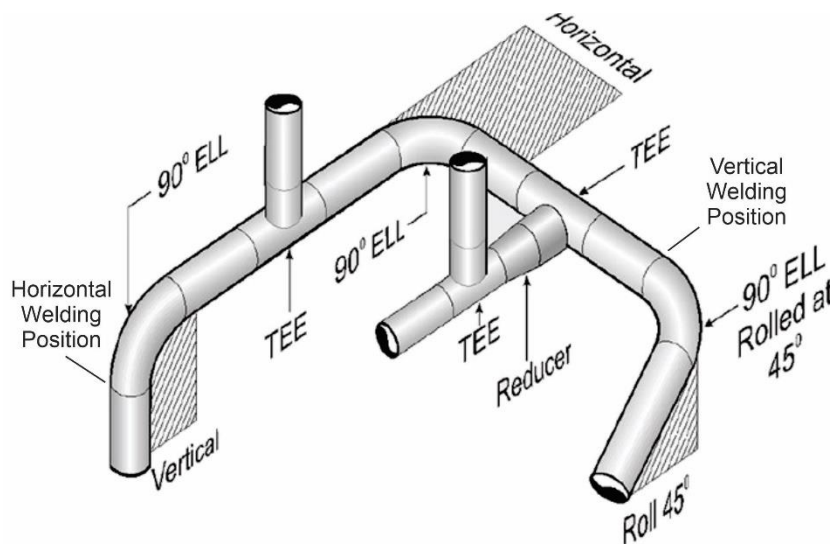


FIGURE 19: GENERIC PIPING SYSTEM CONFIGURATION [36]

Welding positions according to DIN EN ISO 6947

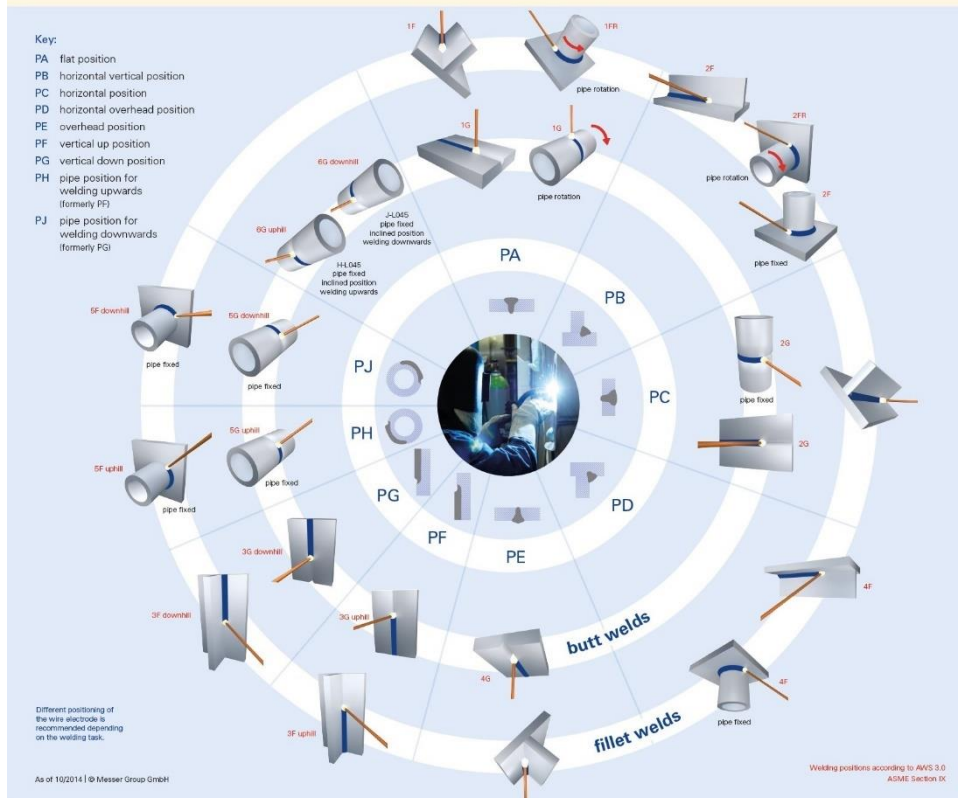


FIGURE 20: WELDING POSITIONS [35]

In addition to typical piping systems layout, it is important to understand typical pipes characteristics to focus this research on solutions and applications that could suit for oil and gas industry. In [26] it is described a probabilistic seismic analysis of a Liquefied Natural Gas (LNG) plant used as a case study (Figure 21).



FIGURE 21: LNG PLANT USED AS CASE STUDY FOR [26] (LEFT) AND 3D MODEL OF THE STORAGE TANK, SUPPORT STRUCTURE AND PIPING SYSTEM (RIGHT)

In the further parts of the thesis is described the piping system connecting the storage tank with the process area. There are characteristics of such structures providing complete information regarding material, sizes and accessory elements locations. In Figure 22 it is depicted a detailed pipe system

section included in the above-mentioned case study and it describes the dimensions of the pipes and their positions, the type of fittings adopted and the constraints between the piping system and the concrete support structure at the bottom of the structure. In this specific case the pipeline installed inside the LNG plant described in [26] consists of two different sections connected each other by a reducer eccentric: the first one is characterized by a 10'' SCH10S pipe, while the latter by a 8'' SCH10S [37]. The first pipe has the external diameter of 273.5 mm and the wall thickness of 4.19 mm while the second pipe has the external diameter of 219.08 mm and the wall thickness of 3.76 mm.

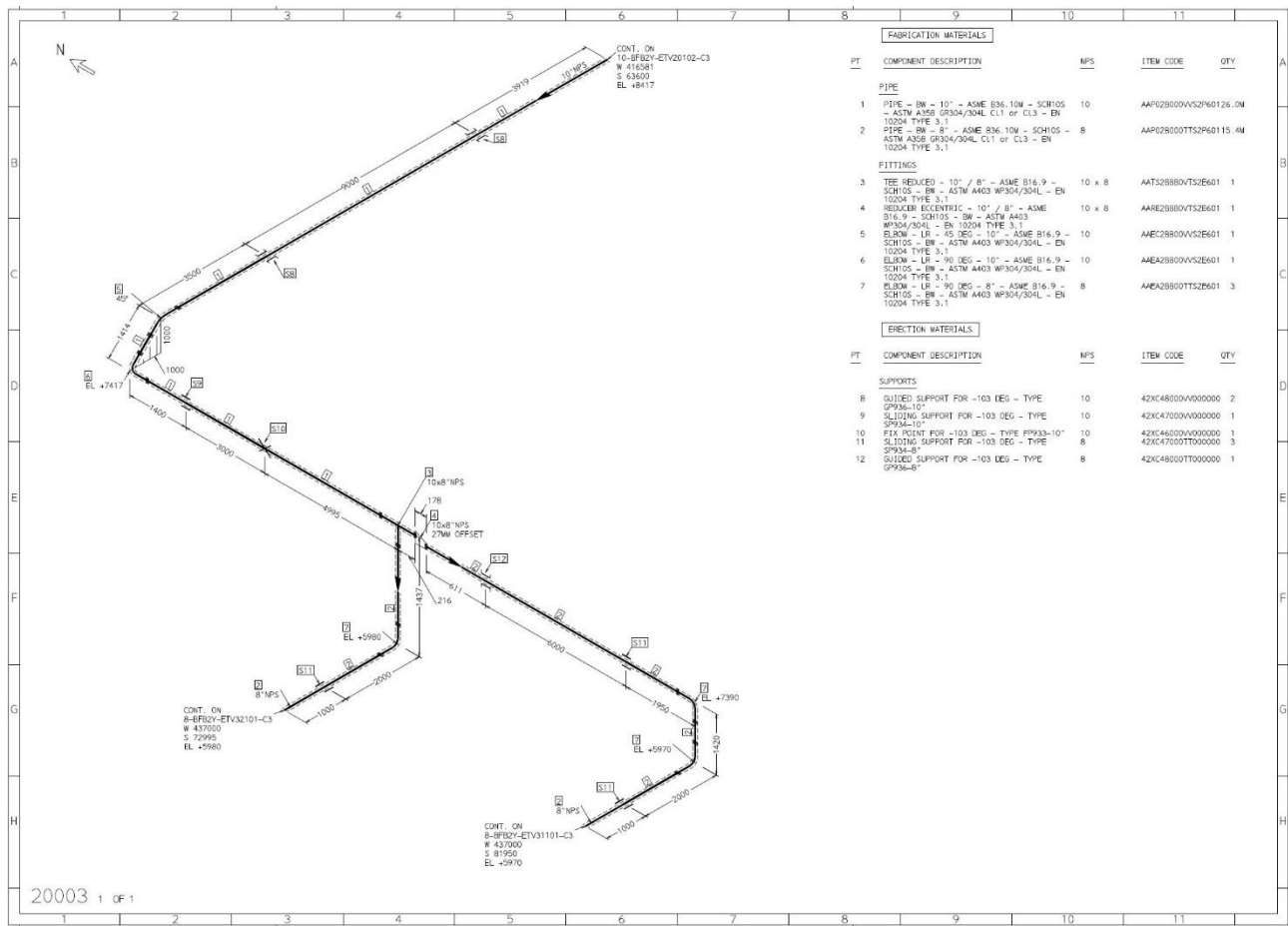


FIGURE 22: DETAILED PIPE SEGMENT [26], [38]

The complete piping system used case study consists of eight main pipes with different dimensions connecting the storage tank to process areas of the plant. The properties of these eight pipes are listed in Table 3: pipes diameters are in a range from 4'' (114,3 mm) to 18'' (457,2 mm).

Pipeline number	Pipe specification	External diameter [mm]	Wall thickness [mm]	Elbows curvature radius [mm]
1	16'' - SCH20	406.4	7.92	610
2	10'' - SCH10S	273.05	4.19	381

3	4'' - SCH10S	114.3	3.05	152
4	6'' - SCH10S	168.28	3.40	229
5	12'' - SCH10S	323.85	4.57	457
6	6'' - SCH10S	168.28	3.40	229
	8'' - SCH10S	219.08	3.76	305
7	6'' - SCH10S	168.28	3.40	229
8	18'' - SCH10S	457.2	4.78	686

TABLE 3: PIPING SYSTEM INSTALLED ON CASE STUDY [26] [37]

2.3 CASE STUDY PIPING SYSTEM

Taking into account the premises described in Paragraph 2.2, it was selected a similar pipe [39]. It was of 10 meters pipe grade API-5L X80 with a 12''^{3/4} diameter (323.9 mm) and 10 mm wall thickness. This pipe was manufactured by Huta Łabędy S.A [24] using hot rolled steel [39]. Significant mechanical properties of hot rolled steel pipes are minimum yield strength $R_{t,0.5}$ and ultimate tensile strength R_m (Figure 23). The first quantity refers to minimum tensile stress that causes an elongation of 0,5% while the second one refers to ultimate tensile stress that causes failure of the material. API-5L [40] standard prescribes for X80 steel minimum yield strength $R_{t,0.5}$ of 555 MPa and minimum ultimate tensile strength R_m of 625 MPa (Table 4). The mill test certificate from the manufacturer (Figure 24), obtained from tensile test on 5 different samples, states a minimum of 615 MPa and a maximum of 634 MPa for yield strength and a minimum of 679 MPa and a maximum of 699 MPa for ultimate tensile strength (Table 5).

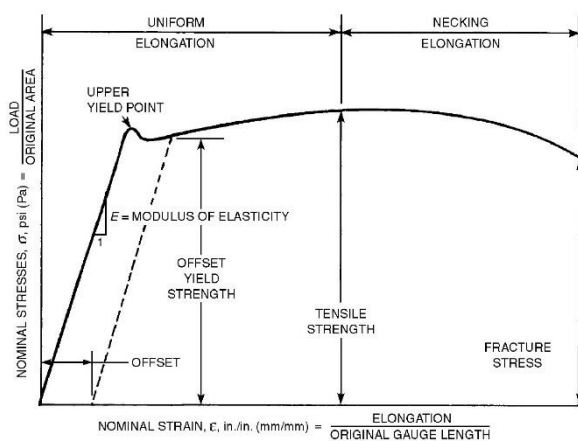


FIGURE 23: DEFINITION OF YIELDING AND ULTIMATE STRENGTH FOR X80 STEEL [41]

API-5L Prescriptions: X80 steel	
Yield strength $R_{t,0.5}$ [MPa]	Ultimate tensile strength R_m [MPa]
555	625

TABLE 4: MECHANICAL PROPERTIES OF X80 STEEL ACCORDING TO API-5L [40]

Manufacturer test on 5 sample	
Yield strength $R_{t,0.5}$ [MPa]	Ultimate tensile strength R_m [MPa]
615 ÷ 634	679 ÷ 699

TABLE 5: MECHANICAL PROPERTIES OF X80 STEEL ACCORDING PIPE MANUFACTURER [39]

posco		Mill Test Certificate										Certificate No. : 160818-FH01KS-0175A1-0001									
Order No. : 01S2283899		PO No. : API-WGK-1601										Date of Issue : Aug., 19, 2016									
Supplier : POSCO DAEWOO CORPORATION		Commodity : HOT ROLLED COIL																			
Customer : HUTA LABEDY S.A.		Spec & Type : API 5L X80M PSL2																			
Size	Product No.	Quantity	Weight (kg)	Heat No.	Position	Tensile Test				Bend Test	Impact Test		Non-metallic Inclusion ASTM E45 A Method (Grade)								F.G.S
						YP (MPa)	TS (%)	EL (%)	YR (%)		V Notch +0°C	Energy SF (Joule)	A	B	C	D	Thin		Heavy		
10x1040xC	HRH039750	1	22,390	SP60921	B	633	696	31	90.9	Good	1: 166 98 2: 179 97 3: 173 97	0.0	0.0	1.5	1.0	0.0	0.0	2.0	1.5	14.0	
10x1040xC	HRH039770	1	22,270	SP60921	B	633	692	33	91.5	Good	A: 179 97 1: 176 97 2: 184 98 3: 177 97	0.0	0.0	2.0	0.0	0.0	0.0	2.0	1.5	14.0	
10x1040xC	HRH039790	1	22,300	SP60921	B	615	679	31	90.8	Good	A: 179 97 1: 182 95 2: 172 97 3: 160 96	0.0	0.0	1.5	1.5	0.0	0.0	2.0	1.5	14.0	
10x1040xC	HRH039740	1	22,430	SP60921	B	634	699	32	91.0	Good	A: 186 96 1: 193 98 2: 206 100 3: 201 100	0.0	0.0	1.5	1.5	0.0	0.0	1.5	1.5	14.0	
10x1040xC	HRH039780	1	22,430	SP60921	B	632	698	31	91.9	Good	A: 200 99 1: 181 98 2: 191 98 3: 170 97	0.0	0.0	0.5	0.0	0.0	0.0	0.5	0.5	14.0	
10x1040xC	HRH039800	1	22,330	SP60921	B	616	680	32	91.0	Good	A: 181 98 1: 191 98 2: 199 98 3: 206 100 A: 166 98	0.0	0.0	1.5	0.5	0.0	0.0	0.5	0.0	14.0	
*** Sub Total (C10) ***		6	134,240 (kg)																		
*** Grade Total ***		6	134,240 (kg)																		
*** Brand Total ***		6	134,240 (kg)																		
* Position - T: Top, M: Middle, B: Bottom * Tensile Test: Direction: Transversal, Gauge Length: 50mm(Rectangular), YP Method: 0.5% underload * Bend Test: Direction: Transversal, Angle: 180° * Impact Test: Direction: Transversal, Sub-Size: 10mmX7.5mm * F.G.S: Ferrite Grain Size * Division - 1: Ladle Analysis										We hereby certify that the material herein has been made in accordance with the order and above specification. This material has been fully killed and made by basic oxygen process. This material has been made by vacuum degassing & calcium treated process. This material is fine grained steel. Test Certificate is issued according to EN10204 3.1.											
Surveyor To:										Legal sanction can be imposed on forging. Improper use of product can cause safety issues. Kim, Young-Ha Chief of material testing section											
POSCO										Gwangyang Works, 20-26, Pokposarang-gil, Gwangyang-si, Jeollanam-do, 57807, Korea											

FIGURE 24: MILL TEST CERTIFICATE FOR SELECTED PIPE STEEL [39]

The chemical composition of the pipe is reported in Table 6, while its geometrical properties are described in Table 7.

Chemical Composition															
C [%]	Si [%]	Mn [%]	P [%]	S [%]	Cr [%]	Ni [%]	B [ppm]	Cu [%]	Mo [%]	N [ppm]	Nb [%]	Ti [%]	V [%]	Al [%]	PCM [%]
0.0766	0.232	1.633	0.0072	0.0014	0.242	0.019	2	0.038	0.004	50	0.049	0.214	0.042	0.038	0.186

TABLE 6: CHEMICAL COMPOSITION OF THE PIPE SELECTED [39]

Geometrical Properties		
External Diameter [inches]	External Diameter [mm]	Wall thickness [mm]
12'' 3/4	323.9	10

TABLE 7: GEOMETRICAL PROPERTIES OF THE PIPE SELECTED [40]

To perform the experiments the pipe was cut in segments of about 20-25 cm of length in order to prepare proper samples. As an example, two of these segments clamped are depicted in Figure 25 ready for the experimental activity. As described in Figure 11 twelve samples similar to the one depicted in Figure 25 were manufactured with induced imperfection in the welded joint, while seven samples were manufactured with optimal joint conditions as described in Figure 12.

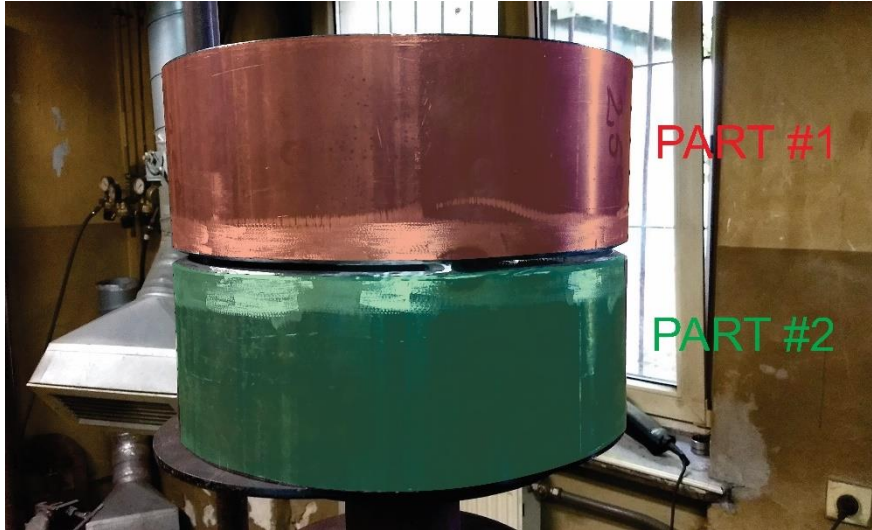


FIGURE 25: EXAMPLE OF TWO SEGMENTS OF THE 10 M PIPE BEFORE EXPERIMENTAL ACTIVITY

3 WELDING PROCESSES AND DIAGNOSTIC METHODS

The welding technologies used in the experiments carried out during this PhD programme and the diagnostic methods which were applied to assess the quality and reliability of welded joints are discussed in this chapter.

A series of twelve butt-welded joint pipe specimens were manufactured during the first step of the experimental activity adopting traditional welding technologies i.e., Gas Metal Arc Welding (GMA), Manual Metal Arc Welding (MMA) and Self Shielded Flux cored arc welding (SSA). An additional set of pipe samples was produced with the use of an innovative method called hybrid welding technology. This solution combines Laser Welding and Gas Metal Arc welding technologies. In this case the root area is welded using the laser source while the groove is subsequently welded using GMA technology. All these welding technologies are briefly described in next paragraphs, providing basic information while a more complete illustration is left to dedicated appendix section. The manufacturing of all the specimens was a preliminary step towards the actual aim of the thesis that was the study of the mechanical properties of butt-welded joints in high strength steel pipes, the influence on them of the imperfections that might develop during welding procedure and the methods of detection of these imperfections.

Once all the pipe specimens necessary for the further processing were produced, they were tested with radiographic methods assessing the quality of the welded joints. The use of this technique allowed to detect possible discontinuities inside the joints and evaluate their compatibility with acceptance quality levels suggested by the standards. Two specific paragraphs are devoted to a description of the various type of weld discontinuities and the radiographic method useful for their detection.

The welding process was also monitored with an infrared camera, recording welding pool temperature inside the welded joint. The data recorded were subsequently analysed to obtain precise information regarding the development of imperfections inside the welded material. In this chapter it is provided a brief review of thermographic technique as non-destructive evaluation method.

3.1 WELDING TECHNOLOGIES

The goal of the joining processes is to cause different pieces of material to become a unified whole. In case of two pieces of metal, when the atoms at the edge of one piece come close enough to the atoms at the edge of another piece for interatomic attraction to develop, the two pieces become one

[41]. Welding processes achieve this result with the use of heat or pressure, or both. In the thesis the technologies of the first group and in particular arc welding technologies and laser welding technology were only considered. In the first case the source of heat is generated by an electric arc that is struck between the workpiece and the tip of the electrode. The effect of the intense heat produced by the arc is the melting of a portion of the base metal and the subsequent formation of the weld. In the second case the thermal input that is necessary to melt the metal is provided by a laser beam that impacts on the portion of the material where the joint is planned. During the experiments were used three types of arc welding technologies and another hybrid one consisting in the combination of laser and arc welding technologies. Their concepts and their applications for different purposes are briefly described in the next paragraphs and extensively in the appendix

In gas metal arc welding technology (GMA) the process of joining two metal pieces involves the use of a metal arc and consumable electrode with externally added shielding gas. For this thesis, during the experimental activity, the electrode wire adopted is classified according to EN ISO 16834-A [42] as G 69 4 M Mn3Ni1CrMo; the commercial name from Lincoln Electric is LNM Moniva [43] (Figure 26) and has section diameter of 1,2 mm. This wire is suitable for welding of high strength steels with yield strength up to 690 MPa. The shielding gas selected was Argon with 20% of CO₂ (Figure 27) classified as M21-ArC-20 according to EN ISO 14175 [44].



FIGURE 26: LNM MoNiVA WIRE [43]



FIGURE 27: M21ARCO2 [45]

Manual metal arc welding technology is one of the most known welding methods and is sometimes referred as stick welding. Electric arc is generated between the tip of a covered electrode and the base material as depicted in Figure A2. The electrodes used during experimental activity are Conarc 85 from Lincoln Electric (Figure 28). This product is classified as E 69 5 Mn2NiCrMo B 3 2 H5 according to EN ISO 18275-A [46]. For root welding passes were used electrodes with a diameter of 2,5 mm, while with a diameter of 3,2 mm for filler/cap passes.



FIGURE 28: CONARC 85 ELECTRODES [47]

Self-Shielded Flux Cored Arc Welding (SSAW or FCAW) is a welding technology like Gas Metal Arc Welding regarding power sources, wire feeders and welding guns. However, in this case during the welding process there is not an external shielding gas feed, but welding wire incorporates a core containing flux. The electrode used during the preparation of butt-welded joint pipe specimens was PIPELINER NR208-XP (Figure 29) from Lincoln Electric, classified as E81T8-G according to AWS A5.29/A5.29M [48].



FIGURE 29: PIPELINER NR208-XP ELECTRODE [49]

Laser beam welding (LBW) effects the fusion welding of materials with the heat supplied by a laser beam that impinges on the joint. The laser beam is generated from a concentrated beam of coherent, monochromatic light in the infrared or ultraviolet frequency portion of the electromagnetic radiation spectrum [41].

3.2 WELDING IMPERFECTIONS

Weld quality is an area that requires attention in every phase of the manufacturing and service life of welded assemblies. Welded joints with the required reliability throughout its life must exhibit a

sufficient level of quality and fitness for purpose. To guarantee the adequate level of quality, each weldment should be:

- adequately designed to meet the intended service for the required life.
- manufactured with the use of specified materials and in accordance with the design standards.

In the research performed in the framework of the thesis, the focus was especially put on the manufacturing conditions of welding processes. These processes, if not correctly performed, can lead to the growth of discontinuities inside the weld material. These unwanted occurrences can affect the mechanical behaviour of the joint and specifically to steel pipes for oil and gas industry, resulting in spill and leakages. The most severe of these events can result in explosions or dispersion of hazardous substances. The American Welding Society issued Standard Welding Terms and Definitions, AWS A3.0:2001; the term discontinuity is defined as “an interruption of the typical structure of a material, such as a lack of homogeneity in its mechanical, metallurgical, or physical characteristics” [50]. It should be noted that a discontinuity is not necessarily a defect. A defect is defined as “a discontinuity or discontinuities that by nature or accumulated effect render a part or product unable to meet minimum applicable acceptance standards or specifications” [50].

Typical discontinuities associated with fusion welding are:

- porosity, which is a cavity-like discontinuity that forms when gas is entrapped in solidifying weld metal. It occurs on the surface or in the subsurface of the weld and it assumes various configurations and shapes based on welding conditions. Scattered porosity appears to be distributed throughout one pass of single or multiple pass welding and occurs on the surface or in the subsurface of the weld. The cluster porosity is a localized group of pores. The linear porosity consists of spherical pores oriented in a line. On wormholes or elongated porosity, the pores assume a length greater than the width and extends from the root of the weld toward the face. The different occurrences of porosity imperfection are schematically depicted in Figure 30.

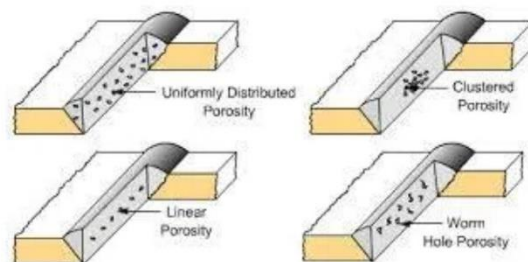


FIGURE 30: DIFFERENT OCCURRENCES OF POROSITY IMPERFECTION [51]

- inclusions are discontinuities produced by solid materials trapped in the weld metal or the interfaces of the weld metal.

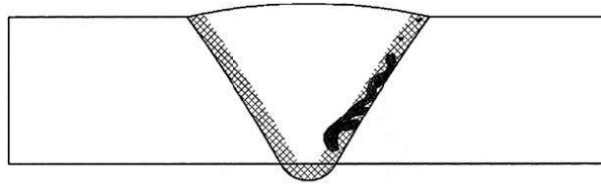


FIGURE 31: SLAG INCLUSION [52]

- incomplete fusion is a situation in which the fusion does not completely occur between weld metal and parent material or between consecutive weld beads.

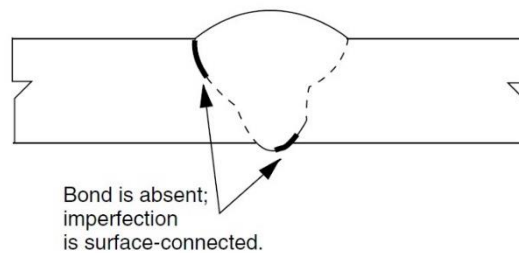


FIGURE 32: INCOMPLETE FUSION IMPERFECTIONS [53]

- incomplete joint penetration is a root condition that occurs when weld metal does not completely extend through the joint thickness (Figure 33). It is the result of incorrect groove design as well as welding procedures. This type of discontinuity, due to stress concentration, can facilitate the initiation and propagation of cracks when the element is subject to bending or tensile loads. Pipe elements are prone to this kind of imperfections because the internal surface is usually inaccessible; for the same reason it is more difficult to detect with visual inspection.

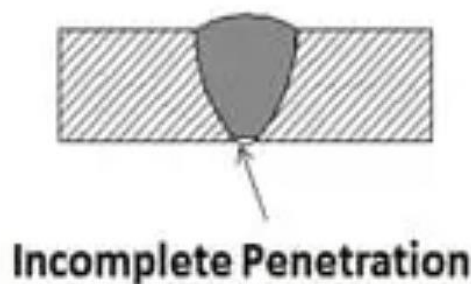


FIGURE 33: INCOMPLETE JOINT PENETRATION [54]

- undercut imperfection occurs when groove portions at the edge of a layer are left unfilled by the weld material forming a recess in the joint face (Figure 34).

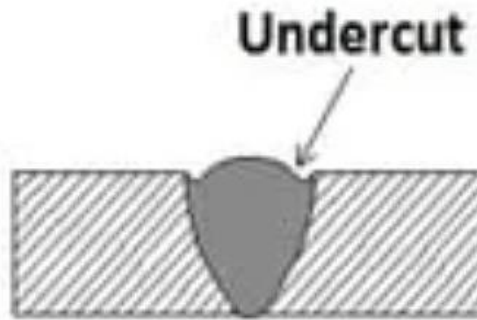


FIGURE 34: UNDERCUT [54]

- excessive overlap imperfection occurs when weld metal protrudes beyond the weld toe or root creating a surface discontinuity (Figure 35). This discontinuity, which can be seen as a mechanical notch, can be the point where the fracture of the joint take place.

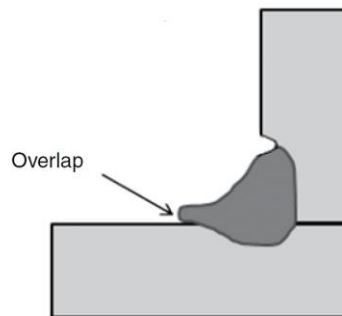


FIGURE 35: OVERLAP [52]

- cracks are small fractures that can develop inside the welded material due to localized stresses exceeding the ultimate strength of the material. They are characterised by sharp tip and high ratio of length and width. This type of discontinuity is particularly severe because its tendency to propagate under stress causing the failure of the joint.

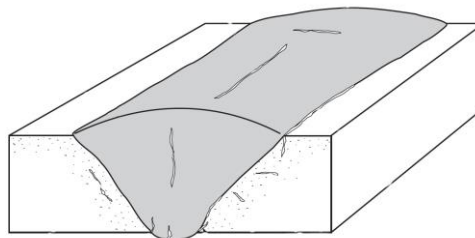


FIGURE 36: CRACKS [41]

3.1 NON-DESTRUCTIVE METHODS OF WELDING PROCESS ASSESSMENT

Non-destructive Evaluation (NDE) is a common term for non-invasive methods of testing, evaluation and characterization based on physical principles of sensing and assessment [55]. NDE methods for technical diagnostics include:

- radiography which is a method that allows to obtain a two-dimensional projection of a three-dimensional object hit by a penetrating radiation. All the imperfections and discontinuities lying along the path of the radiation are therefore impressed on a detector film.
- ultrasound which uses ultrasonic waves propagating into a solid to assess its properties and quality. The waves, travelling through the objects, interact with discontinuities, change in thickness or variation of the elasticity of the material.
- eddy current which is a method that can be used to assess the response of conductive materials to electromagnetic fields.
- magnetic particle inspection which is a simple and economical methods to detect near the surface defects. The procedure consists of the analysis of the behaviour of ferromagnetic particles over the surface of a magnetized object. The magnetic field is affected by the defects the particles to be attracted by these zones that can be therefore easily highlighted.
- liquid penetration method which allows to detect surface discontinuities using a penetrant liquid. This liquid, which must have a contrast colour from the surface analysed, penetrate into the discontinuity and therefore can reveal its edges.
- thermography which refers to a technique based on the analysis of infrared images obtained from a heated object. On these images it is possible to isolate and detect the imperfections based on the differences of thermal properties from base material.

In the next paragraphs two selected techniques are described. They were used during the experiments carried out according to the PhD programme: radiography and thermography. The first technique was applied to locate and evaluate the magnitude of imperfections inside butt-welded joints of steel pipe, while the second was used during the welding process, recording welding pool temperature in order to subsequently evaluate welding conditions that favour the development of the same imperfections detected with radiographic test.

3.1.1 RADIOGRAPHIC AND THERMOGRAPHIC TECHNIQUES

One of the techniques available for non-destructive quality evaluation of elements and structures is radiography. This approach allows to detect hidden flaws of an object subjected to X-rays or gamma rays. It is based on the principle that flaws in components show different exposure levels on a radiographic film due to differential absorption of radiation penetrating the object. Considering the case of quality assessment procedure, the radiation penetrating the object is absorbed, scattered or transmitted through the object to the recording medium. The amount of radiation transmitted depends upon several factors:

- relative densities of the metal,
- characteristics of the radiation,
- through-thickness variations
- inclusions or discontinuities.

An industrial radiographic test is performed using special X-rays systems (Figure 37) that are of different sizes, shapes and duty cycles and are essentially characterized by the following parameters:

- energy – measured in kV
- current – measured in mA



FIGURE 37: GAS-FILLED TUBE HEAD X-RAY EMITTER [56]

Thermography is a diagnostic technique that analyses the space distribution and the time evolution of the surface temperature of an element and based on these measures, establishes its technical state.

The possibility to measure electromagnetic radiation of an object and subsequently infer its temperature is called infrared thermography. Infrared thermography is a non-destructive, non-intrusive, non-contact method that allows the mapping of thermal patterns, i.e., thermograms, on the surface of objects, bodies or systems through the use of an infrared imaging instrument, such as an infrared camera [57].

Two approaches are generally adopted in thermal non-destructive evaluation: passive, in which materials and structures emit electromagnetic radiation due to their temperature usually higher than room temperature, and active, in which an external energy source stimulates the material to be inspected. The first approach is typically implemented in the manufacturing of the materials, in the diagnosis of abnormalities or hot spots with respect to the surroundings. In the second case an external source of energy excites the object of the analysis. Defective and non-defective areas, due to different thermo-physical properties, produce thermal contrast that can be measured with the thermographic apparatus. The two approaches are depicted in Figure 38.

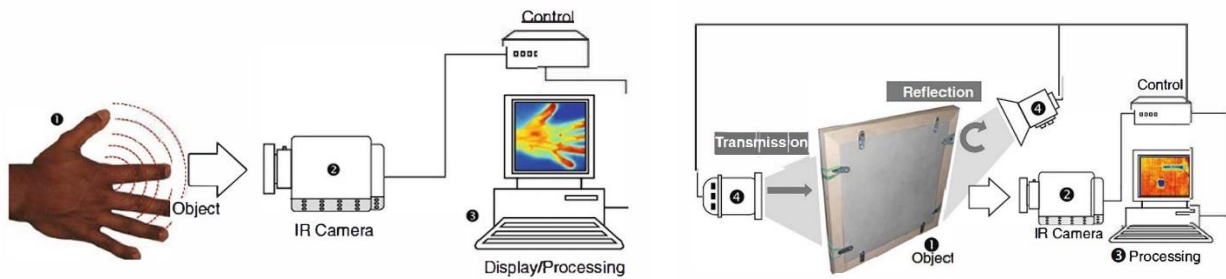


FIGURE 38: PASSIVE AND ACTIVE APPROACHES IN THERMOGRAPHY [55]

For the purpose of the experimental activity described in this thesis, the thermal monitoring of the welding process was carried out adopting the passive approach and a focal plane array camera setup with a resolution of 640 x 480 pixels and a 50 Hz sample frequency.

4 PREPARATION OF CASE STUDY BUTT-WELDED JOINT PIPE SPECIMENS

The properties of the pipe used for experiments were discussed in Paragraph 2.3. It is a 12''^{3/4} pipe of grade API 5L X80 that was cut into segments approximately 25 cm long. These segments were the base components for manufacturing of butt-welded joints as described in the next paragraphs. Two different groups of butt-welded joint pipe specimens were manufactured during the first step of the experiments: the first group includes pipe specimens with induced imperfections inside the butt-welded joints (Figure 11), while the second one includes pipe specimens with optimal quality acceptance levels of welded joints (Figure 12).

The two groups are described in detail in the next two paragraphs. The first group was the basis for detailed analysis of the effects of induced imperfections on the resistance of butt-welded joints. The data, information and knowledge obtained from this analysis were subsequently combined with the thermal data and electrical records collected during welding process. The goal was to understand critical conditions for the development of the imperfections. The pipe specimens included in the second group were used as basis for destructive test, simulating the effect of the impact of collapsing structures due to extreme events.

4.1 SPECIMENS WITH INDUCED IMPERFECTIONS

The manufacturing of the first group of pipe specimens with induced imperfections inside the butt-welded joint was performed in Mostostal Zabrze SA (Figure 39).

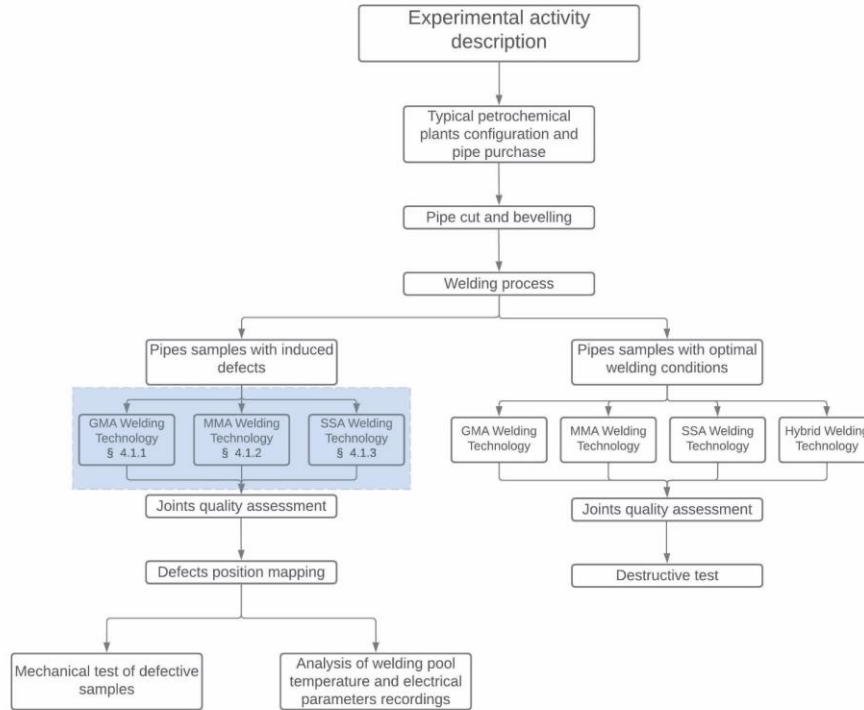


FIGURE 39: DETAIL OF EXPERIMENTAL ACTIVITY PERFORMED FOR PIPES WITH INDUCED IMPERFECTIONS

All pipe segments were bevelled, in general with angles of 25 or 30 degrees, and then clamped together as depicted in Figure 40, ready for being welded together using different welding technologies: Gas Metal Arc Welding (GMA), Manual Metal Arc Welding (MMA) and Self Shielded Flux Cored Wire Welding (SSW).



FIGURE 40: BEVELLING OF THE PIPES BEFORE WELDING PROCESS

To perform the experiments twelve butt-welded joint pipes were manufactured during this stage, four samples for each welding technology abovementioned. The four specimens manufactured for each welding technology had different configurations to simulate as much as possible real conditions of the process: two of them were manufactured applying horizontal welding position (PC) while the other two applying vertical welding position (PH) as depicted in Figure 41.

In addition, for each welding position, imperfections, i.e., porosity, lack of penetration, lack of fusion and undercut, were introduced on the root or the cap/filler bead. The summary of the properties of each pipe sample is included in Table 8 reporting the name of the sample, welding technology used, welding position, i.e., vertical or horizontal, and the position of the imperfection inside the joint.

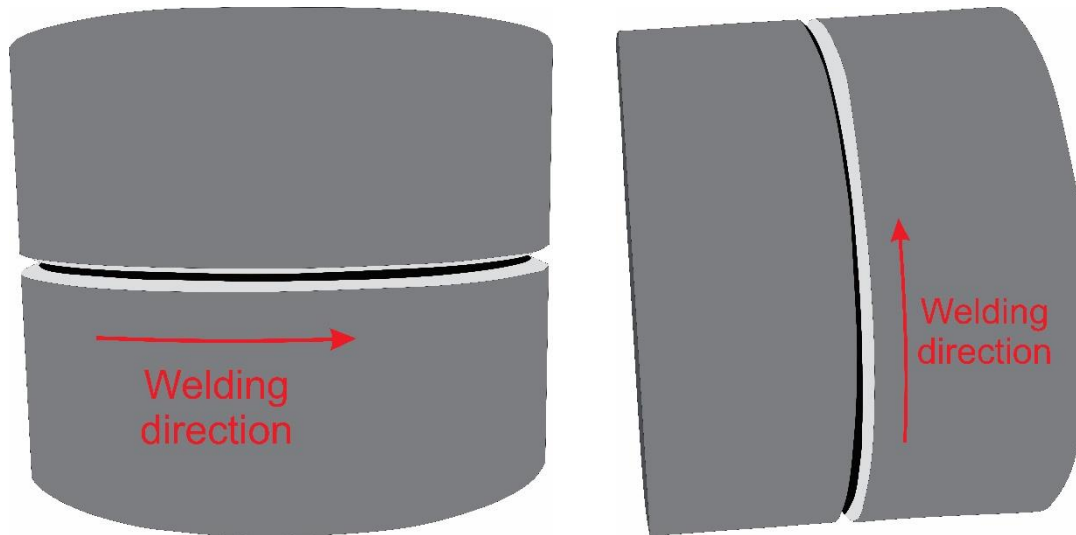


FIGURE 41: HORIZONTAL WELDING POSITION (PC) ON THE LEFT AND VERTICAL WELDING POSITION (PH) ON THE RIGHT

Specimen ID	Welding Technology	Welding Position	Imperfections Position
GMA1	Gas Metal Arc	Horizontal (PC)	Root pass
GMA2	Gas Metal Arc	Horizontal (PC)	Cap/filler pass
GMA3	Gas Metal Arc	Vertical (PH)	Root pass
GMA4	Gas Metal Arc	Vertical (PH)	Cap/filler pass
MMA1	Manual Metal Arc	Vertical (PH)	Root pass
MMA2	Manual Metal Arc	Vertical (PH)	Cap/filler pass
MMA3	Manual Metal Arc	Horizontal (PC)	Root pass
MMA4	Manual Metal Arc	Horizontal (PC)	Cap/filler pass
SSA1	Self-Shielded Wire	Horizontal (PC)	Root pass
SSA2	Self-Shielded Wire	Horizontal (PC)	Cap/filler pass
SSA3	Self-Shielded Wire	Vertical (PH)	Root pass
SSA4	Self-Shielded Wire	Vertical (PH)	Cap/filler pass

TABLE 8: SUMMARY OF PIPE SAMPLES MANUFACTURED

Before welding process, each of twelve pipe specimens were marked approximatively into 8-9 different segments along the circumference (Figure 42). Different welding parameters i.e., voltage, current, shielding gas have been applied for each of the segments during welding process trying to facilitate proper conditions for the generation of imperfections. In the next paragraphs each pipe specimen and Welding Procedure Specifications (WPS) adopted for each welding technology are described in detail. Welding Procedure Specifications (WPS) are the prescriptions that the welder must follow for the correct manufacturing of the workpiece. The manufacturer then demonstrates that the specification meets the standards required by the manufacturing design [41]. For the purpose of the experimental activity WPS provided by the manufacturer include the type of welding technology,

the characteristics of pipe parent material, information regarding filler material i.e., chemical composition and expected mechanical performances, the attributes of shielding gas if present and in the end the optimal welding parameters, current and voltage of the electric arc. WPS applied during the manufacturing of each pipe specimen groups will be introduced in the next paragraphs.



FIGURE 42: SEGMENTS ALONG THE PIPE CIRCUMFERENCE WITH DIFFERENT WELDING PARAMETERS APPLIED

On pipe specimens manufactured using horizontal welding position (PC) the procedure consisted in the deposition of six weld beads (one root pass, two filler passes and three final cap passes). For the case of vertical welding position (PH) were instead deposited three weld beads (one root pass, one filler pass and one cap pass). The two conditions are displayed in Figure 43.

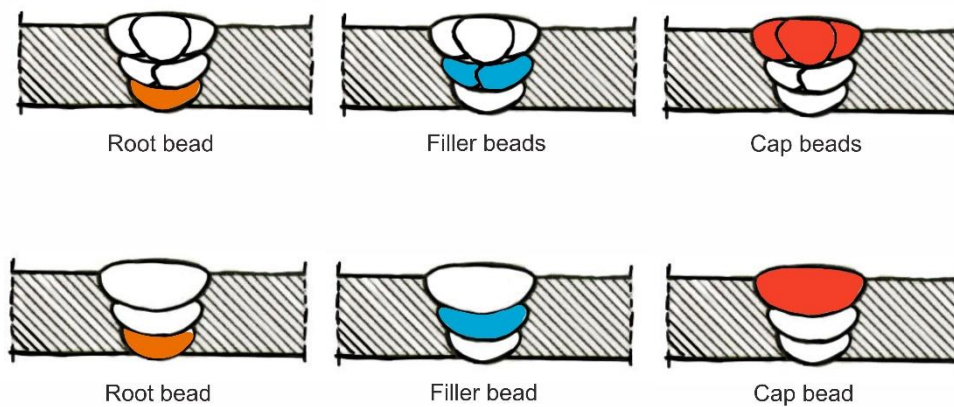


FIGURE 43: BEADS DEPOSITIONS

4.1.1 GMA PIPE SPECIMENS

The number and type of pipe samples marked as GMA and prepared in Mostostal Zabrze SA laboratories are highlighted in Figure 44.

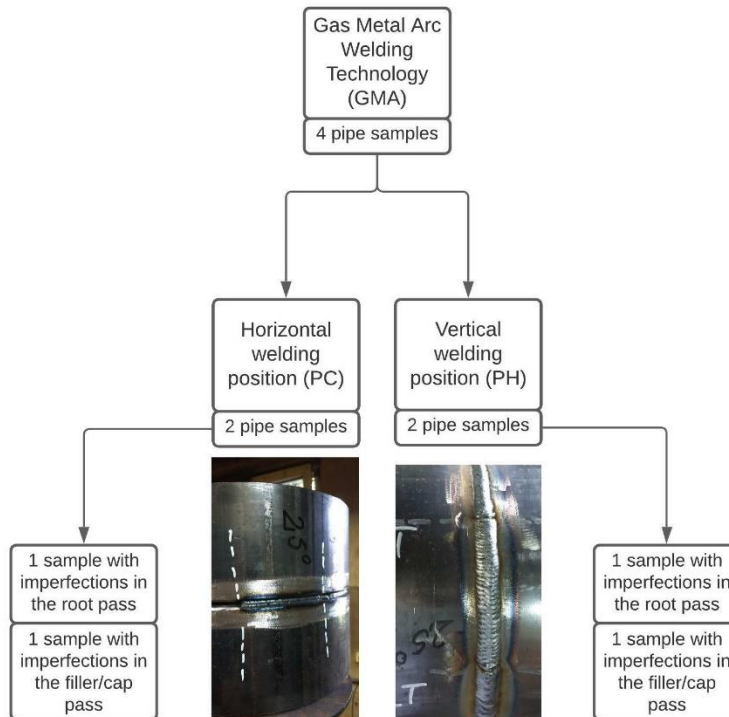


FIGURE 44: NUMBER AND TYPE OF GMA SPECIMENS

For each pipe sample the circumference was divided into 8-9 segments where different welding conditions were applied. On some of them butt-welded joints were manufactured according to Welding Procedure Specifications trying to create as much as possible some segments free from defects. These segments, prepared applying optimal welding conditions, were intended as benchmarks for the other segments where welding conditions were different from WPS specifications. Condition different from those prescribed in WPS were supposed to include imperfections inside welded joints. For each welding position these conditions were applied alternatively in the root pass on one pipe sample and on the cap/filler pass on another pipe sample. Power source device was adopted from Fronium company [58] (Figure 45). WPS for GMA welding technology are included in Figure 46: bevelling angle α was set to 50 degrees, filler material is LNM MoNiVa from Lincoln Electric [43] and shielding gas is 20% $C0_2$ in Argon [45] with a flow rate between 12 and 16 l/min. Three welding beads were deposited into the workpiece in the case of vertical welding position and six beads for horizontal welding position. Moreover, after each beads the workpiece was grinded accurately. The arrangement and the properties of the different segments for each of the four pipe specimens are discussed in detail in the next paragraphs.



FIGURE 45: POWER SOURCE DEVICE FOR GMA APPLICATIONS

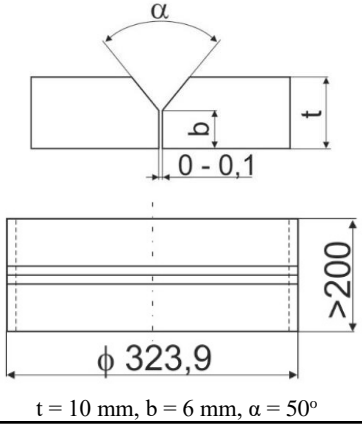
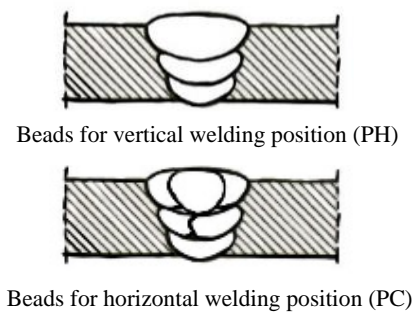
Welding Procedure Specification acc. to EN ISO 15609-1:2019		WPS – GMA - 01																											
Manufacturer: MOSTOSTAL ZABRZE KONSTRUKCJE PRZEMYSŁOWE S.A. Production II : 44-100 Gliwice, 11 Towarowa St.		Welding Process: Metal active gas welding (135) acc. to EN ISO 4063:2011																											
Parent Material Specification: API 5L X80 Wall thickness: 10,0 mm Root face: 6,0 mm Pipe Outside Diameter: 323,9 mm																													
Filler or other additional material classification: AWS A5.28 ER110S-G EN ISO 16834-A G 69 4 M Mn3Ni1CrM LNM MoNiVa Chemical composition [w%] <table style="width: 100%; border-collapse: collapse;"> <tr> <td style="text-align: center;">C</td> <td style="text-align: center;">Mn</td> <td style="text-align: center;">Si</td> <td style="text-align: center;">Ni</td> <td style="text-align: center;">Cr</td> <td style="text-align: center;">Mo</td> <td style="text-align: center;">V</td> <td style="text-align: center;">Cu</td> </tr> <tr> <td style="text-align: center;">0,08</td> <td style="text-align: center;">1,7</td> <td style="text-align: center;">0,44</td> <td style="text-align: center;">1,35</td> <td style="text-align: center;">0,23</td> <td style="text-align: center;">0,3</td> <td style="text-align: center;">0,08</td> <td style="text-align: center;">0,25</td> </tr> </table> Mechanical Properties: <table style="width: 100%; border-collapse: collapse;"> <tr> <td style="text-align: center;">Yield strength [MPa]</td> <td style="text-align: center;">Tensile strength [MPa]</td> <td style="text-align: center;">Elongation [%]</td> </tr> <tr> <td style="text-align: center;">710</td> <td style="text-align: center;">790</td> <td style="text-align: center;">20</td> </tr> </table>								C	Mn	Si	Ni	Cr	Mo	V	Cu	0,08	1,7	0,44	1,35	0,23	0,3	0,08	0,25	Yield strength [MPa]	Tensile strength [MPa]	Elongation [%]	710	790	20
C	Mn	Si	Ni	Cr	Mo	V	Cu																						
0,08	1,7	0,44	1,35	0,23	0,3	0,08	0,25																						
Yield strength [MPa]	Tensile strength [MPa]	Elongation [%]																											
710	790	20																											
Shielding Gas (Acc. to ISO 14175): M21 ArCO ₂ : 20% CO ₂ in Argon Flow rate: 12 ÷ 16 l/min																													
Joint design  <p style="text-align: center;">t = 10 mm, b = 6 mm, $\alpha = 50^\circ$</p>				Weld section 																									
Welding Details																													
Run	Process	Size of filler metal	Current	Voltage	Type of Current	Travel Speed	Heat Input																						
		[mm]	[A]	[V]		[cm/min]	[kJ/cm]																						
Welding Position PC																													
Root pass	135	1,2	100 ÷ 110	16,0 ÷ 19,0	DC	10,0 ÷ 13,0	5,9 ÷ 10,0																						
Layer of filling pass	135	1,2	190 ÷ 220	21,5 ÷ 23,5	DC	28,0 ÷ 34,0	5,8 ÷ 8,9																						
Layer of capping pass	135	1,2	190 ÷ 220	21,5 ÷ 23,5	DC	28,0 ÷ 34,0	5,8 ÷ 8,9																						
Welding Position PH																													
Root pass	135	1,2	90 ÷ 105	16,0 ÷ 18,0	DC	9,0 ÷ 12,0	5,8 ÷ 10,1																						
Layer of filling pass	135	1,2	160 ÷ 180	18,0 ÷ 20,0	DC	22,0 ÷ 28,0	5,0 ÷ 12,3																						
Layer of capping pass	135	1,2	190 ÷ 220	21,5 ÷ 23,5	DC	12,0 ÷ 16,0	8,6 ÷ 14,4																						

FIGURE 46: WPS FOR GMA WELDING TECHNOLOGY [59]

4.1.1.1 GMA1 SPECIMEN

The specimen marked as GMA1 was manufactured adopting Gas Metal Arc Welding Technology and horizontal welding position (PC) with six welding beads. In this case the circumference was divided into nine different segments and desired imperfections, i.e., porosity, undercut, lack of

penetration and lack of fusion, were planned to be reproduced inside the root pass of the welded joint. However, the first two segments of the root pass were manufactured adopting the parameters contained in the Welding Procedure Specification. A complete resume of each segment is reported in Table 9. The pipe specimen is depicted in Figure 47 during the welding process.

GMA1 Root Pass		
Segment Number	Segment code	Segment conditions/Desired imperfection
1	GMA1_1	Optimal Conditions
2	GMA1_2	Optimal Conditions
3	GMA1_3	Porosity
4	GMA1_4	Lack of penetration
5	GMA1_5	Lack of fusion
6	GMA1_6	Undercuts
7	GMA1_7	Porosity
8	GMA1_8	Undercuts
9	GMA1_9	Lack of penetration

TABLE 9: SEGMENTS OF GMA1 ROOT PASS

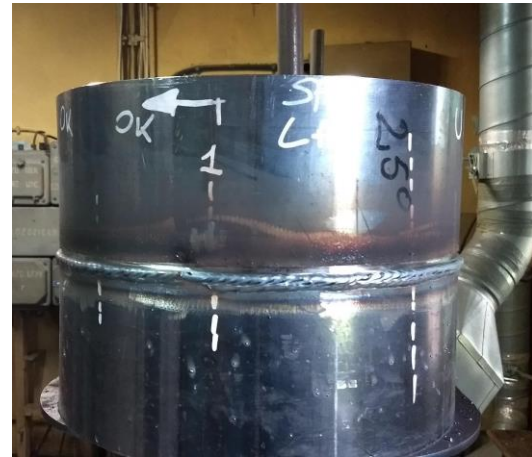


FIGURE 47: GMA1 SPECIMEN DURING MANUFACTURING PROCESS

4.1.1.2 GMA2 SPECIMEN

Similarly to the procedure described in the previous paragraph, the second specimen of the GMA batch (GMA2) was manufactured using Gas Metal Arc welding technology and horizontal welding position (PC). The specimens GMA1 and GMA2 differ from each other for the disposition of the segments manufactured following WPS prescriptions and segments with induced imperfections. On GMA2 pipe specimens the beads with induced imperfection were assigned to the filler or cap passes. Complete resume of each segment is reported in Table 10 and Table 11. A detail of the welded joint of this pipe specimen is depicted in Figure 48.

GMA2 Filler Pass		
Segment Number	Segment code	Segment conditions/Desired imperfection
1	GMA2_1	Porosity
2	GMA2_2	Lack of fusion
3-8	GMA2_3 – GMA2_8	Optimal Conditions

TABLE 10 SEGMENTS OF GMA2 FILLER PASS

GMA2 Cap Pass		
Segment Number	Segment code	Segment conditions/Desired imperfection
1	GMA2_1	Optimal Conditions
2	GMA2_2	Optimal Conditions
3	GMA2_3	Porosity
4	GMA2_4	Undercut



FIGURE 48: GMA2 SPECIMEN DURING MANUFACTURING PROCESS

5	GMA2_5	Lack of fusion
6	GMA2_6	Undercut
7	GMA2_7	Lack of fusion
8	GMA2_8	Porosity

TABLE 11: SEGMENTS OF GMA2 CAP PASS

4.1.1.3 GMA3 SPECIMEN

The specimen marked as GMA3 was manufactured in the same way of GMA1 specimen but vertical welding position instead of horizontal was chosen. Imperfections were planned to be produced inside the root pass of the welded joint, while the filler passes were manufactured in the way that simulate the optimal conditions contained in the Welding Procedure Specification. Complete description of each segment is reported in Table 12 and details of the welded joint of this pipe specimen are depicted in Figure 49.

GMA3 Root Pass		
Segment Number	Segment code	Segment conditions/Desired imperfection
1	GMA3_1	Optimal Conditions
2	GMA3_2	Optimal Conditions
3	GMA3_3	Porosity
4	GMA3_4	Lack of penetration
5	GMA3_5	Lack of fusion
6	GMA3_6	Undercuts
7	GMA3_7	Porosity
8	GMA3_8	Undercuts

TABLE 12: SEGMENTS OF GMA3 ROOT PASS



FIGURE 49: GMA3 SPECIMEN DURING MANUFACTURING PROCESS

4.1.1.4 GMA4 SPECIMEN

The specimen marked as GMA4 had same welding position of GMA3 specimens and the same positions of the imperfections in the filler/cap passes like GMA2 specimen. Complete description of each segment is reported in Table 13 and Table 14. Details of the welded joint of this pipe specimen are depicted in Figure 50.

GMA4 Filler Pass		
Segment Number	Segment code	Segment conditions/Desired imperfection
1-5	GMA4_1 – GMA4_5	Optimal Conditions
6	GMA4_6	Lack of fusion
7	GMA4_7	Porosity
8	GMA8_8	Optimal Conditions

TABLE 13: SEGMENTS OF GMA4 FILLER PASS

GMA4 Cap Pass		
Segment Number	Segment code	Segment conditions/Desired imperfection



FIGURE 50: GMA4 SPECIMEN DURING MANUFACTURING PROCESS

1	GMA4_1	Lack of Fusion
2	GMA4_2	Undercut
3	GMA4_3	Lack of Fusion
4	GMA4_4	Undercut
5	GMA4_5	Porosity
6	GMA4_6	Optimal Conditions
7	GMA4_7	Optimal Conditions
8	GMA4_8	Porosity

TABLE 14: SEGMENTS OF GMA4 CAP PASS

4.1.2 MMA PIPE SPECIMENS

The procedures described in Paragraph 4.1.1 were also applied to the manufacture of MMA pipe specimens. The number and type of each specimen is depicted in Figure 51. The butt-welded joint segments were alternatively manufactured according to the WPS and with non-standard parameters.

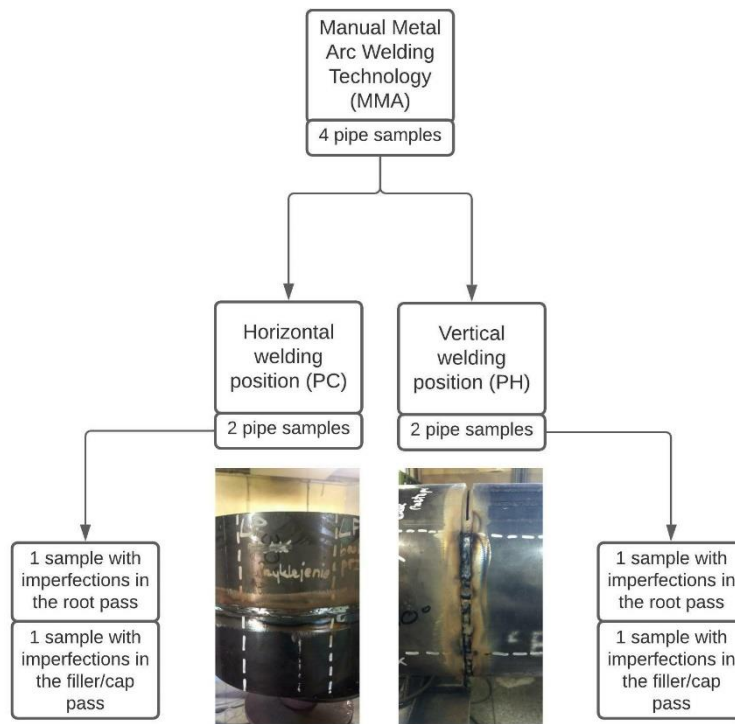


FIGURE 51: NUMBER AND TYPE OF MMA SPECIMENS

Power source device, model Invertec V270, was from Lincoln Electric company (Figure 52). WPS for MMA welding technology are depicted in Figure 53: beveling angle α was set to 60 degrees, filler material electrodes were Conarc 85 from Lincoln Electric. Three welding beads were deposited into the workpiece in the case of vertical welding position and six beads for horizontal welding position. Moreover, after each beads the workpiece was grinded accurately. The arrangement and the properties of the different segments for each of four pipe specimens are discussed in detail in the next paragraphs.



FIGURE 52: POWER SOURCE DEVICE FOR MMA APPLICATIONS

Welding Procedure Specification acc. to EN ISO 15609-1:2019		WPS – MMA - 01						
Manufacturer: MOSTOSTAL ZABRZE KONSTRUKCJE PRZEMYSŁOWE S.A. Production II : 44-100 Gliwice, 11 Towarowa St.		Welding Process: Manual metal arc welding (111) acc. to EN ISO 4063:2011						
Parent Material Specification: API 5L X80 Wall thickness: 10,0 mm Root face: 6,0 mm Pipe Outside Diameter: 323,9 mm								
Filler or other additional material classification: AWS A5.5 18275-A: E69 5 Mn2NiCrMo B 3 2 H5 Conarc 85								
Chemical composition [wt%]								
C	Mn	Si	P	Ni	Mo	Cr		
0,06	1,4	0,3	0,010	2,0	0,4	0,4		
Mechanical Properties:								
Yield strength (0,2%) [MPa]		Tensile strength [MPa]			Elongation [%]			
840		890			20			
Joint design				Weld section				
<p style="text-align: center;">$t = 10 \text{ mm}, b = 6 \text{ mm}, \alpha = 60^\circ$</p>				<p style="text-align: center;">Beads for vertical welding position (PH)</p>				
Welding Details								
Run	Process	Size of filler metal	Current	Voltage	Type of Current	Travel Speed	Heat Input	
		[mm]						[A]
Welding Position PC								
Root pass	111	2,5	65 ÷ 75	21,0 ÷ 23,0	DC	5,0 ÷ 7,0	9,4 ÷ 16,6	
Layer of filling pass	111	3,3	115 ÷ 125	23,0 ÷ 26,0	DC	16,0 ÷ 24,0	5,8 ÷ 9,8	
Layer of capping pass	111	3,2	115 ÷ 125	23,0 ÷ 26,0	DC	16,0 ÷ 24,0	5,5 ÷ 9,8	
Welding Position PH								
Root pass	111	2,5	65 ÷ 75	21,0 ÷ 23,0	DC	3,0 ÷ 5,0	13,1 ÷ 27,6	
Layer of filling pass	111	3,2	110 ÷ 120	23,0 ÷ 26,0	DC	12,0 ÷ 16,0	7,6 ÷ 12,5	
Layer of capping pass	111	3,2	110 ÷ 120	23,0 ÷ 26,0	DC	12,0 ÷ 16,0	7,6 ÷ 12,5	

FIGURE 53: WPS FOR MMA WELDING TECHNOLOGY [59]

4.1.2.1 MMA1 SPECIMEN

The specimen marked as MMA1 was manufactured with the use of Manual Metal Arc Welding and vertical welding position (PH) with three welding passes applied. Imperfections were planned to be induced inside the root pass of the welded joint. The filler and cap passes were manufactured

according to WPS. A complete summary of each segment is reported in Table 15. The pipe specimen is depicted in Figure 54 during the welding process of the root pass.

MMA1 Root Pass		
Segment Number	Segment code	Segment conditions/Desired imperfection
1	MMA1_1	Undercut
2	MMA1_2	Lack of fusion
3	MMA1_3	Optimal Conditions
4	MMA1_4	Porosity
5	MMA1_5	Lack of fusion
6	MMA1_6	Lack of penetration
7	MMA1_7	Undercut
8	MMA1_8	Porosity

TABLE 15: SEGMENTS OF MMA1 ROOT PASS



FIGURE 54: MMA1 SPECIMEN DURING MANUFACTURING PROCESS

4.1.2.2 MMA2 SPECIMEN

The specimen marked as MMA2 is similar to the specimen MM1 regarding welding position PH but it differs for the position of the imperfections. In this case beads with induced imperfections are those placed alongside the filler and cap passes. A complete description of each segment is reported in Table 16 and Table 17. The pipe specimen is depicted in Figure 55 during the welding process.

MMA2 Filler Pass		
Segment Number	Segment code	Segment conditions/Desired imperfection
1	MMA2_1	Lack of Fusion
2	MMA2_2	Porosity
3	MMA2_3	Optimal conditions
4	MMA2_4	Optimal conditions
5	MMA2_5	Optimal Conditions
6	MMA2_6	Optimal Conditions
7	MMA2_7	Optimal Conditions
8	MMA2_8	Optimal Conditions

TABLE 16: SEGMENTS OF MMA2 FILLER PASS

MMA2 Cap Pass		
Segment Number	Segment code	Segment conditions/Desired imperfection
1	MMA2_1	Optimal conditions
2	MMA2_2	Optimal conditions
3	MMA2_3	Porosity
4	MMA2_4	Lack of Fusion
5	MMA2_5	Undercut
6	MMA2_6	Lack of Fusion
7	MMA2_7	Undercut
8	MMA2_8	Porosity

TABLE 17: SEGMENTS OF MMA2 CAP PASS



FIGURE 55: MMA2 SPECIMEN DURING MANUFACTURING PROCESS

4.1.2.3 MMA3 SPECIMEN

To manufacture the pipe marked as MMA3 the Manual Metal Arc Welding and horizontal welding position (PC) with six welding passes was applied. The imperfections were planned to be induced inside root pass of the welded joint while all the segments in the filler and cap passes were manufactured according to WPS. A complete summary of each segment is reported in Table 18. The pipe specimen is depicted in Figure 56 during the welding process.

MMA3 Root Pass		
Segment Number	Segment code	Segment conditions/Desired imperfection
1	MMA3_1	Optimal Conditions
2	MMA3_2	Optimal Conditions
3	MMA3_3	Porosity
4	MMA3_4	Lack of Penetration
5	MMA3_5	Lack of Fusion
6	MMA3_6	Undercut
7	MMA3_7	Porosity
8	MMA3_8	Undercut

TABLE 18: SEGMENTS OF MMA3 ROOT PASS

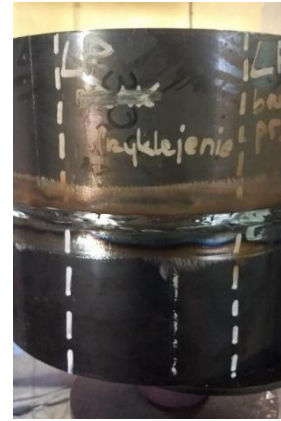


FIGURE 56: MMA3 SPECIMEN DURING MANUFACTURING PROCESS

4.1.2.4 MMA4 SPECIMEN

The specimen marked as MMA4 was manufactured with the same specifics applied for the specimen MMA3 in terms welding position (PC) with six welding passes. The difference was another position of the defective beads. These were planned to be produced inside filler/cap passes of the welded joint while all the segments in the root pass were manufactured according to WPS. A complete characterization of each segment is reported in Table 19 and Table 20. The pipe specimen is depicted in Figure 57 during the welding process.

MMA4 Filler Pass		
Segment Number	Segment code	Segment conditions/Desired imperfection
1	MMA4_1	Porosity
2	MMA4_2	Lack of Fusion
3	MMA4_3	Optimal Conditions
4	MMA4_4	Optimal Conditions
5	MMA4_5	Optimal Conditions
6	MMA4_6	Optimal Conditions
7	MMA4_7	Optimal Conditions
8	MMA4_8	Optimal Conditions

TABLE 19: SEGMENTS OF MMA4 FILLER PASS



FIGURE 57: MMA4 SPECIMEN DURING MANUFACTURING PROCESS

MMA4 Cap Pass		
---------------	--	--

Segment Number	Segment code	Segment conditions/Desired imperfection
1	MMA4_1	Optimal Conditions
2	MMA4_2	Optimal Conditions
3	MMA4_3	Porosity
4	MMA4_4	Undercut
5	MMA4_5	Lack of fusion
6	MMA4_6	Undercut
7	MMA4_7	Lack of fusion
8	MMA4_8	Porosity

TABLE 20: SEGMENTS OF MMA4 CAP PASS

4.1.3 SSA PIPE SPECIMENS

Another set of four pipe specimens was manufactured with the use of Self Shielded Flux Core Wire welding technology (SSA). The number and type of each specimen are characterized in Figure 58. Certain butt-welded joint segments were manufactured according to the WPS while other segments with the application of non-optimal conditions.

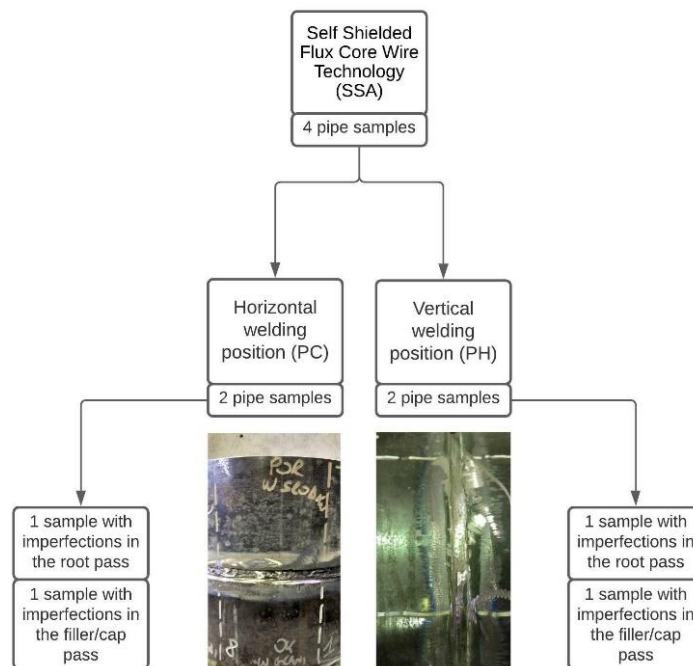


FIGURE 58: NUMBER AND TYPE OF SSA SPECIMENS

I was the power source device Fronium company [58] (Figure 45) that was applied in these experiments. WPS for SSA welding technology are depicted in Figure 59: beveling angle α was set to 60 degrees, filler material was PIPELINER NR-208-XP [60]. Three welding beads were located into the workpiece in the case of vertical welding position and six beads for horizontal welding position. Moreover, after each beads the workpiece was grinded accurately. The arrangement and the

properties of the different segments for each of the four pipe specimens are discussed in details in next paragraphs.

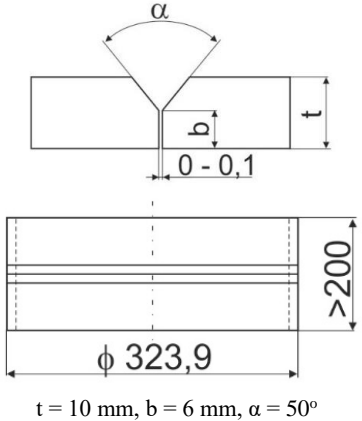
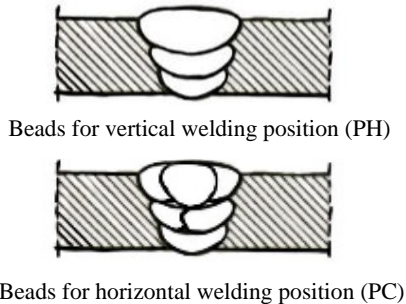
Welding Procedure Specification acc. to EN ISO 15609-1:2019		WPS – SSA - 01																															
Manufacturer: MOSTOSTAL ZABRZE KONSTRUKCJE PRZEMYSŁOWE S.A. Production II : 44-100 Gliwice, 11 Towarowa St.		Welding Process: Self-shielded tubular-cored arc welding (114) acc. to EN ISO 4063:2011																															
Parent Material Specification: API 5L X80 Wall thickness: 10,0 mm Root face: 6,0 mm Pipe Outside Diameter: 323,9 mm																																	
Filler or other additional material classification: AWS A5.29: E81T8-G PIPELINER NR-208-XP Chemical composition [w%] <table style="width: 100%; border-collapse: collapse;"> <tr> <td style="text-align: center;">C</td> <td style="text-align: center;">Mn</td> <td style="text-align: center;">Si</td> <td style="text-align: center;">P</td> <td style="text-align: center;">S</td> <td style="text-align: center;">Ni</td> <td style="text-align: center;">Cr</td> <td style="text-align: center;">Mo</td> <td style="text-align: center;">V</td> <td style="text-align: center;">Al</td> </tr> <tr> <td style="text-align: center;">0,01-0,04</td> <td style="text-align: center;">2,21-2,53</td> <td style="text-align: center;">0,12-0,14</td> <td style="text-align: center;">0,013</td> <td style="text-align: center;">0,003</td> <td style="text-align: center;">1,04-1,26</td> <td style="text-align: center;">0,04-0,7</td> <td style="text-align: center;"><0,02</td> <td style="text-align: center;"><0,006</td> <td style="text-align: center;">0,9-1,2</td> </tr> </table> Mechanical Properties: <table style="width: 100%; border-collapse: collapse;"> <tr> <td style="text-align: center;">Yield strength [MPa]</td> <td style="text-align: center;">Tensile strength [MPa]</td> <td style="text-align: center;">Elongation [%]</td> </tr> <tr> <td style="text-align: center;">500-550</td> <td style="text-align: center;">575-615</td> <td style="text-align: center;">21-28</td> </tr> </table>								C	Mn	Si	P	S	Ni	Cr	Mo	V	Al	0,01-0,04	2,21-2,53	0,12-0,14	0,013	0,003	1,04-1,26	0,04-0,7	<0,02	<0,006	0,9-1,2	Yield strength [MPa]	Tensile strength [MPa]	Elongation [%]	500-550	575-615	21-28
C	Mn	Si	P	S	Ni	Cr	Mo	V	Al																								
0,01-0,04	2,21-2,53	0,12-0,14	0,013	0,003	1,04-1,26	0,04-0,7	<0,02	<0,006	0,9-1,2																								
Yield strength [MPa]	Tensile strength [MPa]	Elongation [%]																															
500-550	575-615	21-28																															
Joint design  <p style="text-align: center;">$t = 10 \text{ mm}, b = 6 \text{ mm}, \alpha = 50^\circ$</p>				Weld section  <p style="text-align: center;">Beads for vertical welding position (PH)</p> <p style="text-align: center;">Beads for horizontal welding position (PC)</p>																													
Welding Details																																	
Run	Process	Size of filler metal	Current	Voltage	Type of Current	Travel Speed	Heat Input																										
		[mm]						[A]	[V]	[cm/min]	[kJ/cm]																						
Welding Position PC																																	
Root pass	114	2,0	110 ÷ 120	16,0 ÷ 19,0	DC	8,0 ÷ 12,0	7,0 ÷ 13,7																										
Layer of filling pass	114	2,0	180 ÷ 200	21,0 ÷ 24,0	DC	25,0 ÷ 35,0	5,2 ÷ 9,2																										
Layer of capping pass	114	2,0	180 ÷ 200	21,0 ÷ 24,0	DC	25,0 ÷ 35,0	5,2 ÷ 9,2																										
Welding Position PH																																	
Root pass	114	2,0	110 ÷ 120	16,0 ÷ 19,0	DC	7,0 ÷ 9,0	9,4 ÷ 15,6																										
Layer of filling pass	114	2,0	150 ÷ 170	20,0 ÷ 23,0	DC	15,0 ÷ 20,0	7,2 ÷ 12,5																										
Layer of capping pass	114	2,0	150 ÷ 170	20,0 ÷ 23,0	DC	15,0 ÷ 20,0	7,2 ÷ 12,5																										

FIGURE 59: WPS FOR SSA WELDING TECHNOLOGY [59]

4.1.3.1 SSA1 SPECIMEN

The specimen marked as SSA1 was manufactured with the use of Self Shielded Flux Core Wire welding technology and horizontal welding position (PC) with six welding passes. In this case the circumference was divided into eight different segments and imperfections were designed to be induced inside the root pass of the welded joint. The filler and cap passes were manufactured according to WPS. The complete characteristics of each segment are reported in Table 21. The pipe specimen is depicted in Figure 60 during the welding process of the root pass.

SSA1 Root Pass		
Segment Number	Segment code	Segment conditions/Desired imperfection
1	SSA1_1	Optimal Conditions
2	SSA1_2	Optimal Conditions
3	SSA1_3	Porosity
4	SSA1_4	Lack of Penetration
5	SSA1_5	Lack of Fusion
6	SSA1_6	Undercut
7	SSA1_7	Porosity
8	SSA1_8	Undercut

TABLE 21: SEGMENTS OF SSA1 ROOT PASS



FIGURE 60: SSA1 SPECIMEN DURING MANUFACTURING PROCESS

4.1.3.2 SSA2 SPECIMEN

The specimen marked as SSA2 was also manufactured with the use of Self Shielded Flux Core Wire welding technology and horizontal welding position (PC). Imperfections were planned to be induced inside the cap/filler passes of the welded joint instead of inside root weld bead. A complete description of each segment is reported in Table 22 and Table 23. The pipe specimen is depicted in Figure 61 during the welding process of the root pass.

SSA2 Filler Pass		
Segment Number	Segment code	Segment conditions/Desired imperfection
1	SSA2_1	Optimal Conditions
2	SSA2_2	Optimal Conditions
3	SSA2_3	Optimal Conditions
4	SSA2_4	Optimal Conditions
5	SSA2_5	Optimal Conditions
6	SSA2_6	Optimal Conditions
7	SSA2_7	Lack of Fusion
8	SSA2_8	Porosity

TABLE 22: SEGMENTS OF SSA2 FILLER PASS

SSA2 Cap Pass		
Segment Number	Segment code	Segment conditions/Desired imperfection
1	SSA2_1	Lack of Fusion
2	SSA2_2	Undercut
3	SSA2_3	Lack of Fusion
4	SSA2_4	Porosity
5	SSA2_5	Undercut
6	SSA2_6	Porosity
7	SSA2_7	Optimal Conditions
8	SSA2_8	Optimal Conditions

TABLE 23: SEGMENTS OF SSA2 CAP PASS



FIGURE 61: SSA2 SPECIMEN DURING MANUFACTURING PROCESS

4.1.3.3 SSA3 SPECIMEN

The specimen marked as SSA3 was manufactured with the application of Self Shielded Flux Core Wire welding technology and vertical welding position (PH) with three welding passes. The position of the imperfections inside the welded joints follows the same scheme that was used for SSA1 pipe. Imperfections were in fact planned to be induced inside the root pass of the welded joint. The filler/cap passes were manufactured according to WPS. A complete description of each segment is reported in Table 24. The pipe specimen is depicted in Figure 62 during the welding process of the root pass.

SSA3 Root Pass		
Segment Number	Segment code	Segment conditions/Desired imperfection
1	SSA3_1	Optimal Conditions
2	SSA3_2	Optimal Conditions
3	SSA3_3	Porosity
4	SSA3_4	Lack of Penetration
5	SSA3_5	Lack of Fusion
6	SSA3_6	Undercut
7	SSA3_7	Porosity
8	SSA3_8	Undercut

TABLE 24: SEGMENTS OF SSA3 ROOT PASS



FIGURE 62: SSA3 SPECIMEN DURING MANUFACTURING PROCESS

4.1.3.4 SSA4 SPECIMEN

The last specimen, which was marked as SSA4, was manufactured with the use of Self Shielded Flux Core Wire welding technology and vertical welding position (PH) like SSA3 specimen. The difference between these two pipes consisted in the different layout of the weld beads. In the SSA4

pipe the defects were placed inside filler/cap beads instead of the root pass of SSA3 specimen. A complete characterization of each segment is reported in Table 25 and Table 26. The pipe specimen is depicted in Figure 63 during the welding process of the root pass.

SSA4 Filler Pass		
Segment Number	Segment code	Segment conditions/Desired imperfection
1	SSA4_1	Optimal Conditions
2	SSA4_2	Optimal Conditions
3	SSA4_3	Optimal Conditions
4	SSA4_4	Optimal Conditions
5	SSA4_5	Optimal Conditions
6	SSA4_6	Optimal Conditions
7	SSA4_7	Undercut
8	SSA4_8	Porosity

TABLE 25: SEGMENTS OF SSA4 FILLER PASS

SSA4 Cap Pass		
Segment Number	Segment code	Segment conditions/Desired imperfection
1	SSA4_1	Undercut
2	SSA4_2	Lack of Fusion
3	SSA4_3	Undercut
4	SSA4_4	Porosity
5	SSA4_5	Lack of Fusion
6	SSA4_6	Porosity
7	SSA4_7	Optimal Conditions
8	SSA4_8	Optimal Conditions

TABLE 26: SEGMENTS OF SSA4 CAP PASS



FIGURE 63: SSA4 SPECIMEN DURING MANUFACTURING PROCESS

4.2 SPECIMENS WITH OPTIMAL QUALITY ACCEPTANCE LEVEL

The second part of the experimental activity (Figure 64) was devoted to the preparation of additional butt-welded joint pipe samples with optimal quality acceptance levels that subsequently were submitted to impact load test. The preliminary procedures were the same as those adopted for the previous pipe specimens manufacturing: two pipe sections of 12''^{3/4} diameter and 20-25 cm long were bevelled and then clamped together before being welded. Subsequently the first group of four pipes was manufactured adopting the same welding technologies as in the previous experimental activity step, i.e., GMA, MMA and SSA (Figure 65). An additional pipe specimen was manufactured adopting hybrid welding technology; this method consists of two steps welding process: the root pass of the butt-welded joint is manufactured using laser welding technology, while the following groove passes gas metal arc welding technology.

The pipes belonging to the first batch were entirely manufactured at Mostostal Zabrze laboratories while the root pass of the second group of pipes was manufactured in Łukasiewicz Research Network

– Institute of Welding [61] located in Gliwice. These pipes were then moved to Mostostal Zabrze welding department for the final treatment of the groove passes using GMA.

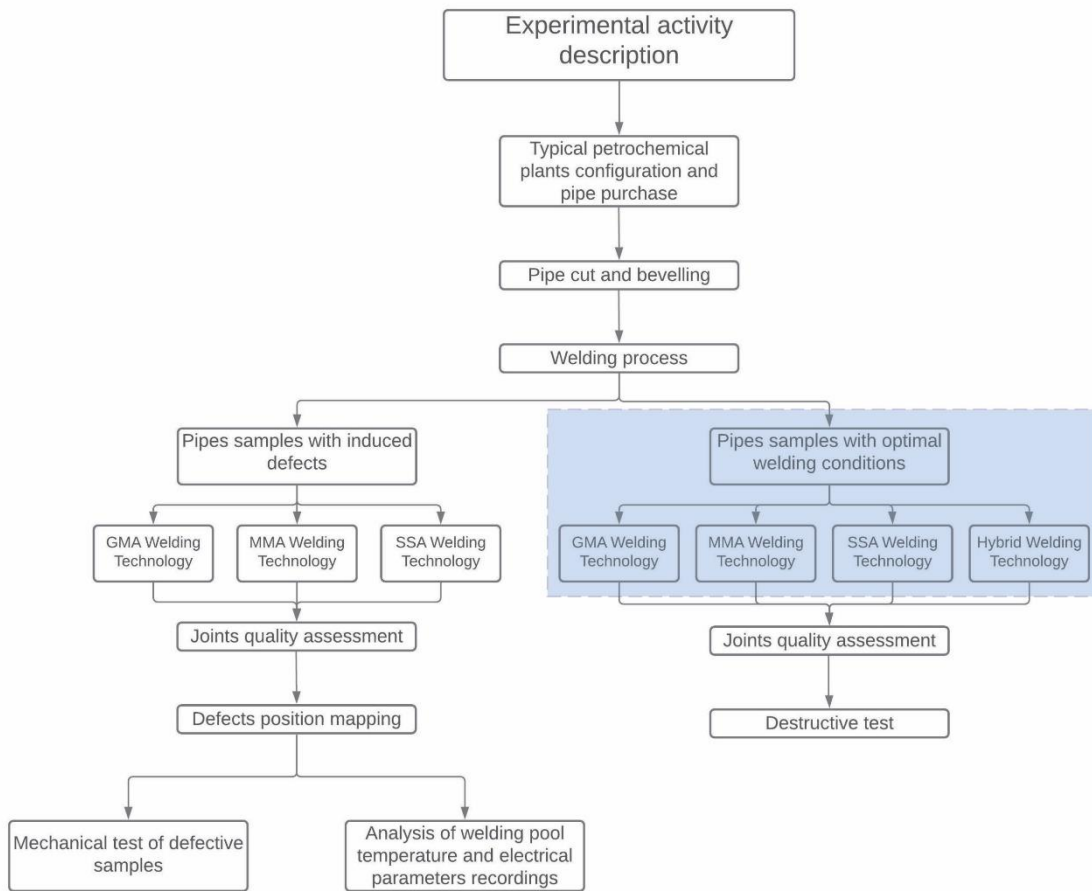


FIGURE 64: DETAIL OF EXPERIMENTAL ACTIVITY PERFORMED FOR PIPES WITH OPTIMAL QUALITY LEVELS

4.2.1 GMA, MMA, SSA PIPE SPECIMENS

The pipe samples which were required for the impact load tests and manufactured with traditional welding technologies were prepared in Mostostal Zabrze laboratories following Welding Procedure Specifications (WPS) described in paragraphs 4.1.1, 4.1.2 and 4.1.3. The goal of these procedures was to achieve the best quality acceptance level for each joint, what let us to reduce the likelihood to introduce possible imperfections inside the welded material. This process was meant to create samples analogous to pipes usually used for oil and gas applications in real conditions. The similarities of the quality requirements to the regularly required in petrochemical installations was based on EN ISO 5817 [62] and EN 12732 [63] standards. The number of pipes produced during this phase is presented in Figure 65.

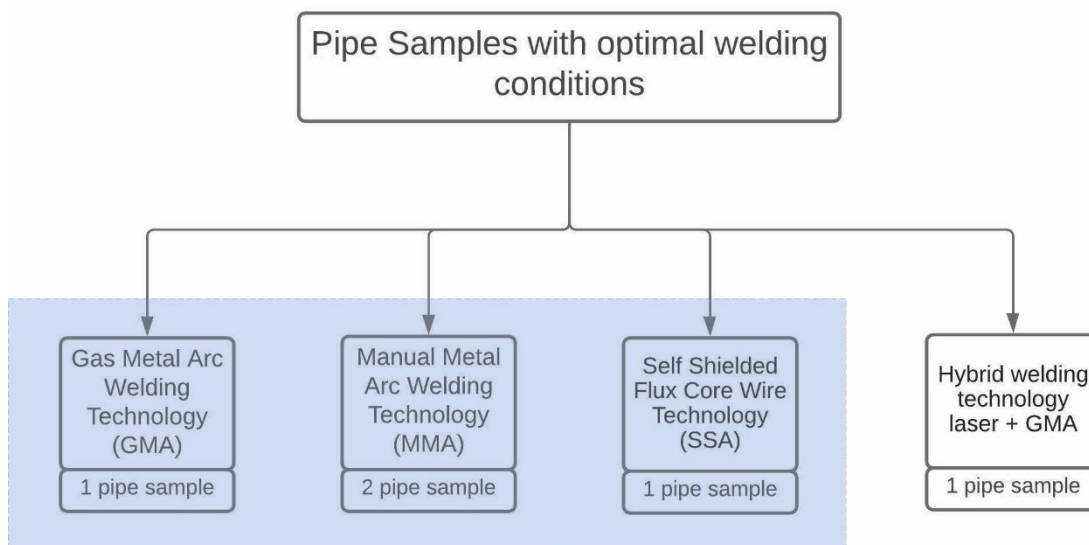


FIGURE 65: TYPE AND NUMBER OF SAMPLES WELDED USING TRADITIONAL METHODS

4.2.2 HYBRID WELDING TECHNOLOGY PIPE SPECIMENS

This procedure was essentially divided into two different stages: the first stage, necessary to produce the root pass was performed in Łukasiewicz Research Network – Institute of Welding, while the latter took place in the laboratories of Mostostal Zabrze where each welded joint was completed with the depositing of filler and cap passes using GMA welding technology.

The preliminary activity necessary to properly prepare the pipe for joining process was the single V shape bevelling of pipes ending sections. The shape and dimensions of the bevelling are presented in Figure 66. The values of root face thickness b , root opening and groove angle α were respectively equal to 6 mm, 0,1 mm and 60° . In the same WPS report it is also included the type of equipment necessary for the correct implementation of the welding process. The procedure took place inside a TruLaser Robot 5120 station (Figure 67) using Kuka robot KR30HA with rotational - tilting positioners KUKA DKP-400 (Figure 68). The laser source was provided by a Yb:YAG TruDisk 12002 [64] device and the laser beam is delivered by a 400 μm fibre optic cable.

Welding Procedure Specification acc. to EN ISO 15609-4:2019	WPS 01LB/IS/B4/301/2019
Manufacturer: ŁUKASIEWICZ - INSTYTUT SPAWALNICTWA 44-100 Gliwice, Bł. Czesława Str. 16-18	Welding Process: solid state laser welding (521) acc. to EN ISO 4063:2011
Parent Material Specification: API 5L X80 Wall thickness: 10,0 mm Root face: 6,0 mm Pipe Outside Diameter: 323,9 mm	

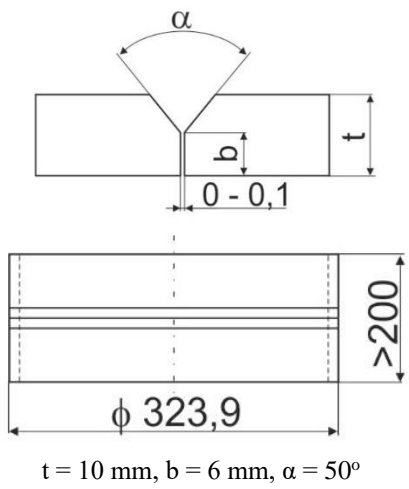
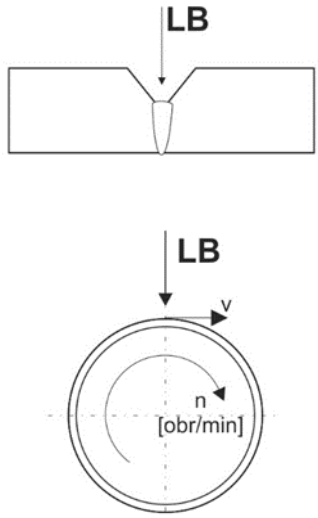
Equipment identification: TruLaser Robot 5120 station (Figure 67) Kuka robot KR30HA with rotational - tilting positioners KUKA DKP-400 (Figure 68) Laser System: TruDisk 12002 Beam Delivery System: fiber 300 μm LLK-D Beam Focusing System: TRUMPF D70	
Beam quality: BPP $\leq 12\text{mm}\cdot\text{mrad}$ Beam Polarisation: random Plasma Suppression Gas System: no Plasma Shielding Gas System: Argon Filler Material Feeding System: no	
Joint design  <p>$t = 10 \text{ mm}, b = 6 \text{ mm}, \alpha = 50^\circ$</p>	Welding technique 

FIGURE 66: WPS FOR LASER WELDING TECHNOLOGY



FIGURE 67 TRULASER ROBOT 5120 STATION [62]



FIGURE 68: KUKA ROBOT KR30HA

Before starting the laser welding process, it was necessary to assess the best operating characteristics for the correct and flawless manufacturing of the root pass. The relevant parameters can be associated with three different categories:

- beam properties, which include power and wavelength of the laser beam
- mechanical equipment properties, which include the speed of the robotic head above the workpiece
- shroud gas properties, which define the composition and usage of the shielding gas.

The combination of these parameters can give in the results different outputs in terms of quality of the joint, penetration, presence of imperfections and required resistance to design loads. For this reason, preliminary tests were carried on. The goal was to establish the best set of parameters that could be applied to the pipe specimens. These tests were performed on a 10 mm thick X80 grade steel plate (Figure 69) applying different values of power, travel speed and focus. These tests were arranged in four series with constant travel speed and five different values of power for a total of twenty configurations.



FIGURE 69: PRELIMINARY TESTS ON THE STEEL PLATE

The first series presented in Table 27 was characterized by constant travel speed value of 1,5 m/min, focus position above the surface set to 0 mm and five different levels of power in the range from 2 kW to 6 kW.

Test laser welding configurations
Fibre delivery system: 300 μ m
Focus distance 300 mm
Beam dimension: 0,45 mm
Shielding gas: Ar 10-12 l/min

Series #1			
Configuration number	Power [W]	Travel speed [m/min]	Focus position[mm]
2	2000	1,5	0
3	3000	1,5	0
4	4000	1,5	0
5	5000	1,5	0
6	6000	1,5	0

TABLE 27: TEST SERIES #1

The second series (Table 28) had similar configuration as the first series except of the travel speed value, in this specific case set at 2 m/min level.

Test laser welding configurations			
Fibre delivery system: 300 μ m			
Focus distance 300 mm			
Beam dimension: 0,45 mm			
Shielding gas: Ar 10-12 l/min			
Series #2			
Configuration number	Power [W]	Travel speed [m/min]	Focus position[mm]
22	2000	2,0	0
23	3000	2,0	0
24	4000	2,0	0
25	5000	2,0	0
26	6000	2,0	0

TABLE 28: TEST SERIES #2

The third series differs from the previous two for the travel speed selection: in this case the value equals to 2,5 m/min as described in Table 29 was selected.

Test laser welding configurations			
Fibre delivery system: 300 μ m			
Focus distance 300 mm			
Beam dimension: 0,45 mm			
Shielding gas: Ar 10-12 l/min			
Series #3			
Configuration number	Power [W]	Travel speed [m/min]	Focus position[mm]
32	2000	2,0	0
33	3000	2,0	0
34	4000	2,0	0
35	5000	2,0	0
36	6000	2,0	0

TABLE 29: TEST SERIES #3

For the last series of tests, the decision was to adopt a procedure where the focus position was not on the surface of the parent material, but it was pointed three mm inside the plate. The travel speed was constant and equal to 2 m/min and the power value was variable and changed from 2 kW to 6 kW (Table 30).

Test laser welding configurations			
Fibre delivery system: 300 μ m			

Focus distance 300 mm
 Beam dimension: 0,45 mm
 Shielding gas: Ar 10-12 l/min

Series #4			
Configuration number	Power [W]	Travel speed [m/min]	Focus position[mm]
42	2000	2,0	-3,0
43	3000	2,0	-3,0
44	4000	2,0	-3,0
45	5000	2,0	-3,0
46	6000	2,0	-3,0

TABLE 30: TEST SERIES #4

The next step was extraction of samples cross sections from all of twenty segments of melted material. All these sections were subjected to macro examination necessary to assess the quality of the fusion. The results of this procedure with the specimens obtained from the configuration number 2 and 6 for all four series are depicted in Figure 70 - Figure 73. It can be observed that different configurations produce different levels of penetration and therefore the possibility to achieve the complete fusion of the root section of the planned hybrid welded joints.

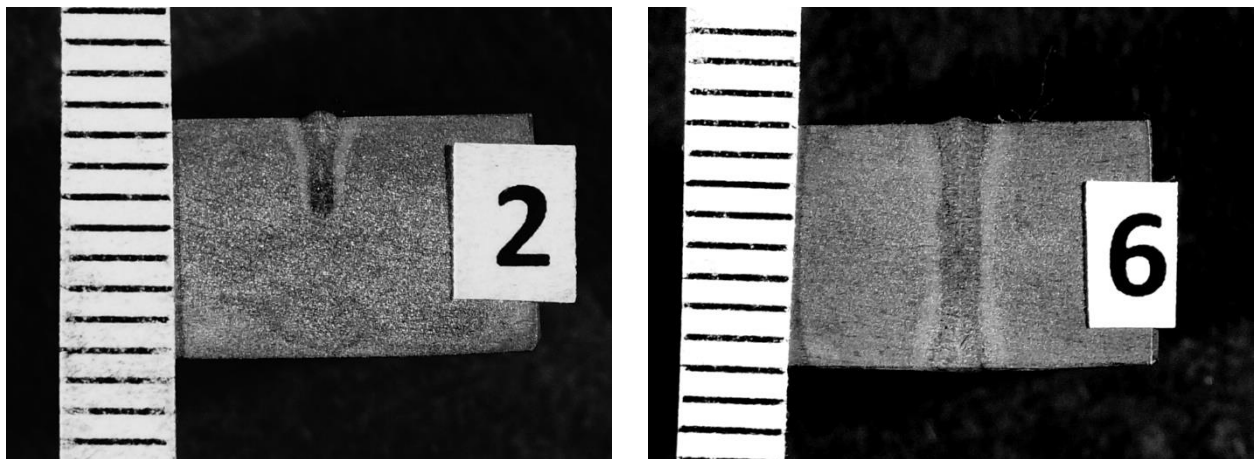


FIGURE 70: MACRO EXAMINATION OF SERIES #1

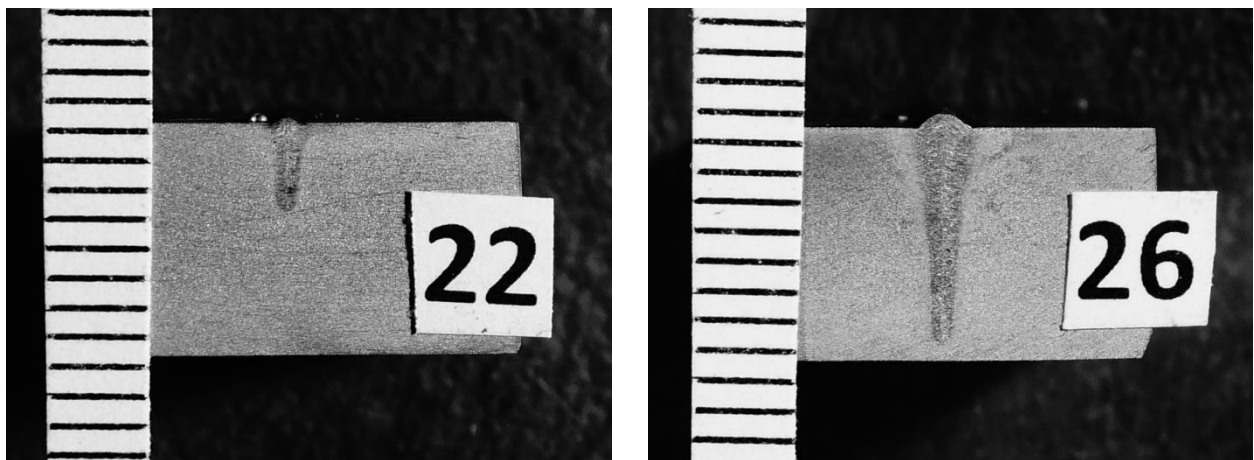


FIGURE 71: MACRO EXAMINATION OF SERIES #2

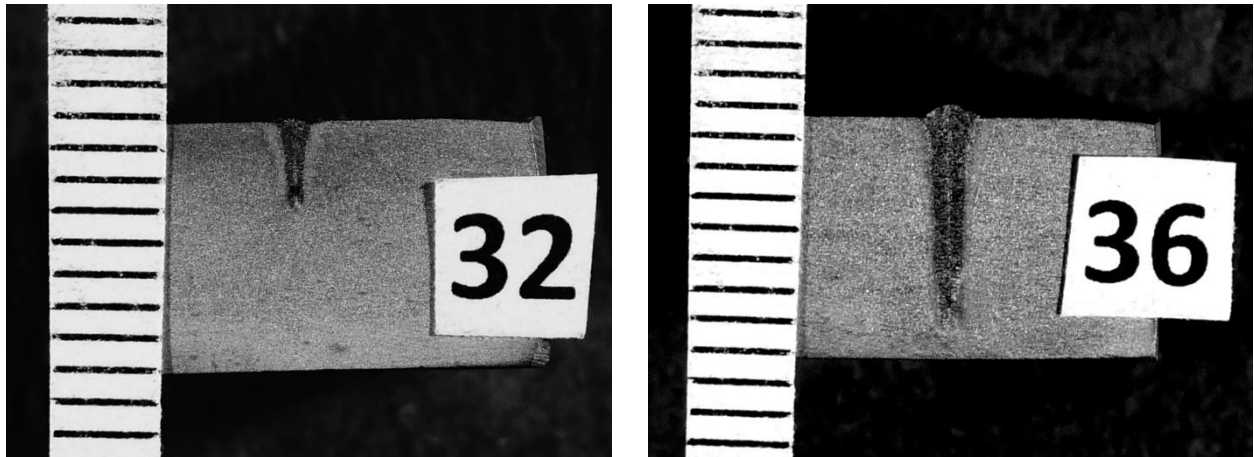


FIGURE 72: MACRO EXAMINATION OF SERIES #3

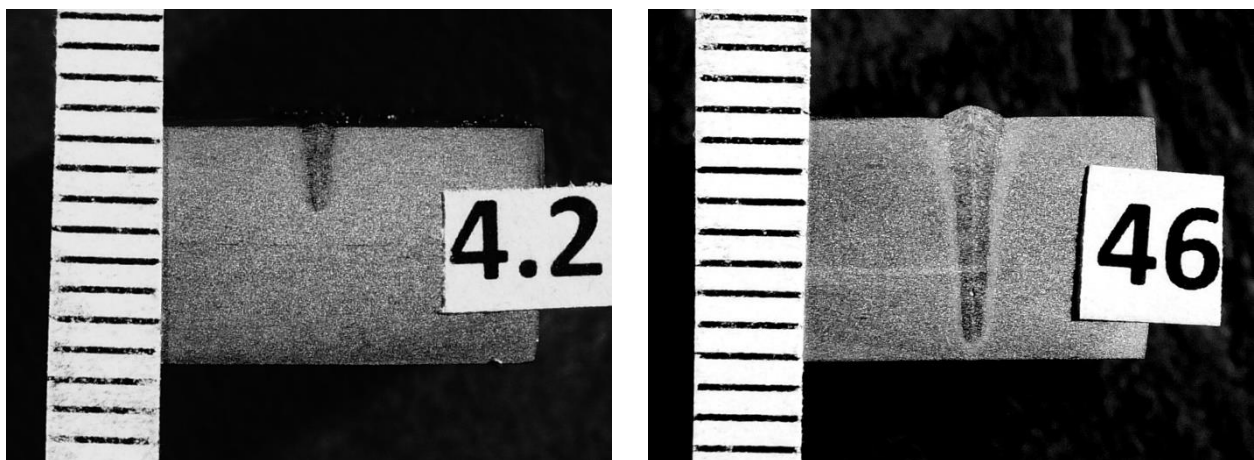


FIGURE 73: MACRO EXAMINATION OF SERIES #4

The assessment of quality of all presented cases on the macro examinations led to the decision to adopt the parameters used for the combination number 25. The effects of this choice were analysed based on samples acquired from the pipe. In Figure 74 the cross section of the pipe sample showing macrostructural properties as well penetration depth of the root pass of the welded joint is presented.

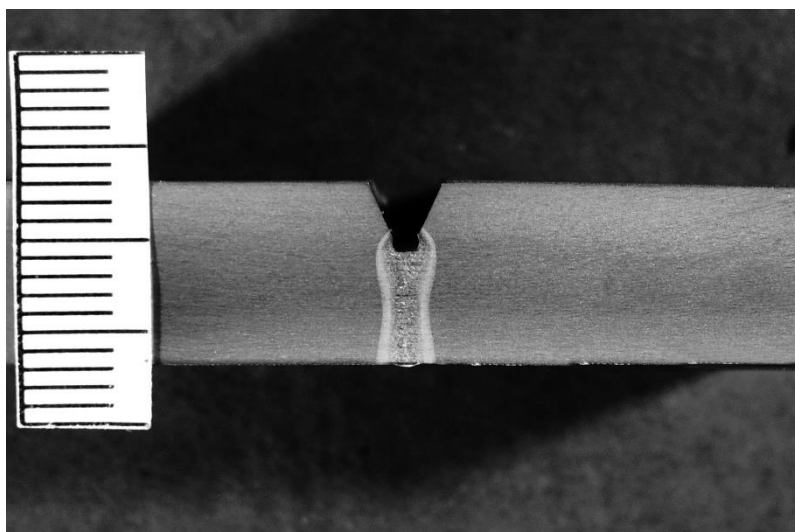


FIGURE 74: MACRO EXAMINATION OF X80 PIPE SECTION

Additionally, the same sample was tested with the use of radiographic analysis that allowed to detect possible defects. The result of this test is shown in Figure 75 where the absence of unwanted imperfections inside the joint area can be observed. They are visible in Figure 76, where the melted metal includes micro-pores. This case refers to the set of parameters number 15.

The pipes were moved to the laboratory of Mostostal Zabrze where the missing groove passes, manufactured according to the welding procedure specification for GMA welding technology, were added. Radiographic examinations were also carried out at the end of the gas metal arc welding process assessing the whole quality of the joint before the subsequent impact load tests.



FIGURE 75: RADIOGRAPHIC TEST OF LASER ROOT PASS FOR COMBINATION 25



FIGURE 76: RADIOGRAPHIC TEST OF LASER ROOT PASS FOR COMBINATION 15

5 QUALITY ASSESSMENT OF DEFECTIVE SAMPLES

The next step of the experimental activity, (Figure 77) was the inspection of the butt-welded joints to assess quality of the joint and detect possible imperfections. Visual inspection and radiographic tests were carried out allowing to determine the type, the magnitude, and the exact position of the imperfections.

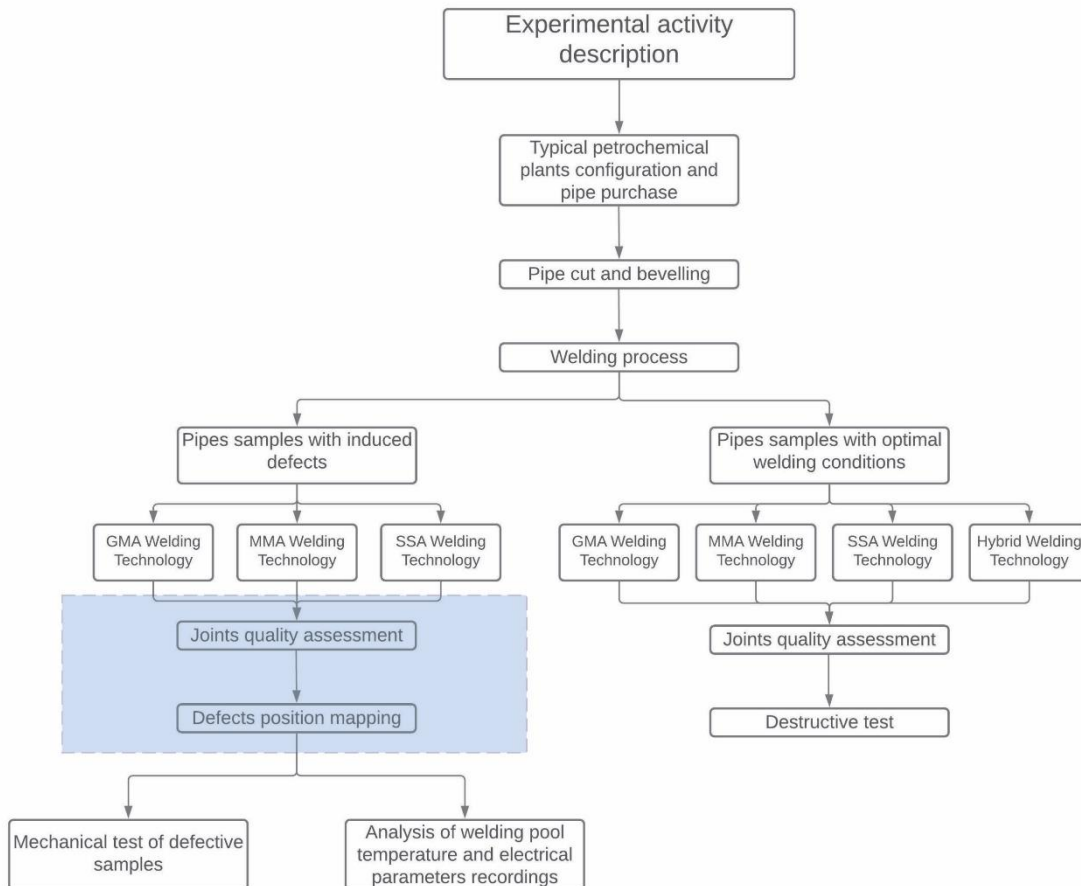


FIGURE 77: EXPERIMENTAL ACTIVITY STAGE

Radiographic test was the primary examination method employed for this purpose. All pipe samples were tested along the circumference of the welded joint. The radiographic tests were also performed at Mostostal Zabrze laboratories following the prescriptions of ISO 17636-1 [65] and the defects were classified according to ISO 6520-1:2007 [66]. The tests were performed using the portable gas-filled tube head x-ray emitter depicted in Figure 78 with the radiation energy set at 190 kV and the current set at 13 mAmin. A single wall exposure setup (Figure 79) was adopted with target to film distance of 450 mm.



FIGURE 78: X-RAY EMITTER

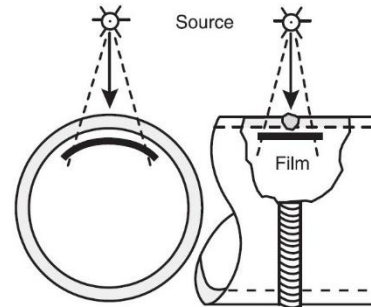
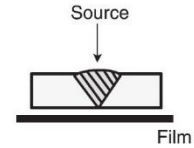


FIGURE 79: SIGLE WALL EXPOSURE SETUP [56]

The type of defects detected during this analysis are listed in Figure 80. A specific colour to better highlight them on the X-rays films displayed in the next paragraphs was assigned.

Defects Legend

Gas Pores (2011)
 Distributed Porosity (2012)
 Cluster Porosity (2013)
 Linear Porosity (2014)

Continuous Undercut (5011)
 Undercut (5012)
 Intermittent Undercut (5012)

Lack of Penetration (402)

Worm holes (2016)

Root Concavity (515)

Incomplete Filled Groove (511)

Elongated Cavity (2015)

Metallic Inclusion (3041)

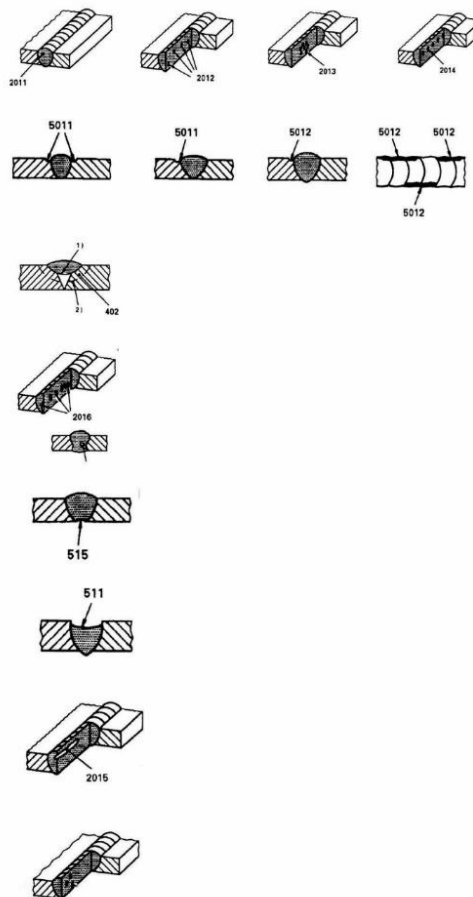


FIGURE 80: LIST OF DEFECTS DETECTED INSIDE THE BUTT-WELDED JOINTS

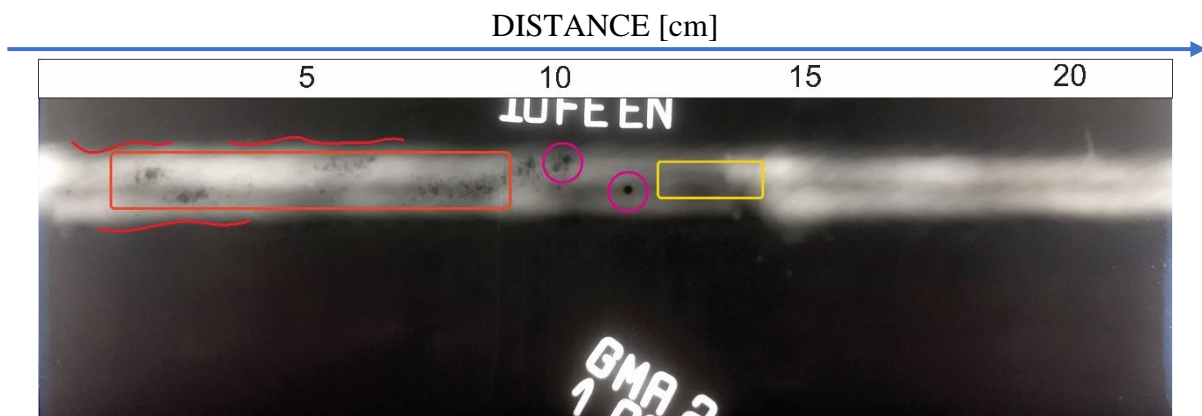
The complete resume of the results obtained from the radiographic inspection is included in the appendix at the end of this thesis. Summary of this research with selected results are discussed in the next paragraph. They are specific cases where the defects were particularly severe and that led to the failure of the welded joint during the destructive tests. The case studies selected belongs to the pipe specimens marked GMA2, GMA3 and MMA1.

5.1 DEFECTS DETECTED ON GMA2 PIPE SPECIMEN

The pipe specimen was manufactured using gas metal welding technology with horizontal welding position (PC). The variety of defects detected along the butt-welded joint is listed in Table 31. The table includes the type of defect detected, its position along the circumference and the name assigned to the portion of the segment that includes the defect for the subsequent mechanical tests. The X-ray films obtained from the radiographic tests are presented in Figure 81. In each film the defects are highlighted using the colours presented in Figure 80.

Defect detected	Position along the circumference [cm]	Section name
Intermittent Undercut (5012) + Uniformly Distributed Porosity (2012)	3	1_G2
Intermittent Undercut (5012) + Uniformly Distributed Porosity (2012)	9	2_G2
Root Concavity (515)	14	3_G2
Distributed Porosity (2012) + Worm holes (2016)	35	4_G2
Distributed Porosity (2012) + Worm holes (2016)	44	5_G2
Incomplete Filled Groove (511) + Gas Pores (2011)	51	6_G2
Lack of Penetration (402) + Gas Pores (2011)	72	7_G2
Lack of Penetration (402) + Gas Pores (2011)	78	8_G2
Cluster Porosity (2013)	93	9_G2

TABLE 31: LIST OF DEFECTS INCLUDED IN GMA2



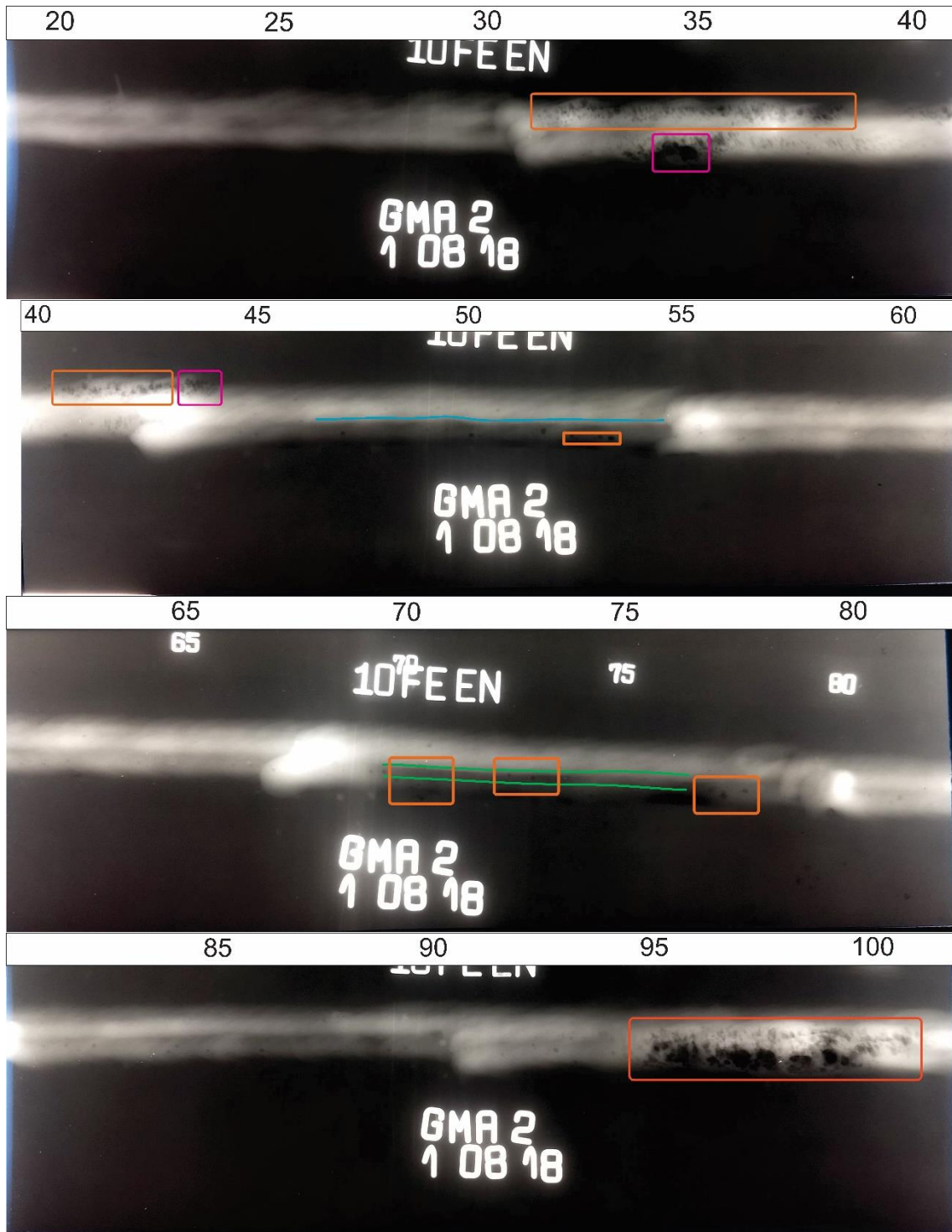


FIGURE 81: RADIOGRAPHIC INSPECTION OF GMA2 PIPE

5.2 DEFECTS DETECTED ON GMA3 PIPE SPECIMEN

This second pipe sample selected as case study was manufactured adopting Gas Metal Arc welding technology and vertical welding position (PH). In the same way as in the previous paragraph the various defects detected were classified and their position along the circumference was recorded for the subsequent mechanical tests. This information is included in Table 32.

Defect detected	Position along the circumference [cm]	Section name
Cluster Porosity (2013)	34	1_G3
Lack of Penetration (402)	43	2_G3
Lack of Penetration (402)	50	3_G3
Lack of Penetration (402)	56	4_G3
Lack of Penetration (402)	67	5_G3
Cluster Porosity (2013) + Worm holes	78	6_G3
Cluster Porosity (2013) + Worm holes	87	7_G3
Lack of Penetration (402)	93	8_G3

TABLE 32: LIST OF DEFECTS INCLUDED IN GMA3

The X-Ray films showing the results of the radiographic test performed on this pipe sample is presented in Figure 82.



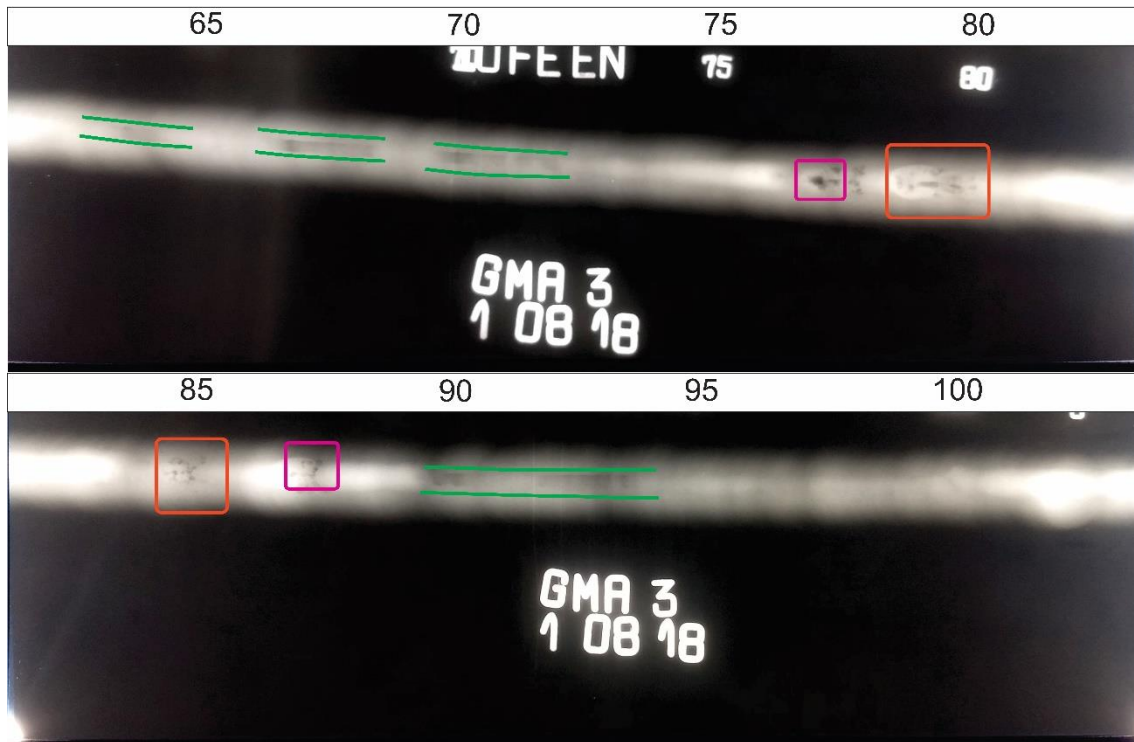


FIGURE 82: RADIOGRAPHIC INSPECTION OF GMA3 PIPE

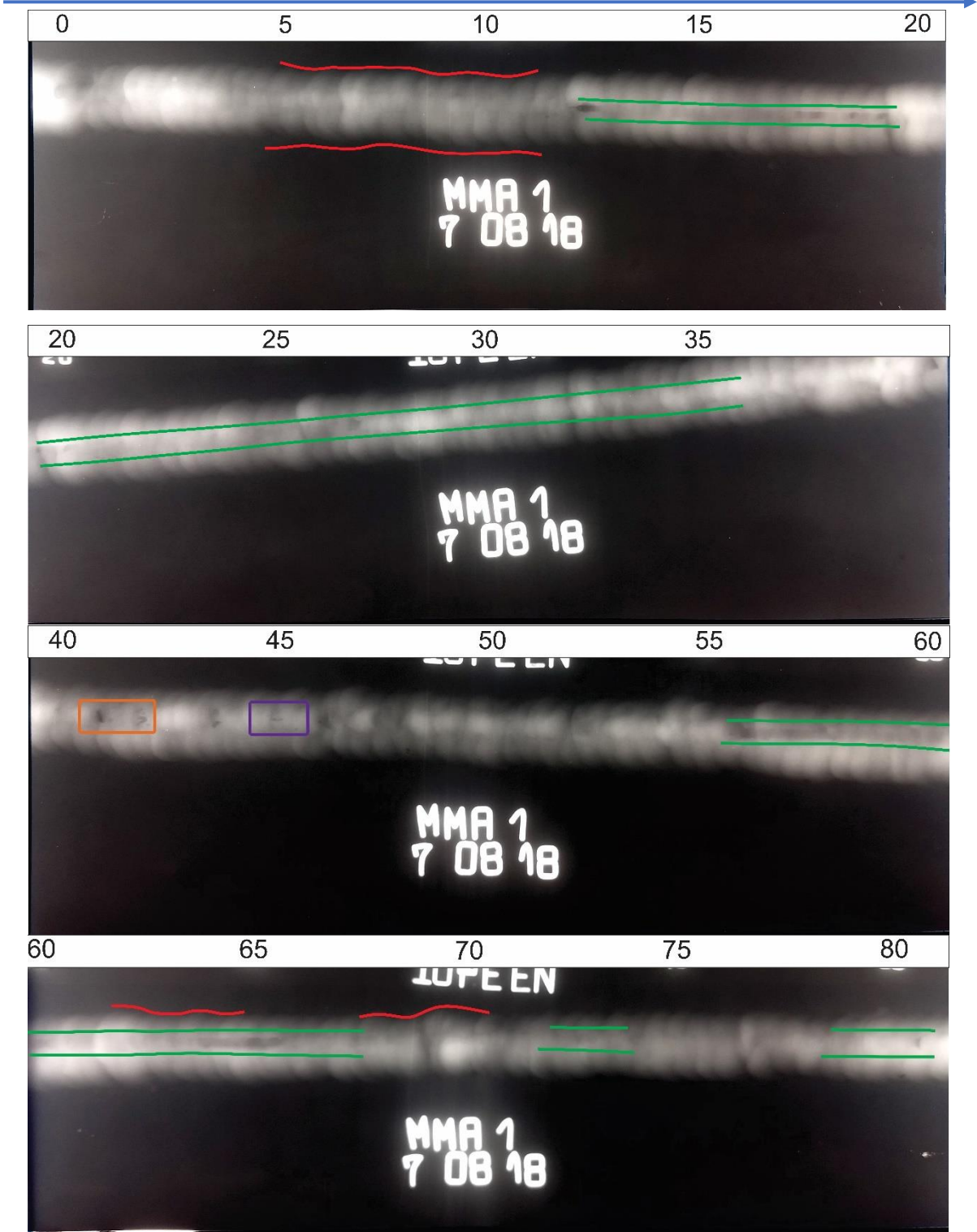
5.3 DEFECTS DETECTED ON MMA1 PIPE SPECIMEN

The last specimen selected as case study is the pipe marked MMA1. This pipe sample was manufactured using Manual Metal Arc welding technology at vertical welding position (PH). The list of the defects detected along the length of the butt-welded joint is included in Table 33. The X-Ray films showing the distribution of the defects are depicted in Figure 83.

Defect detected	Position along the circumference [cm]	Section name
Intermittent Undercut (5012)	5	1_G3
Lack of Penetration (402)	13	2_G3
Lack of Penetration (402)	19	3_G3
Lack of Penetration (402)	25	4_G3
Lack of Penetration (402)	31	5_G3
Lack of Penetration (402)	36	6_G3
Elongated Cavity (2015)	45	7_G3
Lack of Penetration (402)	56	8_G3
Intermittent Undercut (5012) + Lack of Penetration (402)	65	9_G3
Intermittent Undercut (5012) + Lack of Penetration (402)	72	10_G3
Intermittent Undercut (5012) + Lack of Penetration (402)	77	11_G3
Intermittent Undercut (5012) + Lack of Penetration (402)	85	12_G3
Intermittent Undercut (5012) + Lack of Penetration (402)	92	13_G3

TABLE 33: LIST OF DEFECTS INCLUDED IN MMA1

DISTANCE [cm]



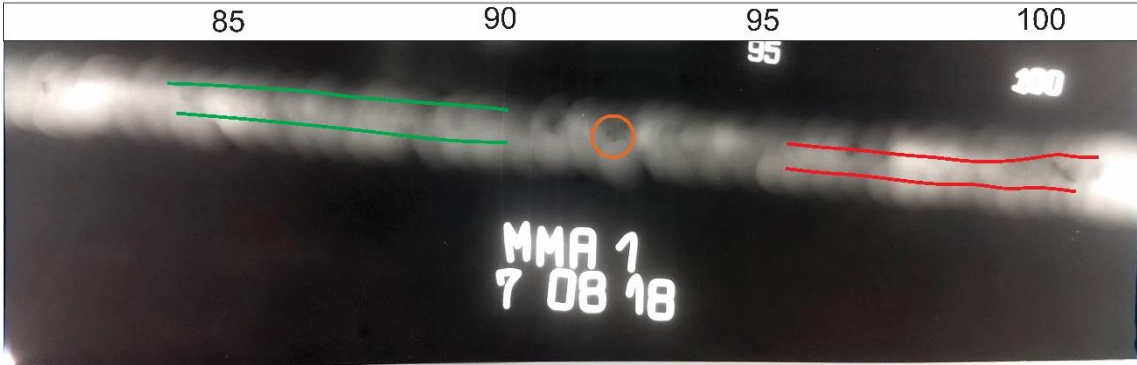


FIGURE 83: RADIOGRAPHIC INSPECTION OF MMA1 PIPE

6 DESTRUCTIVE TEST OF THE PIPE SAMPLES

One of the main goals of the research described in this thesis is to assess the performances of butt-welded joint high strength steel pipes under extreme loadings and therefore validate the possible applications of this type of elements on petrochemical plants. As discussed in the previous chapters two different types of pipe specimens were manufactured:

- the group of pipe specimens, where imperfection inside the welded joints were included
- the group with welded joints complying with optimal acceptance levels prescribed by standards.

After welded joints quality assessment, the pipes were subjected to destructive tests aiming to determine whether they could withstand extreme loadings typical of NaTech events (Figure 84). The mechanical test applied to these two groups of pipes were different. In case of the first group, the pipes were cut into sections including the defects detected with radiographic analysis that were subsequently subjected to tensile and bend tests. In case of the second group of specimens the samples were subjected to the impact load test. The results of these experiments are discussed in the next two paragraphs.

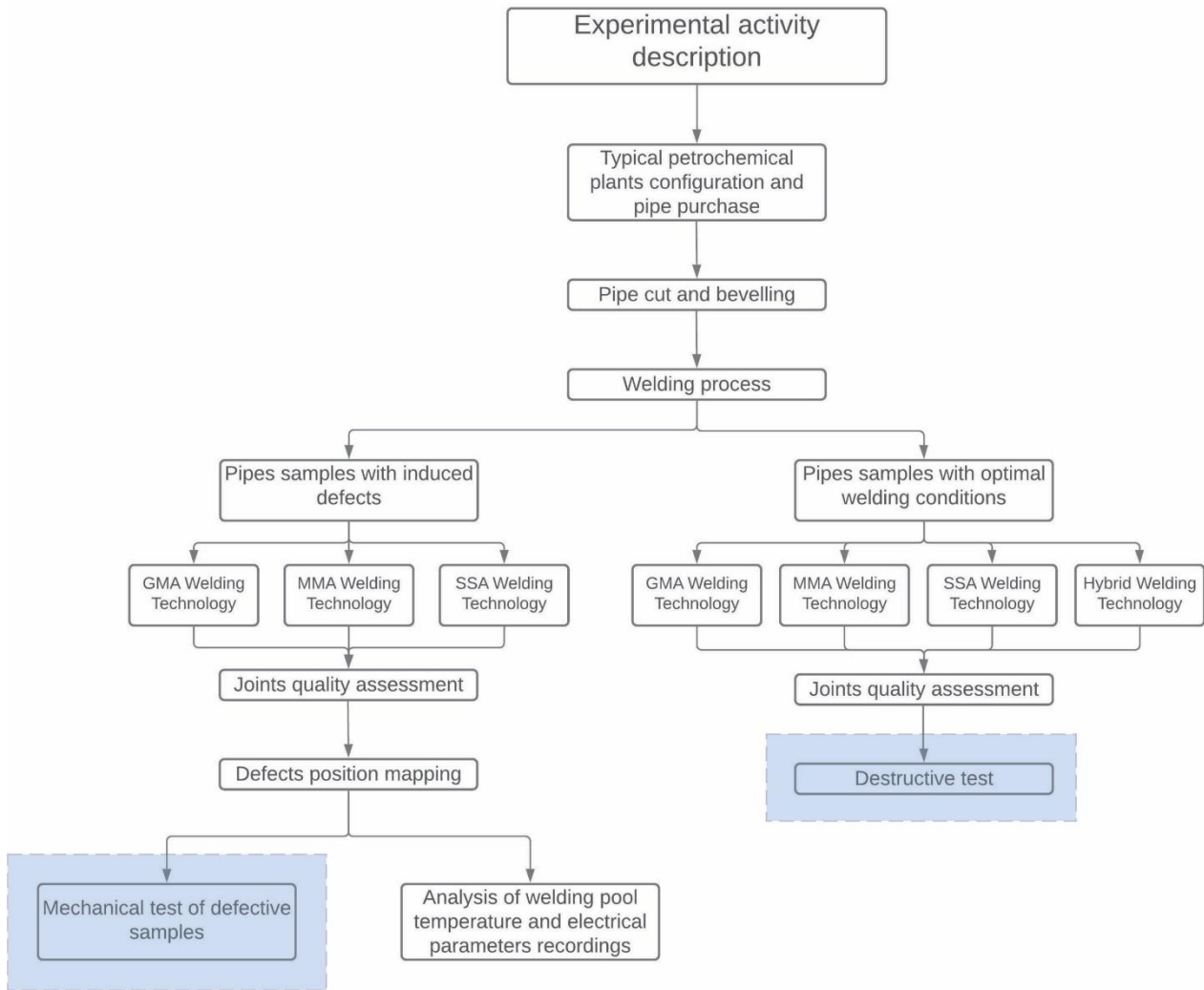


FIGURE 84: EXPERIMENTAL ACTIVITY STAGE

6.1 DESTRUCTIVE TEST OF DEFECTIVE WELDED JOINTS

In this paragraph are discussed the results of the mechanical tests performed on the defective pipe specimens. The sections of the pipe including defective spots were obtained cutting longitudinally (Figure 85) the twelve pipe specimens. These sections included single major defects listed in Chapter 5 specifically for the pipe specimens marked as GMA2, GMA3 and MMA1 and on Appendix A.3A.2 for all the other nine specimens. The shape and the dimensions of this parts are prescribed by [67] for tensile test and by [68] for bend test.

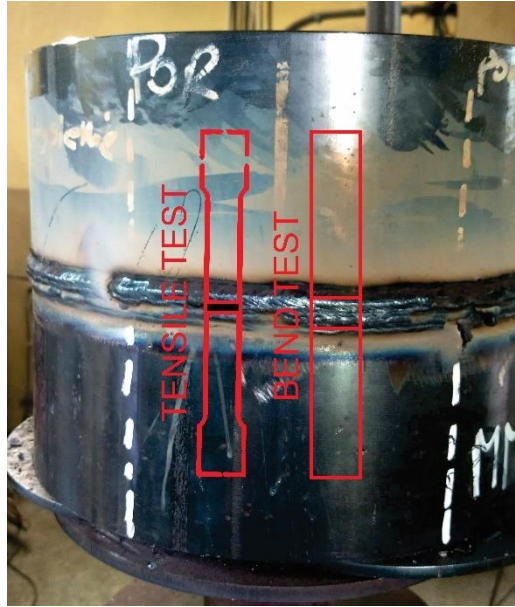


FIGURE 85: POSITION AND SHAPE OF THE SAMPLES FOR DESTRUCTIVE TESTS

The samples for tensile tests are prescribed to be in a dog-bone shape as depicted in Figure 86 with their exact dimensions included in Table 34. An example of one sample obtained from SSA2 pipe specimens is depicted in Figure 87: Sample for tensile test . The tensile tests were performed at controlled crosshead speed $V_1 = 20 \text{ mm/min}$ until the failure of the element.

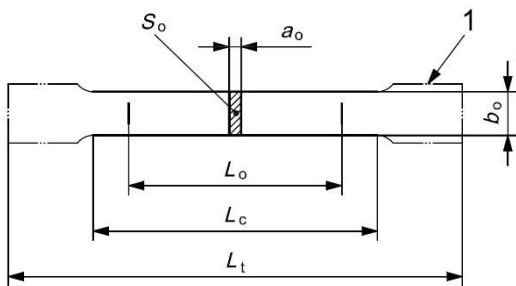


FIGURE 86: SAMPLE FOR TENSILE TEST [67]

	Definition	Value
a_0	Wall thickness of the tube	10,1 mm
b_0	Width of a flat test piece	25 mm
L_0	Original gauge length	80 mm
L_c	Parallel length	110 mm
L_t	Total length of test piece	250 mm
S_0	Original cross section area	252,5 mm ²

TABLE 34: DIMENSIONS OF THE SAMPLE



FIGURE 87: SAMPLE FOR TENSILE TEST OBTAINED FROM SSA PIPE

The samples that are necessary for bend test, according to [68], must have a rectangular shape 30 mm wide and the same length of tensile test samples. One of them, obtained from the pipe specimen marked as SSA3 is showed in Figure 88.



FIGURE 88: SAMPLE FOR BEND TEST OBTAINED FROM SSA3 PIPE

Three-point bend test was performed using the setup described in Figure 89 and Table 35

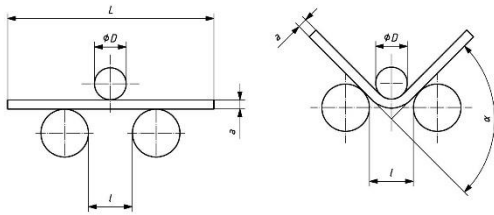


FIGURE 89: THREE-POINT BEND TEST

	Definition	Value
D	Diameter of the former	40 mm
l	Distance between supports	70 mm
L	Total length of test piece	250 mm

TABLE 35: THREE-POINT BEND TEST PRESCRIPTIONS

The results of the destructive test for the samples obtained from the pipe marked as GMA2, GMA3 and MMA1 are presented in the next three paragraphs.

6.1.1 DESTRUCTIVE TEST RESULTS FOR GMA2 PIPE

The samples belonging to the pipe marked as GMA2 were tested according to the scheme of Table 36.

Sample code	Defects included in the sample	Test performed
1_G2	Intermittent Undercut (5012) + Uniformly Distributed Porosity (2012)	Bend
2_G2	Intermittent Undercut (5012) + Uniformly Distributed Porosity (2012)	Bend
3_G2	Root Concavity (515)	Bend
4_G2	Distributed Porosity (2012) + Worm holes (2016)	Bend
5_G2	Distributed Porosity (2012) + Worm holes (2016)	Bend
6_G2	Incomplete Filled Groove (511) + Gas Pores (2011)	Tensile
7_G2	Lack of Penetration (402) + Gas Pores (2011)	Bend
8_G2	Lack of Penetration (402) + Gas Pores (2011)	Bend
9_G2	Cluster Porosity (2013)	Tensile

TABLE 36: DESTRUCTIVE TEST PERFORMED ON GMA2 PIPE SAMPLES

The samples 6_G2 and 9_G2 were subjected to tensile load, and both exhibited a failure of the parent material, outside of the joint area. The values of ultimate tensile strength R_m recorded for these two

samples were respectively 686 MPa and 694 MPa (Figure 90). It must be noted that the two values are higher than the value of 625 MPa required by [40] for the selected steel.

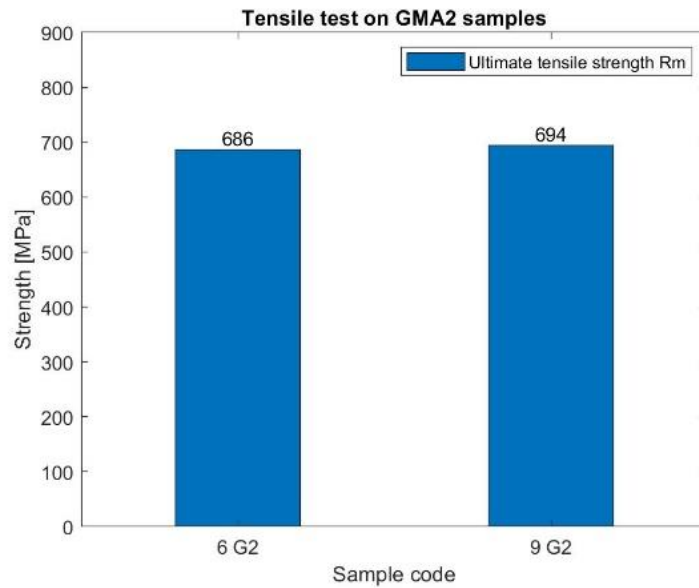


FIGURE 90: ULTIMATE TENSILE STRENGTH FOR G2 SAMPLES

All samples subjected to the bend test showed compliance with the prescriptions for quality acceptance except of the sample marked 4_G2, which included heavy porosity defect. On this sample the bending process resulted in the failure of the butt-welded joint as depicted in Figure 91.



FIGURE 91: FAILURE OF 4_G2 SAMPLE

6.1.2 DESTRUCTIVE TEST RESULTS FOR GMA3 PIPE

The type of tests performed on the samples obtained from the GMA3 pipe are listed in Table 37.

Sample code	Defects included in the sample	Test performed
1_G3	Cluster Porosity (2013)	Tensile
2_G3	Lack of Penetration (402)	Tensile
3_G3	Lack of Penetration (402)	Tensile

4_G3	Lack of Penetration (402)	Bending
5_G3	Lack of Penetration (402)	Bending
6_G3	Cluster Porosity (2013) + Worm holes	Bending
7_G3	Cluster Porosity (2013) + Worm holes	Bending
8_G3	Lack of Penetration (402)	Tensile

TABLE 37: DESTRUCTIVE TEST PERFORMED ON GMA3 PIPE SAMPLES

Ultimate tensile strength values for the samples 1_G3, 2_G3, 3_G3 and 8_G3 are included in the graph presented in Figure 92. The failure on the samples 2_G3 and 3_G3, which were affected by heavy lack of penetration defect, occurred on the welded joint section as shown in Figure 93. The pieces subjected to bend test showed full compliance to optimal quality acceptance requirements.

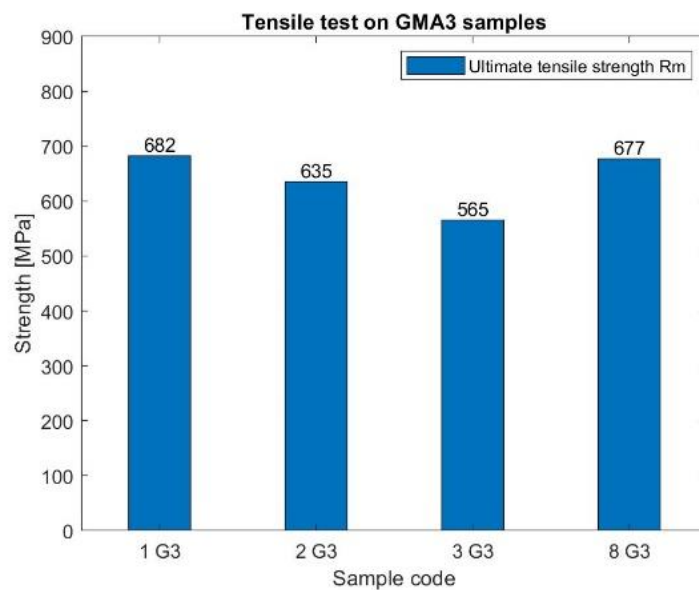


FIGURE 92: ULTIMATE TENSILE STRENGTH FOR G3 SAMPLES



FIGURE 93: FAILURE OF 2_G3 AND 3_G3 SAMPLES

6.1.3 DESTRUCTIVE TEST RESULTS FOR MMA1 PIPE

The test performed with the use of a part of pipes obtained from MMA1 specimen are listed in Table 38.

Sample code	Defects included in the sample	Test performed
1_M1	Intermittent Undercut (5012)	Bending

2_M1	Lack of Penetration (402)	Tensile
3_M1	Lack of Penetration (402)	Bending
4_M1	Lack of Penetration (402)	Bending
5_M1	Lack of Penetration (402)	Bending
6_M1	Lack of Penetration (402)	Bending
7_M1	Elongated Cavity (2015)	Tensile
8_M1	Lack of Penetration (402)	Tensile
9_M1	Intermittent Undercut (5012) + Lack of Penetration (402)	Tensile
10_M1	Intermittent Undercut (5012) + Lack of Penetration (402)	Bending
11_M1	Intermittent Undercut (5012) + Lack of Penetration (402)	Bending
12_M1	Intermittent Undercut (5012) + Lack of Penetration (402)	Bending
13_M1	Intermittent Undercut (5012) + Lack of Penetration (402)	Bending

TABLE 38: DESTRUCTIVE TEST PERFORMED ON MMA1 PIPE SAMPLES

Among these samples subjected to tensile tests, in the sample labelled 9_M1 the failure occurred in the welded joint section (Figure 95).

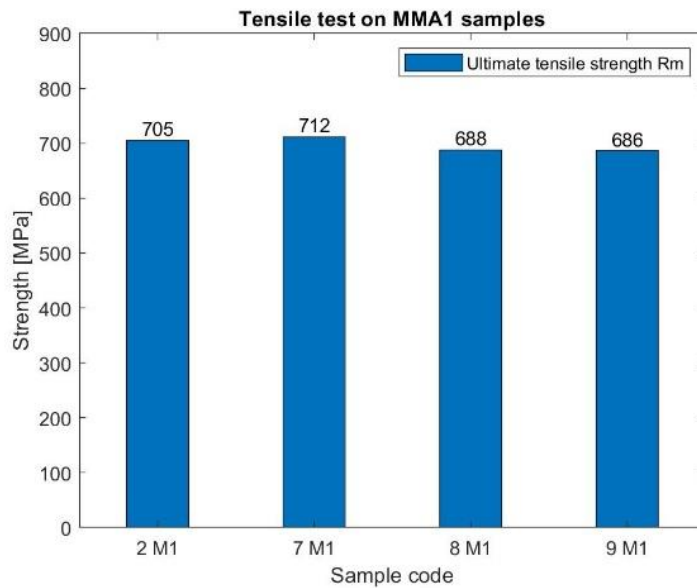


FIGURE 94: ULTIMATE TENSILE STRENGTH FOR M1 SAMPLES

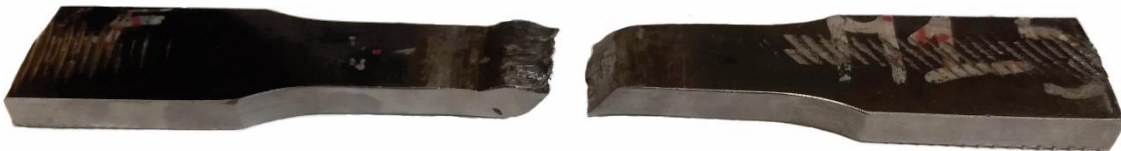


FIGURE 95: FAILURE OF 9_M1 SAMPLE

6.2 IMPACT LOAD TEST ON OPTIMAL QUALITY PIPE SAMPLES

As described in Paragraph 4.2, the first steps of the experimental activity were dedicated to the manufacturing of both defective and optimal quality acceptance level butt-welded joint pipes. The performances of specific pipe sections including various defects submitted to tensile and bend test were discussed in the previous paragraphs. In this paragraph the application and observation of impact load test on full-size butt-welded joint pipes are described. The purpose of these experiments was to simulate the catastrophic impact of a nearby collapsing structure on a piping system. The goal was also to evaluate the ability to undergo plastic deformation by flattening without damages of the piping system. The tests on the GMA, MMA, SSA and laser+GMA butt welded joint pipes, which were described in Paragraph 4.2, were carried out at KUZNIA ŁABĘDY S.A. factory [69] using the die forging hammer SKM-3T machine (Figure 96) with freely dropping mass of 3000 kg.



FIGURE 96: FORGING HAMMER SKM-3T

6.2.1 EXPERIMENTAL SETUP

The configuration for the impact load test was adopted following the prescriptions from [70] where the freely dropping hammer was put at different initial height H_s (measured from the lower plater) in order to obtain different levels of flattening expressed by the parameters H (partial flattening) and b (complete flattening).

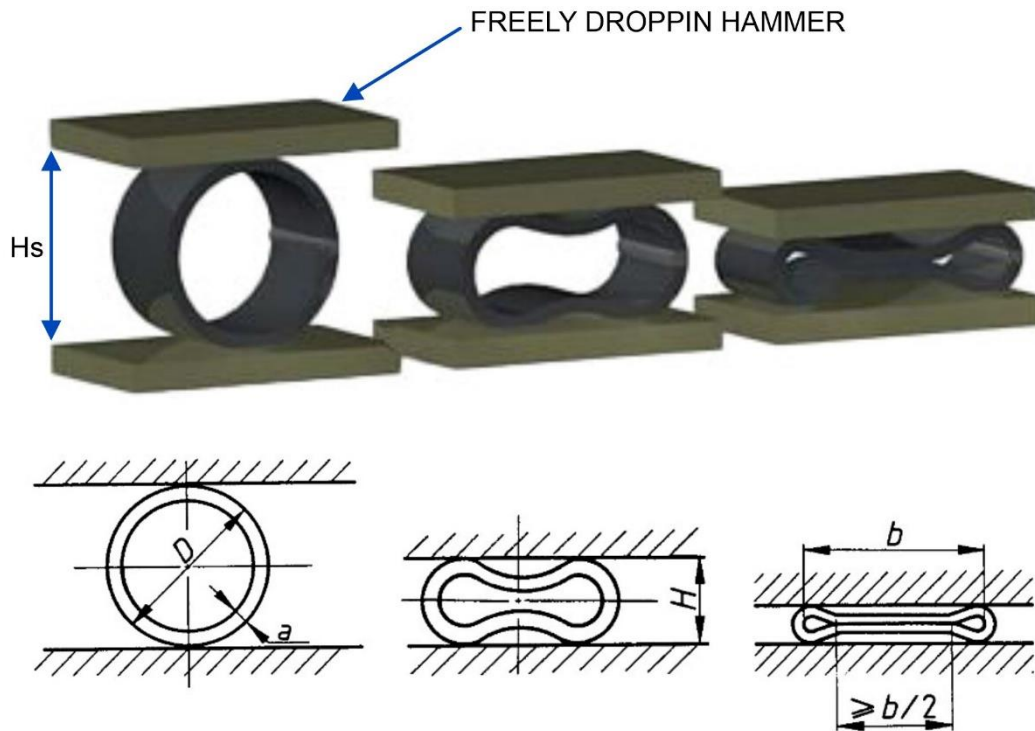


FIGURE 97: IMPACT LOAD TEST CONFIGURATION [70]

The value for the initial height H_s of the dropping platen was chosen considering the yield strength and ultimate tensile strength on the butt-welded joint section. The selection of the optimal value of this parameter is described in [71]. In that research the pipe specimens manufactured during this experimental activity were numerically modelled and then impact load test was simulated.

The numerical model of the MMA, GMA, SSA, LASER+GMA butt welded joints (Figure 98) consisted of two sections 120 mm wide of API 5L X80 steel pipes welded together. Significant geometrical information regarding the design of the numerical model is presented in Table 39.

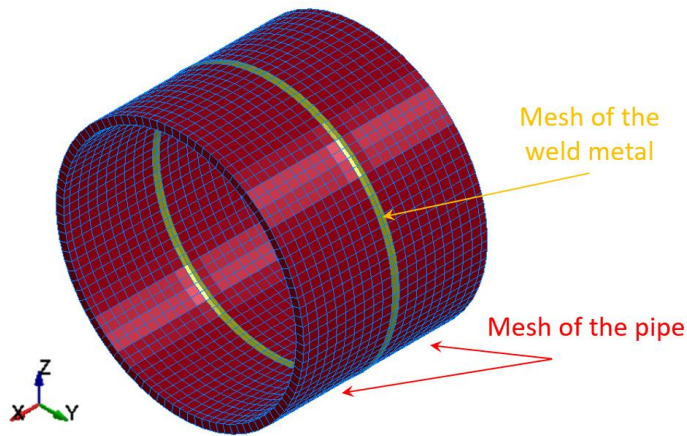


FIGURE 98: NUMERICAL MODEL OF BUTT-WELDED JOINT PIPE

[71]

Pipe section width [mm]	120
Pipe section diameter [mm]	323,9
Pipe wall thickness [mm]	10
Welded joint reinforcement thickness [mm]	12
Weld face width [mm]	16

TABLE 39: SIGNIFICANT DIMENSIONS OF THE NUMERICAL MODEL

The material properties were modelled assuming bilinear elastic-plastic behaviour (Figure 99) with significant values reported in Table 40.

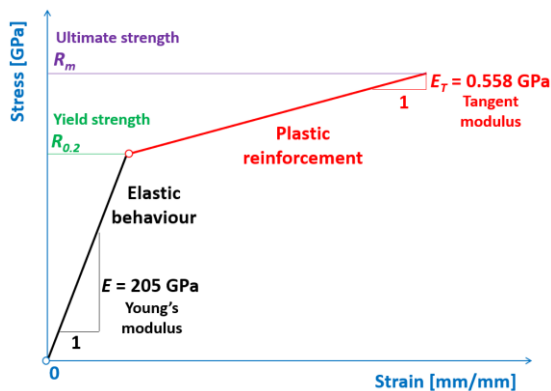


FIGURE 99: MECHANICAL BEHAVIOUR ADOPTED FOR API

X80 STEEL [71]

Basic Material Properties	Value
Young's modulus E [GPa]	205
Poisson's coefficient ν	0.28
Kirchhoff's modulus G [GPa]	80
Tangent modulus E_T [MPa]	558
Yield strength $R_{t 0,5}$ [MPa]	618
Ultimate tensile strength R_m [MPa]	700

TABLE 40: MECHANICAL PROPERTIES ADOPTED FOR API

X80 STEEL

Both hammer and base plate were modelled using solid elements with three degrees of freedom (Figure 100).

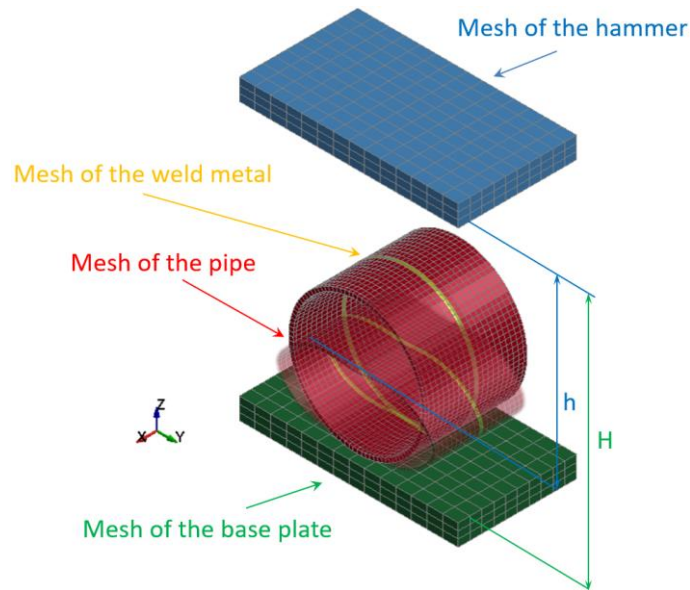


FIGURE 100: NUMERICAL MODEL OF THE COMPLETE IMPACT LOAD TEST [71]

The numerical model was tested with two different values of H_s : 1 meter and 1,5 meters. The results of the simulations in terms of displacements are reported in Figure 101 and Figure 102. It was stated that for an initial value of H_s of 1 meter it is possible to observe partial flattening of the pipe sample, while the complete flattening occurs for a value of H_s of 1,5 meters.

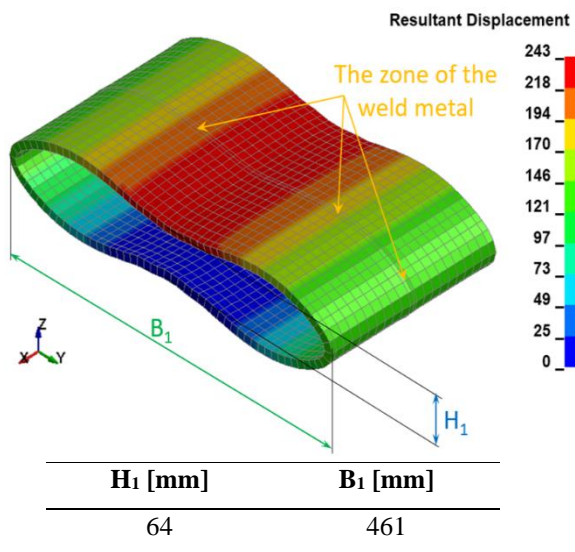


FIGURE 101: TOTAL DISPLACEMENTS FOR $H_s = 1$ M [71]

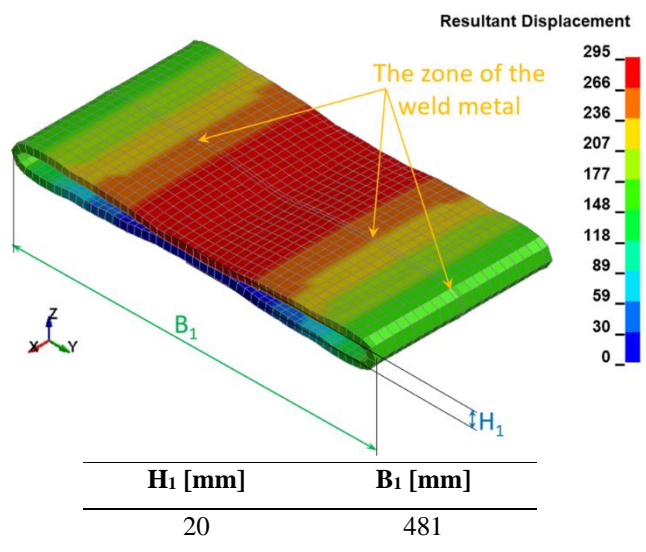


FIGURE 102: TOTAL DISPLACEMENTS FOR $H_s = 1,5$ M [71]

The results of the simulations in terms of Huber-Mises stresses are reported in Figure 103 and Figure 104. It is possible to observe that at the lateral edges of the pipe specimen the values of stress σ_{max} measured on the pipe walls are above the ultimate tensile strength of parent material (Table 5).

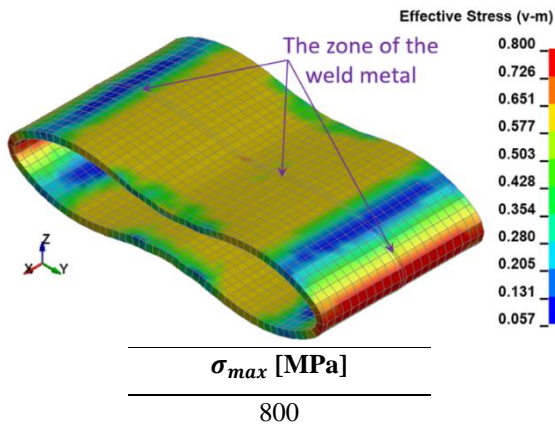


FIGURE 103: HUBER-MISES STRESSES FOR $H_s = 1$ M [71]

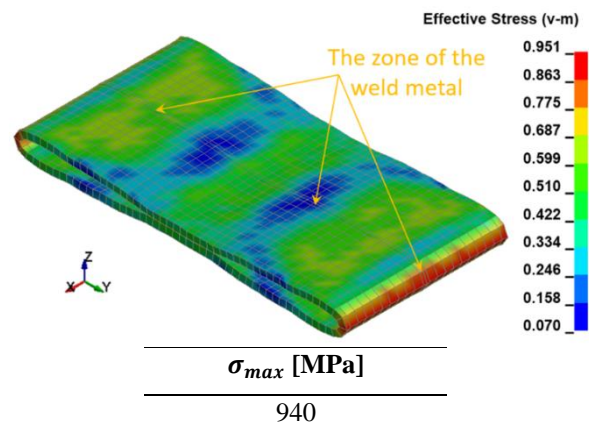


FIGURE 104: HUBER-MISES STRESSES FOR $H_s = 1,5$ M [71]

The results of the simulations showed the effectiveness of values of 1 meter and 1,5 meters as initial height H_s of the impact hammer and therefore they were assumed for the test on the real scale pipe specimens described in Paragraph 4.2.

6.2.2 IMPACT LOAD TEST RESULTS

Initial impact tests were performed with the use of four pipes – one sample for each welding technology. The initial position H_s of the upper plate was set at the height of 1 meter. The expected result, as suggested by the numerical simulations from [71], was supposed to be the partial flattening of the pipe. The actual results from the load test showed this exact behaviour as depicted in the pictures below (Figure 105 -Figure 108). For each pipe specimen can be observed the grade of flattening as well as the condition of the welded and parent material at the edges of the pipe where curvature and resulting stresses are higher. For all the specimens it can be observed the absence of cracks both on the parent material as well as on the area of the welded joint.

GMA PIPE SPECIMEN



H_1 [mm]	B_1 [mm]
75	466

TABLE 41: FLATTENING PARAMETERS GMA SPECIMENS



FIGURE 105: EFFECTS OF IMPACT LOAD TEST ON GMA PIPE SPECIMEN (1 M)

MMA PIPE SPECIMEN



H₁ [mm]	B₁ [mm]
74	456

TABLE 42: FLATTENING PARAMETERS MMA SPECIMEN

FIGURE 106: EFFECTS OF IMPACT LOAD TEST ON GMA PIPE SPECIMEN (1 M)

SSA PIPE SPECIMEN



H₁ [mm]	B₁ [mm]
78	463

TABLE 43: FLATTENING PARAMETERS SSA SPECIMENS

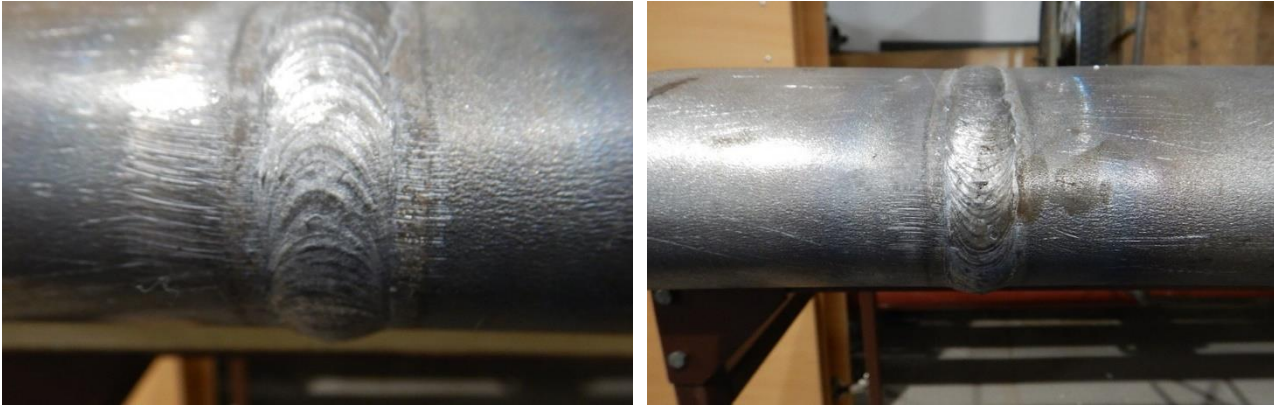


FIGURE 107 EFFECTS OF IMPACT LOAD TEST ON SSA PIPE SPECIMEN (1 M)

LASER + GMA PIPE SPECIMEN



H_1 [mm]	B_1 [mm]
55	474

TABLE 44: FLATTENING PARAMETERS LASER + GMA SPECIMEN

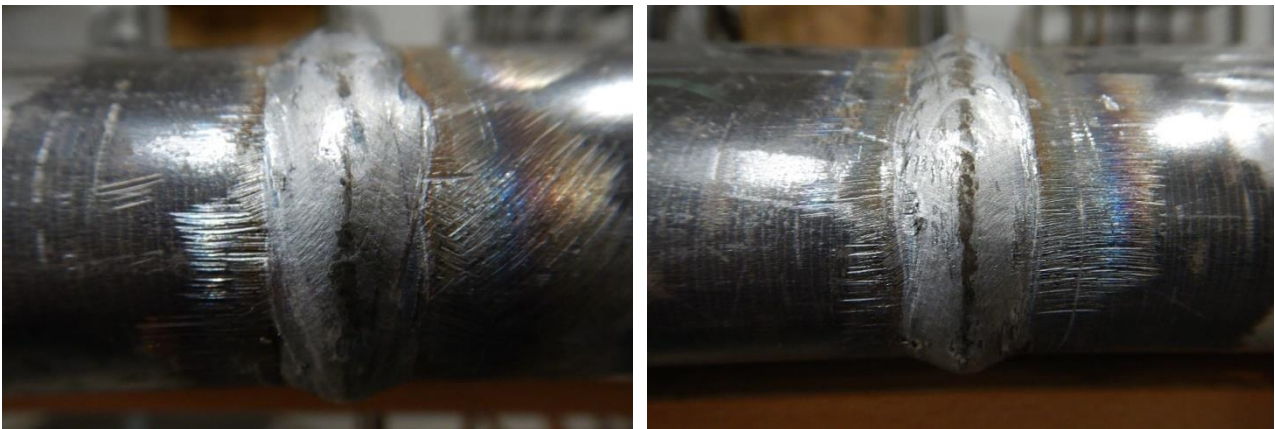


FIGURE 108: EFFECTS OF IMPACT LOAD TEST ON LASER + GMA PIPE SPECIMEN (1 M)

One last MMA pipe specimen was subsequently subjected to complete flattening placing the forging hammer at the initial height of 1,5 meters. It can be observed the complete flattening of the pipe section, as predicted by the numerical model, and the appearance of crack at the extreme portion of the pipe on the welded joint area; these cracks does not anyway propagate on the parent material resulting in the complete failure of the specimen.

MMA PIPE SPECIMEN



H₁ [mm]	B₁ [mm]
20	485

TABLE 45: FLATTENING PARAMETERS MMA SPECIMENS

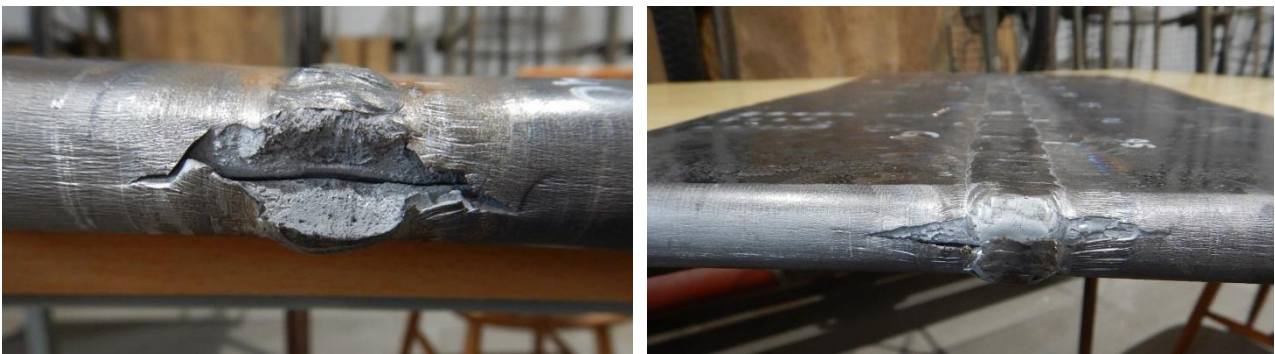


FIGURE 109: EFFECTS OF IMPACT LOAD TEST ON MMA PIPE SPECIMEN (1,5 M)

7 MONITORING OF WELDING PROCESS

As mentioned before, the whole process involving the manufacturing of the butt-welded joint pipe specimens with induced defects was monitored with an infrared camera, which recorded welding pool temperature, and a device recording welding current and arc voltage. The idea was to provide a complete overview of critical conditions that are related to the growth of imperfections inside the welded material. This knowledge could be a useful for a future development consisting of a non-destructive automated system for the detection of the imperfections on high strength steel welded joints. In this thesis the focus is put on the specific cases described in the previous paragraphs where massive defects detected led to the failure of the welded joints. This occurrence was observed on the samples obtained from the pipe marked GMA2, GMA3 and MMA1. However, the sets of data from all the other pipes can be used in the future for refined quality assessment method for less severe defects detection. Combining this data with the exact position of the defects obtained with Radiographic tests it is possible to have a complete image of the conditions necessary to observe the development of similar imperfections on every butt-welded joint high strength steel pipes.

The welding pool temperature data were obtained with an infrared camera that recorded the process of each bead deposition. The camera was of resolution of 640x480 px with a sampling frequency equals to 50 Hz. The device connected to the welding gun was able to collect the values of welding current and arc voltage with a sampling frequency of 200 Hz.

7.1 CRITICAL CONDITIONS IN GMA2 PIPE SPECIMEN

It was observed that the sample 4_G2, located inside segment number 3 (Paragraph 4.1.1.2), suffered the failure of the welded joint during the bend test. The defect detected was classified as porosity mixed with wormholes and it was located 35 cm along the circumference inside the three cap beads. The data from the infrared camera recorded during the deposition of these three beads were processed to obtain the temperature profiles of the portion of the pipe where the welding process took place. These profiles represent the maximal temperature reached by the welding pool melted material on each single point along the section of the joint monitored. The plain 2D and 3D representations of these three temperature profiles are depicted in Figure 110, Figure 111 and Figure 112.

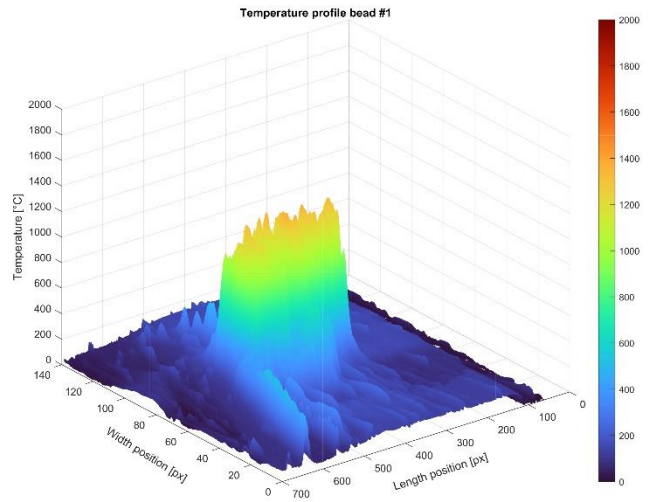
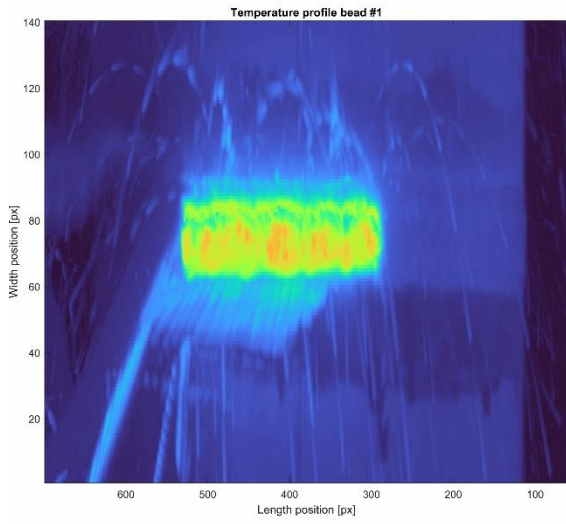


FIGURE 110: PROFILE TEMPERATURE BEAD #1

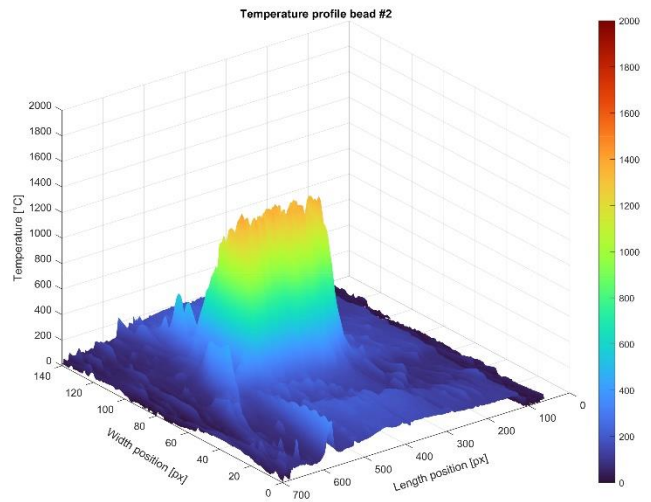
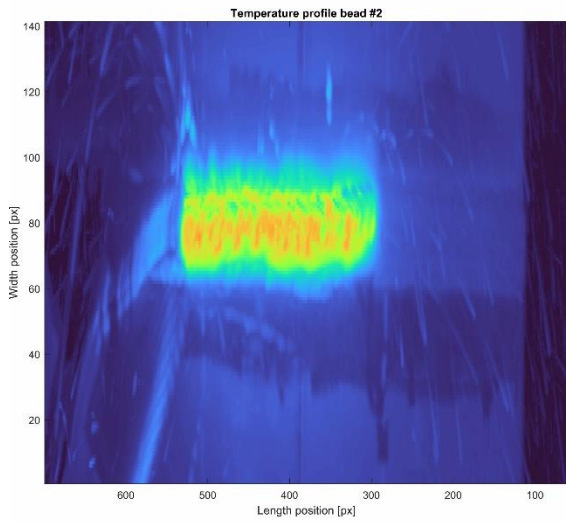


FIGURE 111: PROFILE TEMPERATURE BEAD #2

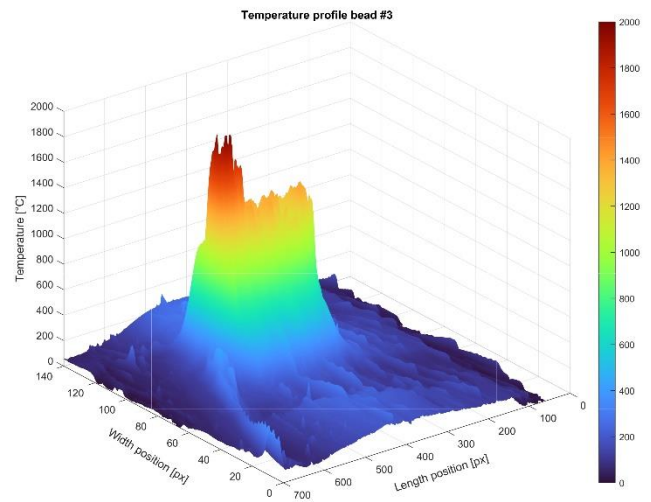
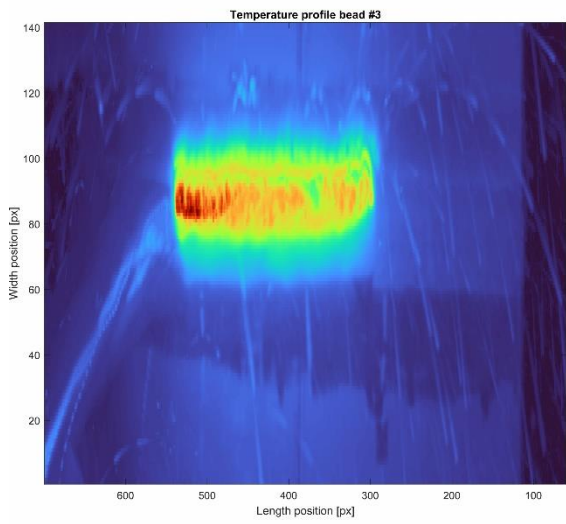


FIGURE 112: PROFILE TEMPERATURE BEAD #3

For better comprehension the temperature profiles are also presented and reported on a 2D representation that was obtained as a collection of the temperature values along a straight line representing the joint length. This graph is placed side by side to the correspondent radiographic film to evaluate the correlation between welding pool temperature and location of defects (Figure 113). For this specific case the segment was affected by the presence of porosity and wormholes.

This temperature profile may be compared with the profile obtained from segment number 2 where any imperfections were detected. The result of the analysis for this set of data is depicted in Figure 114. In this case, due to technical issues of the infrared camera it was possible to record only two of three beads and the temperature values in the first part of the graph are low because the welding operator partially obstructed the view of the pipe sample to the camera. However, the temperature profile along segment number three, which was affected by porosity, appears to be more irregular and less constant in comparison to the one obtained from segment two. Moreover, on the temperature profile of segment number three, specifically for bead number 3, can be observed a sudden peak of the temperature profile in the last part of the graph.

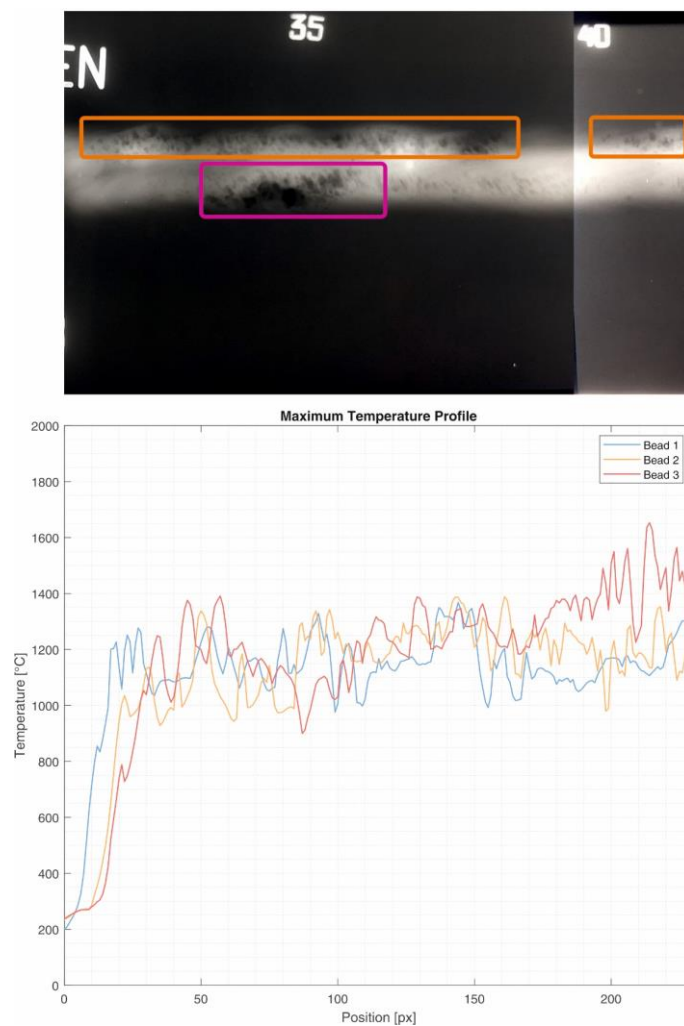


FIGURE 113: TEMPERATURE PROFILE SEGMENT #3

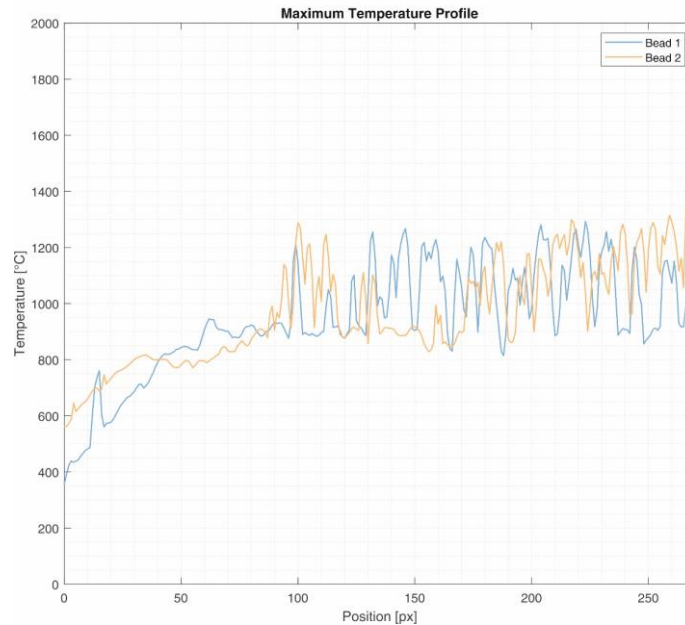
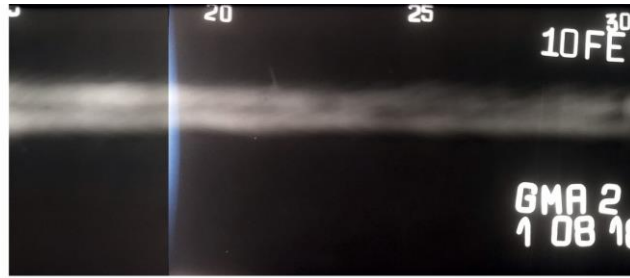


FIGURE 114: TEMPERATURE PROFILE SEGMENT #2

7.2 CRITICAL CONDITIONS IN GMA3 PIPE SPECIMEN

It was observed that the samples 2_G3 and 3_G3 suffered the failure of the welded joint during the tensile test: these samples were located 43 and 50 cm along the pipe circumference on segment number four. For both samples, the type of defect detected was characterized by a heavy lack of penetration in the root pass. The analysis of data collected with the use of infrared camera for this specific bead allowed to obtain the welding pool temperature profile depicted in Figure 115. The maximum temperature reached by the welding pool in the area that includes lack of penetration defect, is approximatively in the range between 600 and 800 °C as it can also be seen from the linear 2D profile temperature of Figure 116.

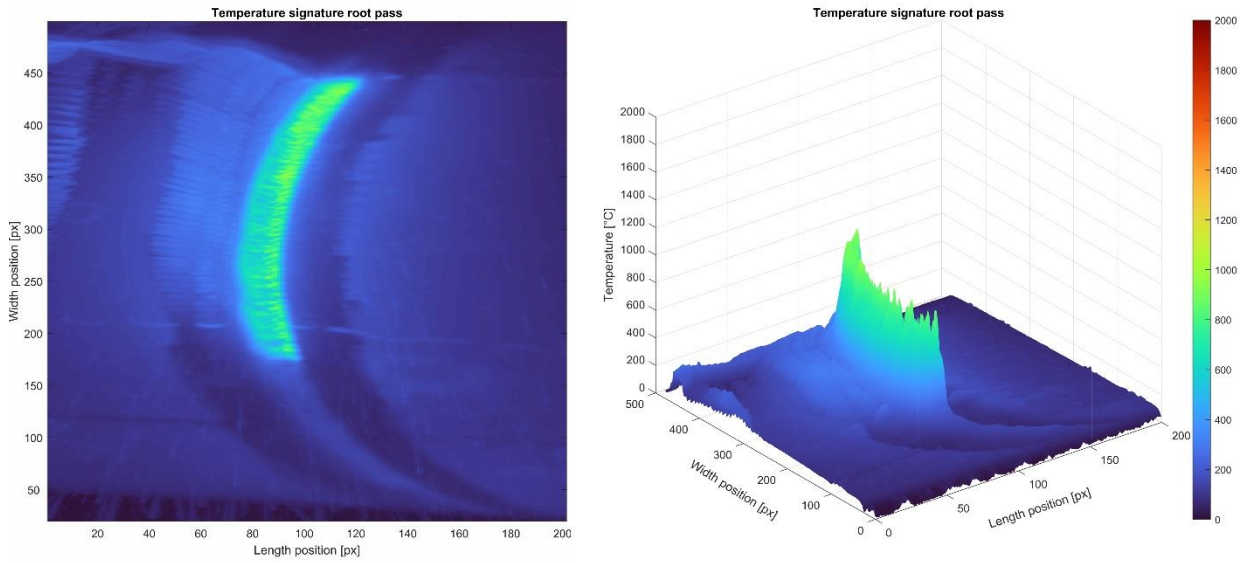


FIGURE 115: PROFILE TEMPERATURE ROOT BEAD SEGMENT 4

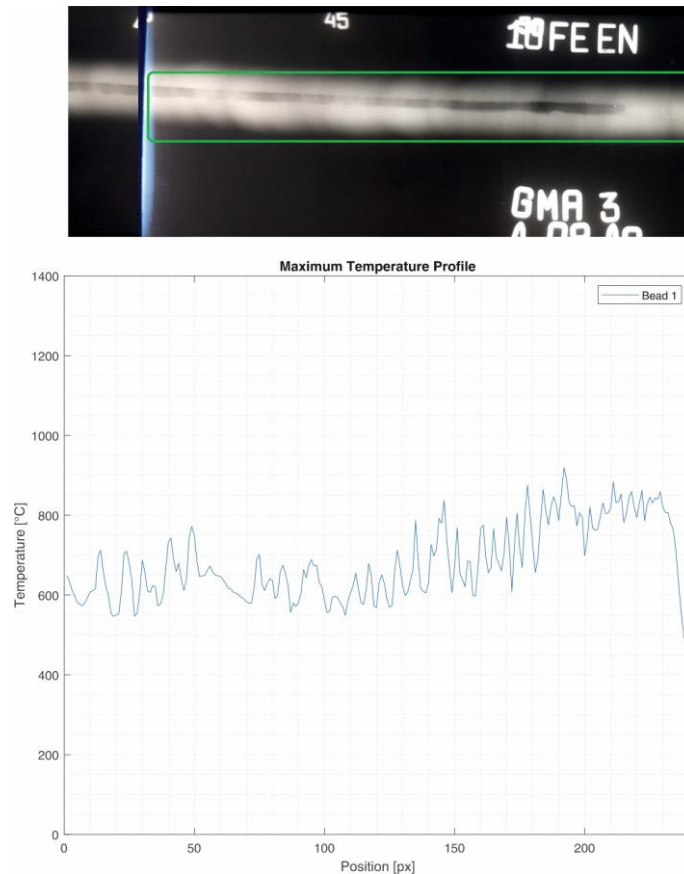


FIGURE 116: TEMPERATURE PROFILE OF SEGMENT 4

This temperature profile can be compared with the temperature profile obtained from segment two where no defects were detected. Except for the initial part and a small part of the central section where the view of the camera was blocked by the welding operator, the temperature is in the range between 800 and 1000 °C, higher to that one recorded in segment 4. The result of low welding pool temperature

is molten metal with poor fluidity and the consequent development of lack of penetration defects. Comparing welding pool temperature of segments two and four it is possible to quantify the difference of temperature that can result in the development of lack of penetration defect.

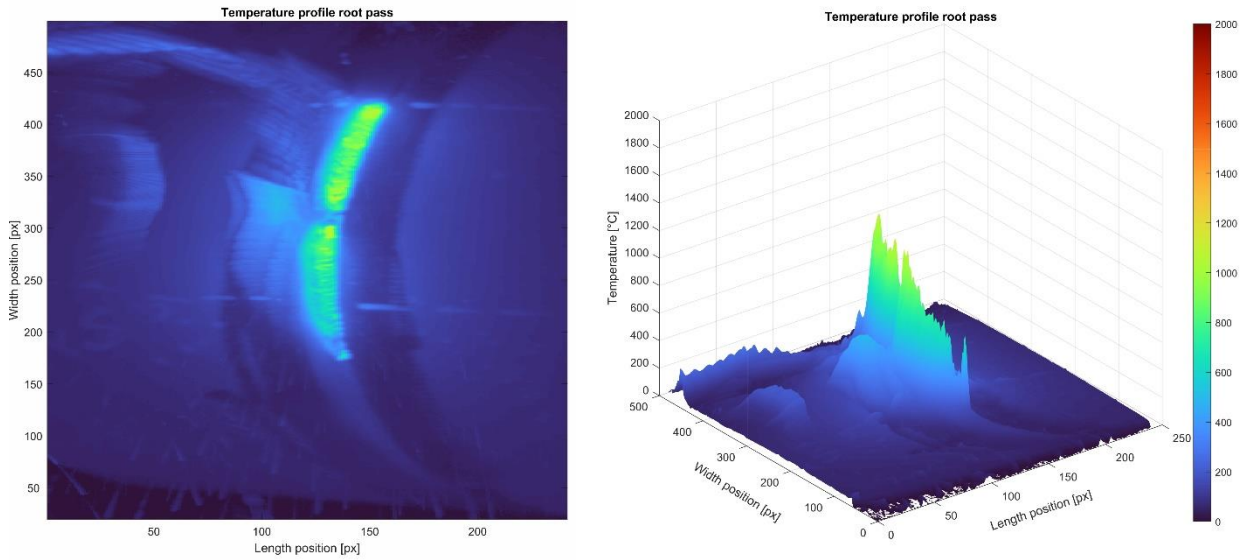


FIGURE 117: PROFILE TEMPERATURE ROOT BEAD SEGMENT 2

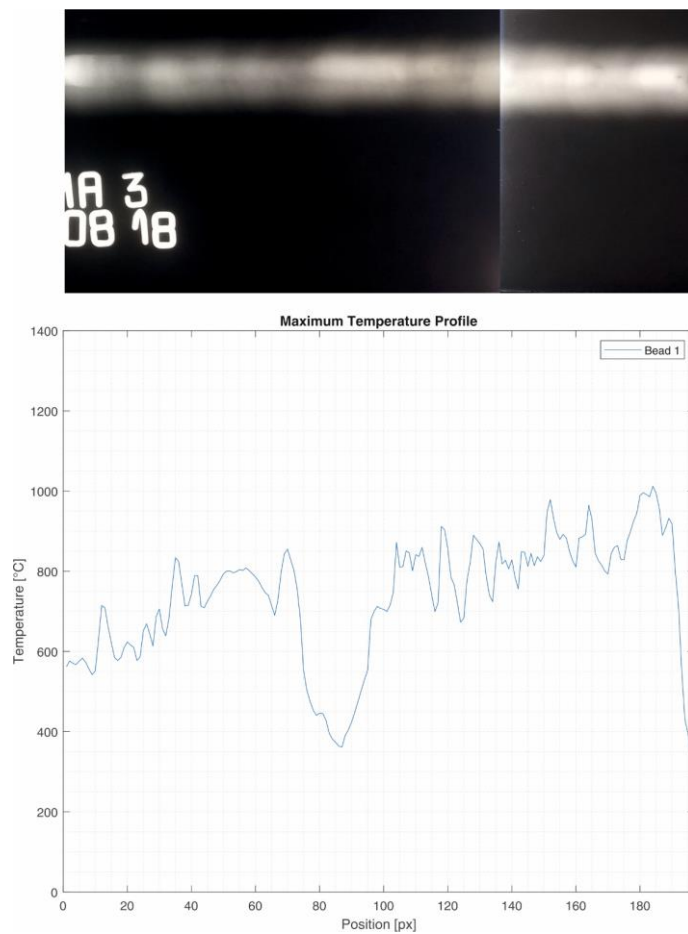


FIGURE 118: TEMPERATURE PROFILE OF SEGMENT 2

Although the sample 1_G3 was not interested by the fracture of the weld metal like the previous two samples it is interesting to show the results of the analysis of the data collected during the manufacturing of segment three. The sample marked as 1_G3 included cluster porosity and the temperature profile for this specific segment is depicted in Figure 119, in which can be observed some peaks of the temperature along the segment length.

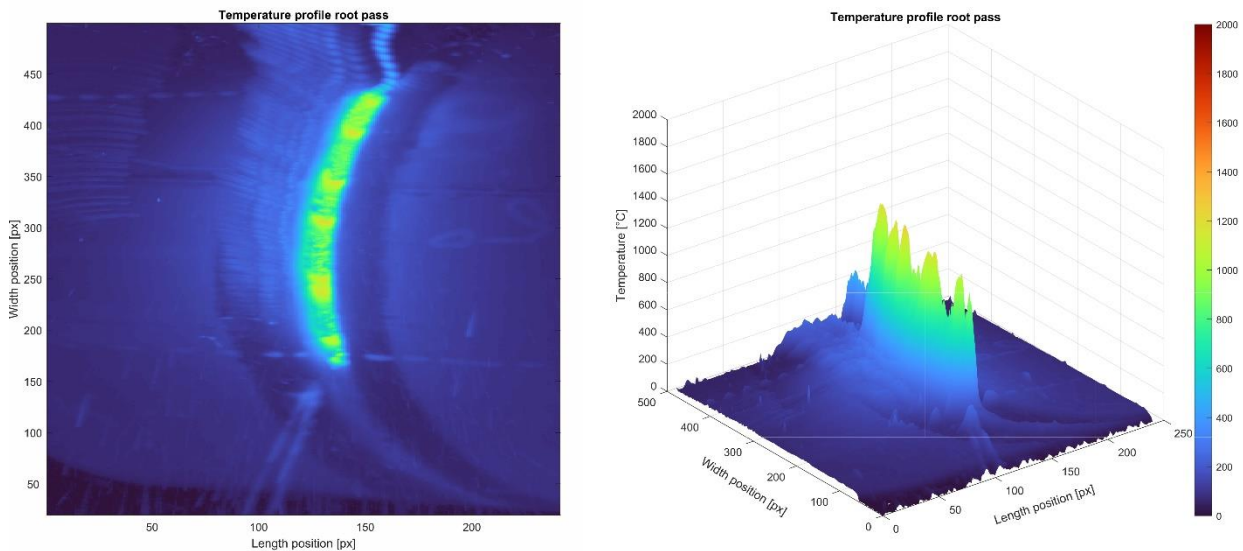


FIGURE 119: PROFILE TEMPERATURE ROOT BEAD SEGMENT 3

This behaviour can be better observed in the linear 2D graph of the profile temperature which is placed side by side with the correspondent radiographic film (Figure 120). Spikes on the temperature profile are clearly visible exactly where porosity was detected inside the welded joint, suggesting that temperature sudden increase could be a possible indicator for porosity development.

In addition, further analyses indicate that also welding parameters have a similar behaviour: the two parameters welding current and arc voltage, depicted in Figure 121, show the same number of spikes located at approximately the same position of the spikes observed on welding pool temperature profile. The analysis of welding current and arc voltage could indeed provide additional information regarding the development of imperfection inside welded joint allowing to refine the results obtained from the thermal analyses.

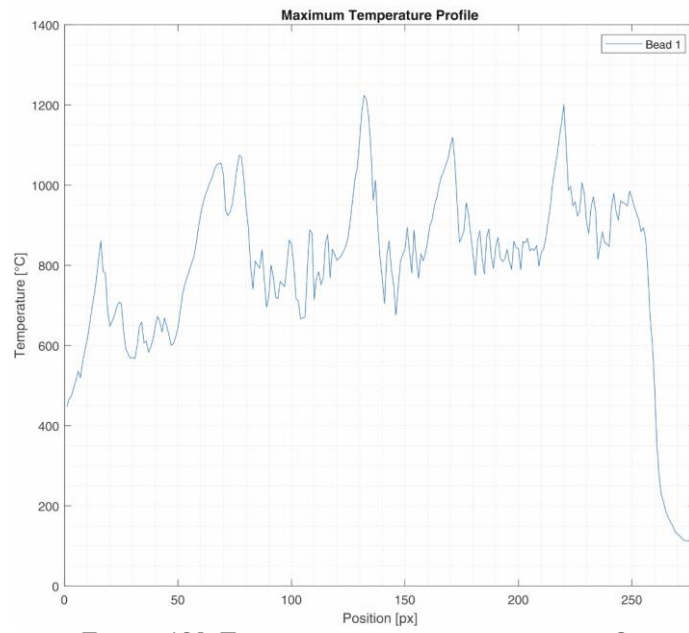


FIGURE 120: TEMPERATURE PROFILE OF SEGMENT 3

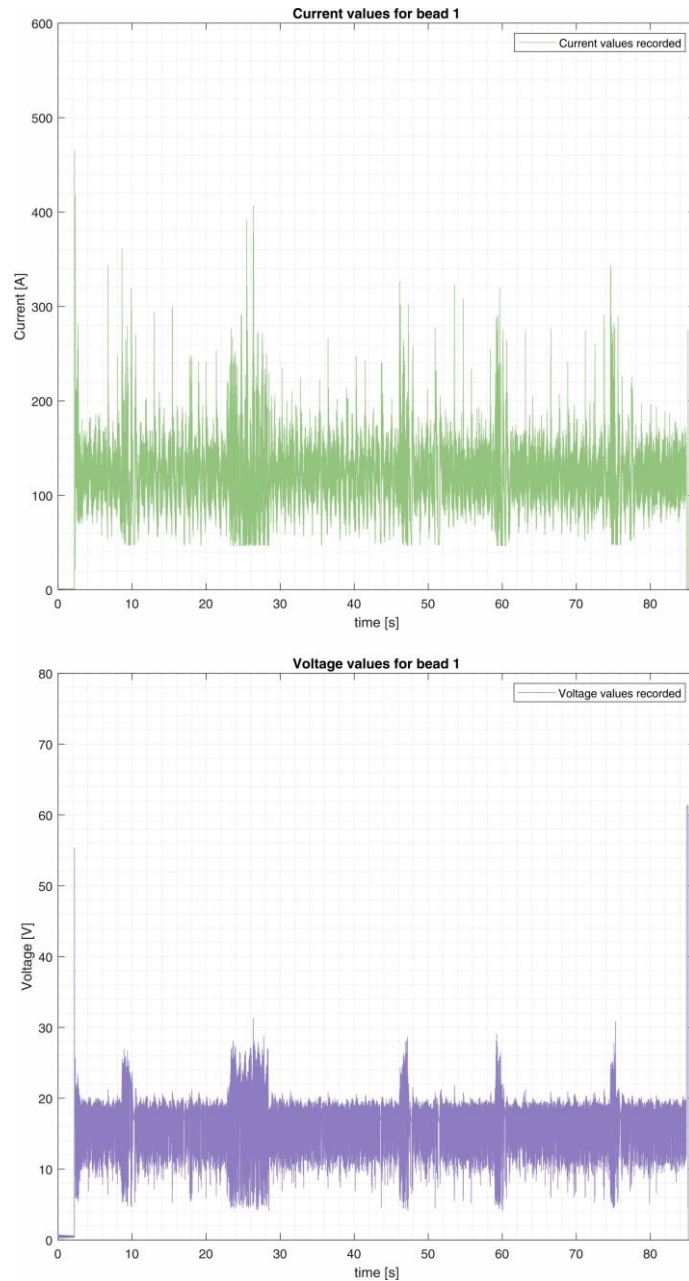


FIGURE 121: WELDING PARAMETERS OF SEGMENT 3

7.3 CRITICAL CONDITIONS IN MMA1 PIPE SPECIMEN

It was observed that the sample 9_M1, which was obtained cutting the pipe marked as MMA1, suffered the failure of the welded joint during the tensile test. This sample was located 65 cm along pipe circumference on segment number 5. The radiographic film for this specific segment showed the presence of heavy lack of penetration with intermittent undercut defect affecting all the root length.

Similarly, to the analyses of the previous paragraphs, it was retrieved the welding pool temperature profile of this segment trying to understand its influence on lack of penetration defect development.

The 2D and 3D temperature profiles obtained are presented in Figure 122. The temperature measured in the very initial part is in the range between 1500 and 2000° and then rapidly decrease between 1000° and 1500° with a slight increase in the central section where the defect is less severe.

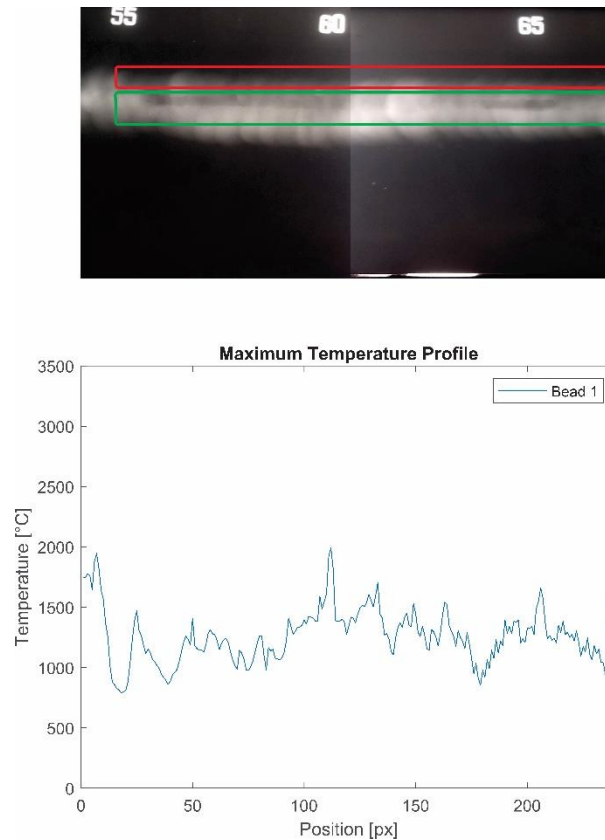


FIGURE 122: TEMPERATURE PROFILE OF SEGMENT 5

It is interesting to compare these values with those from other segments. Although most of the root beads on other segments are affected by lack of penetration defect, as visible in Figure 83, segment 4 can be used as benchmark.

The maximum welding pool temperatures for segment 4 are shown in Figure 123. Unfortunately, the final section of the profile is missing because the data recorded were partial due to the obstruction of the welding operator. However, on the sections where the data were available and not affected by lack of penetration defect, it can be observed that the temperature is higher than the one measured on segment 5. The fact that lack of penetration defect is caused by low welding pool temperature was observed also in the previous paragraphs with other pipe samples. Moreover, the presence of cluster porosity (highlighted in orange) and elongated cavity (highlighted in violet) relates to the two spikes visible in the graph. An abrupt increase of welding pool temperature produces localized porosity imperfections. This phenomenon was observed also in the samples showed in the previous paragraphs and manufactured with different welding technologies.

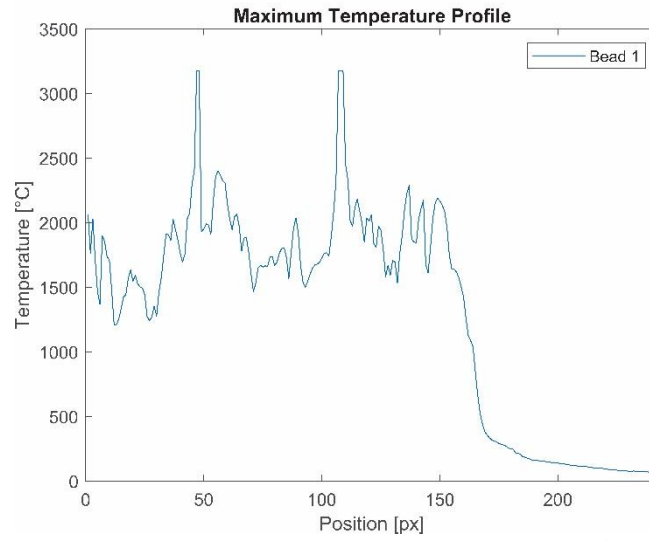
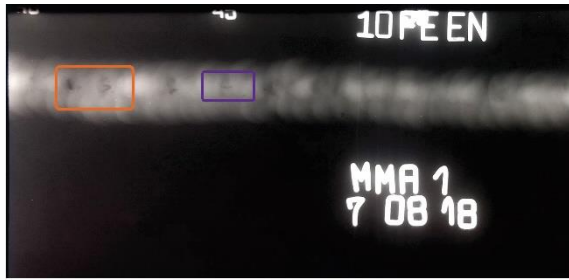


FIGURE 123: TEMPERATURE PROFILE OF SEGMENT 4

8 CONCLUSIONS

The core of this thesis was the study of welded connections of high strength steel pipes used in petrochemical and industrial plants from a mechanical and structural engineering perspective. The activity is the direct consequence of the attempt to apply the concept of resilience to complex infrastructures subjected to extreme loads. The two main aspects of this approach are essentially the effort to minimize the risk and the effects coming from Natech accidents. Piping systems are critical components that are potential source of failures and need particular attention to avoid catastrophic consequences originated by extreme events. This observation combined with the facts exposed in paragraph 1.2 about increasing energy demand are the origin for the research of new cost-effective solutions such as high strength steel pipes. The idea to concentrate the research activity on butt-welded joints originates from the observation that in many cases the manufacturing process is performed not only on controlled conditions but also directly on the installation site with possible negative influences due to atmospheric conditions or external contaminations. These external factors can be the source for the generation of various imperfection inside the joint affecting the final quality of the connection. These considerations highlighted the necessity to obtain a deep knowledge of manufacturing process, quality assessment methods and mechanic behaviour of high strength steel butt-welded joint pipes required for their correct design and installation. For this reason, the activities carried out during the research aimed at the four achievements described in Figure 9. They were:

- Observation of butt-welded joint pipes manufacturing process
- Assessment of the influence of imperfections on the behaviour of welded joints
- Analysis of the behaviour of real scale pipe specimens under catastrophic loads
- Definition of a method for the detection of the imperfections inside the joints

The outcomes of any of these points is discussed in the next paragraphs providing the information obtained during the activity, the results that could be useful for future developments as well as the critical aspects that could be further enquired in following activities.

8.1 MANUFACTURING PROCESS

The investigation of typical petrochemical plants layout carried out in Paragraph 2.3 provided the information about piping systems usually adopted on actual installations allowing to set up the experimental activity using a steel pipe with comparable dimensions. Generally, the likelihood to obtain poor outcomes in terms of quality of the welds is higher when the manufacturing process is

performed manually and directly on the construction site. Indeed, external factors like adverse atmospheric conditions, contaminations from detrimental substances e.g., grease, oil, or welding operators' malpractices could generate the imperfections described accurately in Paragraph 3.2. For these reasons it was decided to recreate this scenario during the experimental activity. The circumstances abovementioned were artificially recreated on twelve pipe samples having various configurations. In details, on some segments along the circumference of the welded joints were alternatively implemented the following actions:

- manual variation of the values of arc voltage and weld current
- the flux of shielding gas in GMA welding was interrupted intermittently
- grease was spread on the surface of the weld groove
- variation of the electric arc length

Immediately after the manufacturing process, visual inspection permitted to detect macroscopic imperfections both on the inner and outer surfaces of the pipes. It was possible to spot heavy porosity on the segments where the shielding gas flow rate was interrupted several times for a couple of seconds during the deposition of the beads. This evidence was observed for example on the external surface of specimen GMA2, specifically on segment eight (Figure 124). The visual assessment allowed also to detect the presence of macroscopic lack of penetration defects on some of the manufactured samples as depicted in Figure 125.



FIGURE 124: POROSITY ON GMA2 PIPE



FIGURE 125: LACK OF PENETRATION ON GMA3 PIPE

In addition, all the pipe specimens were submitted to radiographic test to detect actual presence of imperfection not only on the visible surfaces of the welds but also inside their entire volume. This non-destructive method assessment revealed the presence of various types of imperfections and

inclusions as it was originally planned. All the actions adopted during the manufacturing process, which simulated the effect of external circumstances, gave positive outcomes in terms of the capability to reproduce typical weld defects. This was a fundamental achievement because it granted the possibility to later evaluate two different aspects:

- how the presence and the magnitude of each defect affect the mechanical behaviour of the portion of the pipe including it
- the possibility to build up for each class of defects a set of information regarding critical welding pool temperature and electrical welding parameters that compromise the final quality of the welded joint.

At the same time, it was carried out a specific activity with the final goal to prepare other pipe specimens complying with highest quality acceptance levels. The standard EN-ISO 5817 [62] introduces four classes of requirements as described in Table 46 and for each of them specifies the minimum requirements for quality acceptance. For the purpose of the research, it was decided to adopt class B+ as intended for critical infrastructures such as industrial and petrochemical plants.

Quality level	Particularity of the executions
D	Components with elementary quality requirements of average /low importance
C	Components with normal quality requirements of average importance
B	Components with extended quality requirements of average/high importance
B+	Components with extended quality requirements of high importance. Particularity significant fatigue phenomena

TABLE 46: QUALITY ACCEPTANCE LEVELS

The manufacturing of the pipe specimens using GMA, MMA and SSA welding technologies followed Welding Procedure Specifications described in Paragraphs 4.1.1 - 4.1.3. Visual inspection and radiographic analysis confirmed the absence of significant defects and the complete compliance of the welded joints to quality acceptance levels.

The manufacturing of the pipe specimens using hybrid welding technology was of particular interest because it was necessary to evaluate different set of welding parameters for laser welding technology. Laser beams of different power and travel speed were applied on a steel plate having the same properties of the pipe used during all the experimental activity. The analysis of the fusion in terms of penetration and quality allowed to identify the best parameters that were then adopted during the

manufacturing of the pipe specimens. Two were the aspects that were considered for the selection of these parameters: penetration length and absence of inclusions and imperfections inside the fusion. Among the twenty combinations tested (see Paragraph 4.2.2) it was selected the set identified as number 25: this specific set was characterized by a power source of 5000 W, travel speed of 2 m/min and focus position of 0 mm above the surface. This group of parameters were selected among the others because they granted adequate penetration as can be observed in Figure 74, and the absence of imperfections as can be seen in Figure 75. On the opposite, the choice of other sets of parameters resulted in the development of microporosity inside the joint as it was shown in Figure 76. This optimization process gave the possibility to produce a pipe specimen manufactured using hybrid welding technology having complete compliance with B+ quality acceptance level.

8.2 ANALYSIS OF DEFECTIVE SAMPLES

Once the manufacturing process was completed the activity aimed at the detection of the imperfections inside the welded joints and the subsequent assessment of their influence on the resistance of the connection. As indicated in the previous paragraph, visual inspection confirmed the presence of surface defects i.e., porosity, lack of penetration, on some pipe specimens. After visual inspection, complete assessment was then carried out using radiographic inspection over the whole length of each joint. Changing welding parameters, shielding gas flow rate, or putting some external substances over the surface of the pipes e.g., water, oil, grease, allowed to include the following imperfections. The complete list of the defects detected for selected pipe specimens is reported in the Paragraphs 5.1 - 5.3 and on the appendix for all the others.

- Lack of penetration
- Porosity
- Undercut
- Root concavity
- Incomplete filler groove
- Worm holes

The parts that included these defects, which normally would have not passed quality acceptance level controls, were cut from the pipe specimens, and then divided in two groups for tensile and bending test. These tests were useful to establish how the defects with different grade of severity affect ultimate limit state of the joint. A distinction was made observing the type of failure that occurred on

each specimen and specifically the failure of the parent material or of the weld metal. The first circumstance is preferable when the final goal of the analysis is the evaluation of the quality of the connection because it shows that the mechanical properties of the joint are better than those of the parent material.

Considering the three welding technologies used, were performed 42 tensile tests and 54 bend tests. The different number of samples can be explained with the fact that bending tests were performed alternatively on internal or external surface of the pipe requiring a bigger number of samples. The exact number and the outcomes of each occurrence are described in Table 47. Out of 96 total samples, four of them experienced the failure of the welded joint: three of them during tensile test (2_G3, 3_G3 and 9_M1) while the fourth (4_G2) occurred during bend test. As general observation, it can be noted that just a small number of samples revealed the failure of the welded joint, although on some of them were clearly visible heavy defects, but instead it occurred to the parent material. As mentioned before this is a desirable event because it grants that the connection has at least the same resistance of the parent material. In addition, it is possible to assess that these destructive tests were performed on samples with significant defects suggesting then that the probability of failure for samples with smaller defects could be smaller.

Welding technology	Number weld material failure/ Number of tensile tests	Number weld material failure/ Number of bend tests
Gas Metal Arc Welding (GMA)	2/13	1/19
Manual Metal Arc Welding (MMA)	1/19	0/23
Self-Shielded Flux Core Wire welding (SSA)	0/10	0/12

TABLE 47: NUMBER OF TESTS PERFORMED

The reason of the failure of the joint for the first three specimens was connected to the presence of severe lack of penetration defects inside the weld metal (Figure 82 and Figure 83). The specimen marked 4_G2 was instead affected by porosity combined with worm holes that developed on the external surface of the weld material (Figure 81). This evidence suggested to concentrate the attention on these specimens evaluating the conditions that favour the development of such type of defects. The method used for this analysis was mainly based on the thermal information collected with an infrared camera during the manufacturing process. The data consisted in welding pool temperature measurement, which were recorded with a frequency of 50 Hz. These data gave the possibility to reconstruct the temperature profile of each point along the joint. The comparison between the temperature profile of the segments containing the defects and the segments that did not show any imperfection allowed to define critical conditions for the development of specific defects. This information can be defined as defects signature, and they could be used as a tool for real time quality assessment of welded joints of X80 pipe samples. The idea is to provide a basic tool that can be used

to detect the defects comparing the welding pool temperature measured during the welding process to those responsible of development of induced defects and retrieved during the experimental activity. The important information obtained from the analyses of the temperature profiles suggested that lack of penetration defect is correlated to lower temperatures of the molten material inside welding pool. This behaviour is visible for example in Figure 126 that represent the comparison between the segment 2 (on the left) and segment 4 (on the right) on the pipe sample GMA3.

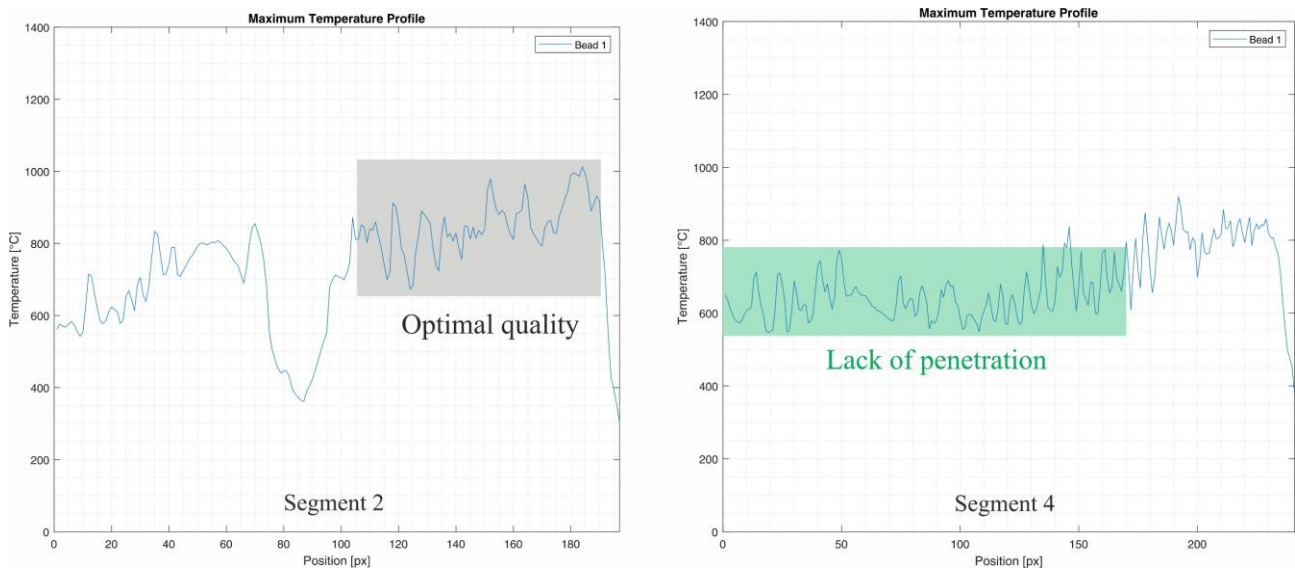


FIGURE 126: COMPARISON BETWEEN SEGMENTS IN GMA3 PIPE

Due to lower temperatures the molten metal is less fluid and therefore it has more difficulty to fill completely the gap between the two elements to be joined. This situation weakens the connection because the discontinuity between the parent and weld material may create the point of origin for the fracture as it exactly happened for the samples 2_G3 and 3_G3 during tensile test.

The second situation studied was the case of porosity defect, which caused the failure of the sample 4_G2 under bend test. Cluster porosity was also detected on segment 3 of GMA3 pipe sample. In the first case, the temperature profile showed irregular behaviour, with visible fluctuations of the values, compared to the profile registered on segments where it was not detected porosity. This occurrence is visually depicted in Figure 127.

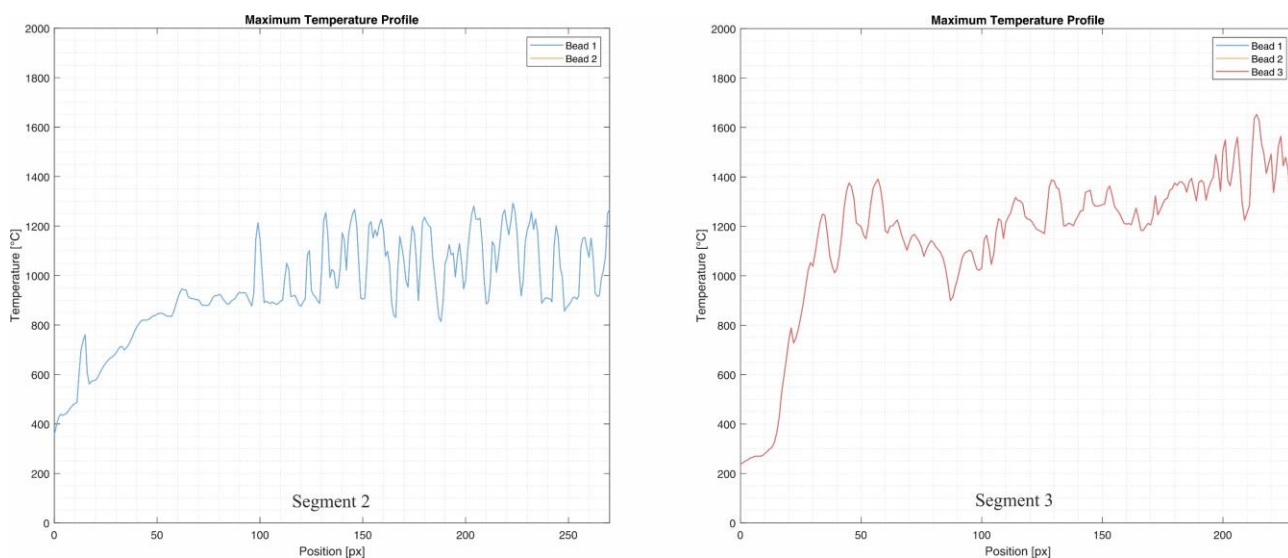


FIGURE 127: COMPARISON BETWEEN SEGMENTS IN GMA2 PIPE

Irregularities are more visible on segment three of GMA3 and on segment 4 of MMA1 pipe specimens. Peaks in the temperature profile on the spots where cluster porosity was detected are clearly visible on Figure 120 and Figure 123.

Just few cases were discussed before, those showing the rupture of the weld metal, but further research activities can concentrate their focus on other samples that have a different configuration regarding defects type and magnitude. In addition, it was showed that the use of arc voltage and weld current data could also provide information regarding weld imperfections development: in Figure 121 it can be noted a change of arc voltage and weld current values on the spots where it was detected porosity development.

8.3 ANALYSIS OF NON-DEFECTIVE SAMPLES

The last part of the research activity was then devoted to the study of the behaviour of complete butt-welded joints pipes under impact load test simulating extreme conditions caused by catastrophic events e.g., earthquakes, explosions. During such circumstances piping systems could be subjected to very high stress produced by the collapse of other buildings resulting in their deformation with different grade of severity. For this reason, it was decided to manufacture some pipe specimens using four welding technologies i.e., GMA, MMA, SSA and hybrid, and then submit them to impact load tests. Differently to the specimens with induced imperfections, these ones had complete compliance with prescriptions regarding quality acceptance levels. In fact, after the manufacturing process all the welded joints were checked using radiographic method that confirmed the absence of imperfections and the possibility to assign them B+ quality category.

Impact tests were performed using a forging hammer with a freely dropping mass of 3000 kg registering then pipe flattening level and the integrity of the welded connection. The scope of this activity was to test real scale butt-welded joint pipes under catastrophic loads evaluating then the condition of the connection and the presence of possible breaks that on real scenarios could result content leakage.

Before starting the activity, it was necessary to consider the initial set up that allowed the desired deformation of the pipes. In particular, the fundamental parameter that had to be carefully considered was the initial position of the hammer above the reference plate. The choice was necessary to induce partial or complete flattening of the pipe due to the load applied. The correct values were retrieved from [71] where impact load test was simulated on a finite elements model of the pipe. The properties of the numerical model and the outcomes of this analysis were described in Paragraph 6.2.1. Based on these analyses it was observed that the initial position of the hammer at 1 meter above the reference plate caused the partial flattening of the pipe specimens. The initial height of 1,5 meters above the reference plane caused instead the complete flattening of the pipe. It was also noted that at the extreme edges of section, where the curvature of the pipe surface is higher due to the deformation caused by the load, were registered the maximum Huber-Mises stress levels.

Four pipe specimens, one for each welding technology, were subjected to impact load test with the dropping hammer placed at the initial height of 1 meter above the plate where the pipe was placed. On all the four attempts it was observed the partial flattening of the pipe with no visible damage of parent material neither the weld material (Figure 105 -Figure 108). The exact deformation of the pipe section for each sample, expressed in terms of H_1 (height) and B_1 (width) were reported in Table 41 - Table 44. This outcome suggests that despite extreme loads and the consequent deformation of the pipe, the welded connections remained intact and were not observed cracks and the rupture of the material that could cause loss of containment.

One additional pipe specimen, manufactured with MMA welding technology, was later tested with the hammer dropping from an initial height of 1,5 meters. In this case the load caused the complete flattening of the pipe and the appearance of a transversal crack on the external parts of the pipe having with the maximum curvature although the overall integrity of the joint was not affected.

8.4 FINAL CONSIDERATIONS

This activity demonstrated the consistency of the choice of X80 high resistance steel pipes for petrochemical and industrial installations in terms of manufacturing process and resistance to extreme loads. Butt-welded joints used to connect two separate pipe sections were the specific subject of the

analysis and their behaviour was studied both under quasi static and dynamic loads. In the first case, working on samples obtained from pipes with quality acceptance level below B+, it was observed the failure of the connection just on some specific cases where severe imperfections were detected inside the welded material. Many samples with various types of defects were tested and in only just 3 samples out of 96 revealed the failure of the welded metal before the parent material. These 3 samples were characterized by clearly visible lack of penetration defect. It is therefore necessary to control and avoid the development of this kind of imperfection inside the welded joint. This control could be achieved using thermographic technique as non-destructive quality assessment method. It was showed in Chapter 7 that analysing the thermal profile of the welding pool temperature recorded during the welding process it could be possible to predict the development not only of lack of penetration but also of other categories of defects. This information could be used to develop an automatic method to detect imperfections based on the measurement of the temperature of the welding pool during the same manufacturing process. For the case of dynamic load test, it was demonstrated that for any welding technology adopted, impact load test causing severe partial flattening of the pipe did not result in the failure of the pipe itself neither of the welded joint. Only when submitted to complete flattening it was observed the appearance of transversal cracks on the external surface of the pipe. The extensive work on the manufacture of different configuration of pipe specimens and the various loads applied to portions or full sections of steel pipes grade X80 showed promising performances in terms of resistance towards extreme loads suggesting the possible adoption for critical infrastructures.

BIBLIOGRAPHY

- [1] “Oxford Dictionary of English.” .
- [2] E. Hollnagel, D. Woods, and N. Leveson, *Resilience Engineering : Concepts and Precepts*. 2006.
- [3] J. P. Visser, “Developments in HSE management in oil and gas exploration and production,” in *Safety Management: The challenge of change*, 1998, pp. 43–65.
- [4] M. Miśkiewicz, D. Bruski, J. Chróścielewski, and K. Wilde, “Safety assessment of a concrete viaduct damaged by vehicle impact and an evaluation of the repair,” *Eng. Fail. Anal.*, vol. 106, p. 104147, Dec. 2019, doi: 10.1016/j.engfailanal.2019.104147.
- [5] E. Krausmann, A. M. Cruz, and E. Salzano, *Natech Risk Assessment and Management Reducing the Risk of Natural-Hazard Impact on Hazardous Installations*. Elsevier, 2017.
- [6] Ronald Eisler, *The Fukushima 2011 disaster*. CRC Press - Taylor & Francis Group, 2013.
- [7] L. J. Steinberg, H. Sengul, and A. M. Cruz, “Natech risk and management: an assessment of the state of the art,” *Nat. Hazards*, vol. 46, no. 2, pp. 143–152, Aug. 2008, doi: 10.1007/s11069-007-9205-3.
- [8] C. Scawthorn and G. . Johnson, “Preliminary report,” *Eng. Struct.*, vol. 22, no. 7, pp. 727–745, Jul. 2000, doi: 10.1016/S0141-0296(99)00106-6.
- [9] M. Shinozuka, G. Deodatis, R. Zhang, and A. S. Papageorgiou, “Modeling, synthetics and engineering applications of strong earthquake wave motion,” *Soil Dyn. Earthq. Eng.*, vol. 18, no. 3, pp. 209–228, 1999, doi: 10.1016/S0267-7261(98)00045-1.
- [10] D. Yang, G. Chen, and Z. Dai, “Accident modeling of toxic gas-containing flammable gas release and explosion on an offshore platform,” *J. Loss Prev. Process Ind.*, vol. 65, p. 104118, 2020, doi: 10.1016/j.jlp.2020.104118.
- [11] “Component fragility evaluation, seismic safety assessment and design of petrochemical plants under design-basis accident conditions (INDUSE-2-SAFETY).” doi: 10.2777/5667.
- [12] M. Vathi, S. A. Karamanos, I. A. Kapogiannis, and K. V. Spiliopoulos, “Performance Criteria for Liquid Storage Tanks and Piping Systems Subjected to Seismic Loading,” *J. Press. Vessel Technol.*, vol. 139, no. 5, Oct. 2017, doi: 10.1115/1.4036916.
- [13] Organization of the Petroleum Exporting Countries, “World Oil Outlook 2040.” 2017, [Online]. Available: https://www.opec.org/opec_web/flipbook/WOO2017/WOO2017/assets/common/downloads/WOO.
- [14] Statista, “Largest oil refineries worldwide as of 2019, based on capacity.” [Online]. Available: <https://www.statista.com/statistics/981799/largest-oil-refineries-worldwide/>.
- [15] R. A. Parish and R. A. Rhea, “Mechanical Equipment,” *Pipe Draft. Des.*, pp. 112–133, Apr. 2012, doi: 10.1016/b978-0-12-384700-3.00006-2.
- [16] US Chemical Safety and Hazard Investigation Board, “Final investigation report - Chevron Richmond refinery pipe rupture and fire. Report No. 2012-03-I-CA,” 2015. [Online]. Available: <https://www.csb.gov/chevron-refinery-fire/>.

- [17] J.-Y. Yoo, S.-S. Ahn, D.-H. Seo, W.-H. Song, and K.-B. Kang, "New Development of High Grade X80 to X120 Pipeline Steels," *Mater. Manuf. Process.*, vol. 26, no. 1, pp. 154–160, Feb. 2011, doi: 10.1080/10426910903202534.
- [18] S. Cheng, X. Zhang, J. Zhang, Y. Feng, J. Ma, and H. Gao, "Effect of coiling temperature on microstructure and properties of X100 pipeline steel," *Mater. Sci. Eng. A*, vol. 666, pp. 156–164, 2016, doi: 10.1016/j.msea.2016.04.066.
- [19] S. Nafisi, M. A. Arafin, L. Collins, and J. Szpunar, "Texture and mechanical properties of API X100 steel manufactured under various thermomechanical cycles," *Mater. Sci. Eng. A*, vol. 531, pp. 2–11, 2012, doi: 10.1016/j.msea.2011.09.072.
- [20] G. Golański, A. Merda, A. Zieliński, P. Urbańczyk, J. Słania, and M. Kierat, "Microstructure and mechanical properties of HR6W alloy dedicated for manufacturing of pressure elements in supercritical and ultrasupercritical power units," *E3S Web Conf.*, vol. 82, p. 01005, Feb. 2019, doi: 10.1051/e3sconf/20198201005.
- [21] Z. Tan *et al.*, "Development mechanism of internal local corrosion of X80 pipeline steel," *J. Mater. Sci. Technol.*, vol. 49, pp. 186–201, 2020, doi: 10.1016/j.jmst.2019.10.023.
- [22] K. Gong, M. Wu, and G. Liu, "Comparative study on corrosion behaviour of rusted X100 steel in dry/wet cycle and immersion environments," *Constr. Build. Mater.*, vol. 235, p. 117440, 2020, doi: 10.1016/j.conbuildmat.2019.117440.
- [23] S. Moeinifar, A. H. Kokabi, and H. R. M. Hosseini, "Role of tandem submerged arc welding thermal cycles on properties of the heat affected zone in X80 microalloyed pipe line steel," *J. Mater. Process. Technol.*, vol. 211, no. 3, pp. 368–375, Mar. 2011, doi: 10.1016/j.jmatprotec.2010.10.011.
- [24] "Huta Łabędy." [Online]. Available: <https://www.hutalab.com.pl/pl/>.
- [25] P. E. Myers, *Aboveground Storage Tanks*, McGraw-Hil. 1997.
- [26] O. S. Bursi, R. di Filippo, V. La Salandra, M. Pedot, and M. S. Reza, "Probabilistic seismic analysis of an LNG subplant," *J. Loss Prev. Process Ind.*, vol. 53, 2018, doi: 10.1016/j.jlp.2017.10.009.
- [27] "Floating Roof Seal System – M.A.T." <http://mat-sarl.com/?product=floating-roof-seal-system>.
- [28] R. A. Parish and R. A. Rhea, "Steel Pipe," *Pipe Draft. Des.*, pp. 4–12, Jan. 2012, doi: 10.1016/B978-0-12-384700-3.00002-5.
- [29] S. B. T.-L. L. P. in the Process Industries (Fourth Edition) Mannan, Ed., "Pressure System Design," *Lees' Loss Prevention in the Process Industries*. Butterworth-Heinemann, pp. 509–617, 2012, doi: doi.org/10.1016/C2009-0-24104-3.
- [30] P. Smith, "Chapter 2 - Piping Components," in *The Fundamentals of Piping Design*, P. Smith, Ed. Gulf Publishing Company, 2007, pp. 49–113.
- [31] "Flanges General - What flanges are used in petrochemical industry?" http://www.wermac.org/flanges/flanges_pipe-connections_pipe-flanges.html.
- [32] V. La Salandra, R. Di Filippo, O. S. Bursi, F. Paolacci, and S. Alessandri, "Cyclic response of enhanced bolted flange joints for piping systems," *Am. Soc. Mech. Eng. Press. Vessel. Pip. Div. PVP*, vol. 8, 2016, doi: 10.1115/PVP2016-63244.
- [33] P. Papa *et al.*, "Structural Safety of Industrial Steel Tanks, Pressure Vessels and Piping

Systems Under Seismic loading,” 2013. doi: 10.2777/49423.

- [34] S. A. Karamanos, “Mechanical Behavior of Steel Pipe Bends: An Overview,” *J. Press. Vessel Technol.*, vol. 138, no. 4, Apr. 2016, doi: 10.1115/1.4031940.
- [35] “Messergroup Gmbh - Welding Positions.” [Online]. Available: <https://www.messergroup.com/documents/20195/58291/Welding+positions+according+to+DIN+EN+ISO+6947/>.
- [36] R. A. Parisher and R. A. Rhea, “Pipe Fittings,” *Pipe Draft. Des.*, pp. 13–55, Jan. 2012, doi: 10.1016/B978-0-12-384700-3.00003-7.
- [37] “ASME - B36.10M - Welded & Seamless Wrought Steel Pipe,” ASME - American Society of Mechanical Engineers, 2018. [Online]. Available: <https://www.asme.org/codes-standards/find-codes-standards/b36-10m-welded-seamless-wrought-steel-pipe>.
- [38] “INDUSE 2 safety | Component fragility evaluation and seismic safety assessment of ‘Special Risk’ petrochemical plants under design basis and beyond design basis accidents.” [Online]. Available: <http://www.induse2safety.unitn.it/>.
- [39] P. D. Corp., “Mill Test Certificate No. 160818-FH01KS-0175A1-0001.” 2016.
- [40] “API 5L, Seamless & welded pipe,” 2018.
- [41] K. Sinnes and W. H. Committee., *Welding handbook. Volume 1, Welding and cutting science and technology.* .
- [42] “ISO 16834:2012 Welding consumables — Wire electrodes, wires, rods and deposits for gas shielded arc welding of high strength steels — Classification,” 2012. [Online]. Available: <https://www.iso.org/standard/57189.html>.
- [43] “LNM MoNiVa- Filler material for GMA.” [https://www.lincolnelectric.com/en-gb/Consumables/Pages/product.aspx?product=Products_ConsumableEU_MIGWires-LNM-LNMMoNiVa\(LincolnElectric_EU_Base\)](https://www.lincolnelectric.com/en-gb/Consumables/Pages/product.aspx?product=Products_ConsumableEU_MIGWires-LNM-LNMMoNiVa(LincolnElectric_EU_Base)).
- [44] “ISO - ISO 14175:2008 - Welding consumables — Gases and gas mixtures for fusion welding and allied processes,” 2008. [Online]. Available: <https://www.iso.org/standard/39569.html>.
- [45] “Shielding Gas for GMA.” <https://www.shopairproducts.co.uk/product.php?id=177178>.
- [46] “ISO - ISO 18275:2018 - Welding consumables — Covered electrodes for manual metal arc welding of high-strength steels — Classification,” 2018. [Online]. Available: <https://www.iso.org/standard/72416.html>.
- [47] “Conarc® 85.” [https://www.lincolnelectric.com/en-gb/consumables/Pages/product.aspx?product=Products_ConsumableEU_StickElectrodes-Conarc-Conarc85\(LincolnElectric_EU_Base\)](https://www.lincolnelectric.com/en-gb/consumables/Pages/product.aspx?product=Products_ConsumableEU_StickElectrodes-Conarc-Conarc85(LincolnElectric_EU_Base)).
- [48] “AWS A5.29/A5.29M:2021 Specification for low-alloy steel electrodes for flux cored arc welding,” 2021. [Online]. Available: <https://pubs.aws.org/p/2053/a529a529m2021-specification-for-low-alloy-steel-electrodes-for-flux-cored-arc-welding>.
- [49] “Pipeliner® NR®-208-XP.” [https://www.lincolnelectric.com/en-za/Consumables/Pages/product.aspx?product=Products_Consumable_Flux-CoredWires-Self-Shielded-Pipeliner-PipelinerNR-208-XP\(LincolnElectric\)](https://www.lincolnelectric.com/en-za/Consumables/Pages/product.aspx?product=Products_Consumable_Flux-CoredWires-Self-Shielded-Pipeliner-PipelinerNR-208-XP(LincolnElectric)).
- [50] AWS A2 Committee on Definitions and Symbols., American National Standards Institute.,

American Welding Society. Technical Activities Committee., and American Welding Society., “Standard welding terms and definitions : including terms for adhesive bonding, brazing, soldering, thermal cutting, and thermal spraying,” American Welding Society, 2001.

- [51] “Causes Of Porosity In Welding (+Prevention) - Weldsmartly.” <https://weldsmartly.com/porosity-in-welding/>.
- [52] D. H. Phillips, *Welding engineering*. John Wiley & Sons, Ltd, 2016.
- [53] “API 1104, Welding of Pipelines and Related Facilities ,” 2021.
- [54] “Welding Defects: Types, Causes and Remedies.” <https://learnmechanical.com/welding-defects/>.
- [55] H. Czichos, Ed., *HANDBOOK OF TECHNICAL DIAGNOSTICS : fundamentals and application to structures*. SPRINGER-VERLAG, 2016.
- [56] C. J. Hellier, *Handbook of Nondestructive Evaluation*. McGraw-Hill Education, 2020.
- [57] X. P. V Maldague and P. Moore, *Nondestructive Testing Handbook: Infrared and Thermal Testing*. American Society for Nondestructive Testing, 2001.
- [58] “Fronium Power Source.” <https://www.fronius.com/en/welding-technology/product-list?filter=2866>.
- [59] “Mostostal zabrze konstrukcje przemysłowe S.A.” [Online]. Available: <https://konstrukcje.mz.pl/kontakt/>.
- [60] “Filler material for SSA.” [https://www.lincolnelectric.com/en-za/Consumables/Pages/product.aspx?product=Products_Consumable_Flux-CoredWires-Self-Shielded-Pipeliners-PipelinersNR-208-XP\(LincolnElectric\)](https://www.lincolnelectric.com/en-za/Consumables/Pages/product.aspx?product=Products_Consumable_Flux-CoredWires-Self-Shielded-Pipeliners-PipelinersNR-208-XP(LincolnElectric)).
- [61] “Instytut Spawalnictwa - The Polish Centre for Welding Technology |.” <http://is.gliwice.pl/en>.
- [62] “ISO - ISO 5817:2014 - Welding — Fusion-welded joints in steel, nickel, titanium and their alloys (beam welding excluded) — Quality levels for imperfections,” 2014. [Online]. Available: <https://www.iso.org/standard/54952.html>.
- [63] “CEN - EN 12732:2021 - Gas infrastructure - Welding steel pipework - Functional requirements,” 2021. [Online]. Available: https://standards.cencenelec.eu/dyn/www/f?p=CEN:110:0::::FSP_PROJECT,FSP_ORG_ID:69619,6215&cs=1A28D49865ABFEC700AC4C85538BA9B16.
- [64] “TruDisk | TRUMPF.” [Online]. Available: https://www.trumpf.com/en_GB/products/laser/disk-lasers/trudisk/.
- [65] “ISO - ISO 17636-1:2013 - Non-destructive testing of welds — Radiographic testing — Part 1: X- and gamma-ray techniques with film,” 2013. [Online]. Available: <https://www.iso.org/standard/52981.html>.
- [66] “ISO - ISO 6520-1:2007 - Welding and allied processes — Classification of geometric imperfections in metallic materials — Part 1: Fusion welding,” 2007. [Online]. Available: <https://www.iso.org/standard/40229.html>.
- [67] “ISO 6892-1 - Metallic materials — Tensile testing — Part 1: Method of test at room temperature,” 2019. [Online]. Available: <https://www.iso.org/standard/78322.html>.

- [68] European Committee for Standardization, “EN ISO 7438:2016 - Metallic materials — Bend test,” 2016.
- [69] “Kuznia Łabędy.” <https://www.kuznia-labedy.pl/>.
- [70] “ISO 8492:2013 - Metallic materials — Tube — Flattening test,” 2013. [Online]. Available: <https://www.iso.org/standard/63853.html>.
- [71] A. Klimpel, A. Timofiejczuk, J. Kaczmarczyk, K. Herbuś, and M. Pedot, “Catastrophic Impact Loading Resilience of Welded Joints of High Strength Steel of Refineries Piping Systems,” *Mater. 2022, Vol. 15, Page 1323*, vol. 15, no. 4, p. 1323, Apr. 2022, doi: 10.3390/MA15041323.
- [72] A. Klimpel, *Technologie laserowe: spawanie, napawanie, stopowanie, obróbka cieplna i cięcie*. Wydawnictwo Politechniki Śląskiej, 2012.
- [73] J. Svenungsson, I. Choquet, and A. F. H. Kaplan, “Laser Welding Process – A Review of Keyhole Welding Modelling,” *Phys. Procedia*, vol. 78, pp. 182–191, Apr. 2015, doi: 10.1016/J.PHPRO.2015.11.042.

A APPENDIX

A.1 WELDING TECHNOLOGIES

The basic concepts of the welding technologies that were used to prepare the pipe specimens were briefly introduced in Paragraph 3.1. More details regarding physical aspects, the necessary procedures and equipment to perform them are included in on this appendix section.

A.1.1 GAS METAL ARC WELDING TECHNOLOGY

Generally, the process is performed manually but it can also be automated. In Figure A1 is depicted the typical setup for gas metal arc welding technology.

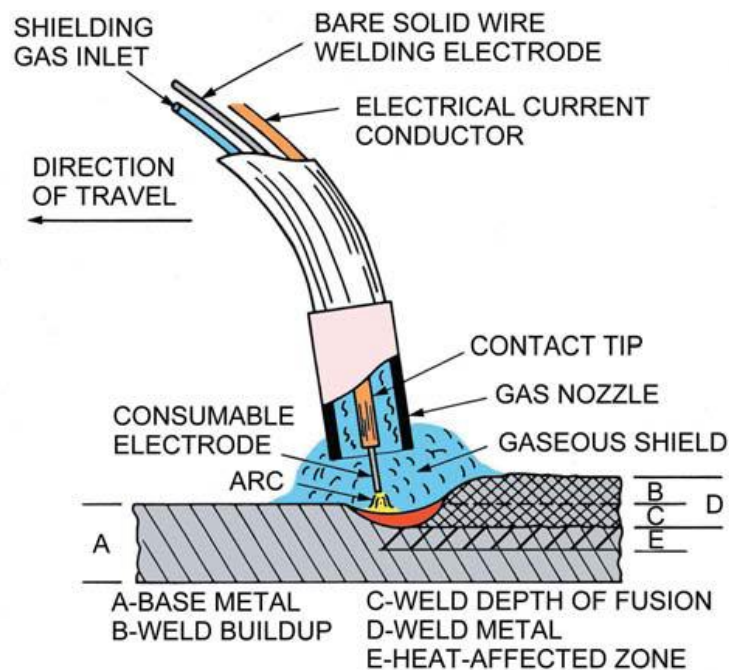


FIGURE A1: TYPICAL SETUP FOR GMA WELDING TECHNOLOGY [41]

Basically, the circuit that allows to generate the arc consists of an electric power source and two cables: one of these is attached to the work piece and another is attached to the electrode holder also called welding gun. Welding process starts when an electric arc is originated between the tip of the electrode and the work piece. The filler wire, which is supplied in coils of solid bare wire and is fed automatically into the joints, is also the electrode. For the effect of the considerable heat the filler wire melts, and it is deposited into the molten weld pool. A shielding gas mixture isolate the arc from the external atmosphere improving the quality of the weld.

The variables affecting the final quality of the welding process are especially:

- the chemical composition and the size of the electrode wire

- the distance between the electrode protrudes past the end of the contact tip to the work
- the properties and correct application of shielding gas
- electrical parameters of the arc
- the travel speed of the arc along the joint

The electrode wire, which may be of ferrous or nonferrous alloys composition, employs either a solid electrode wire or an electrode with a core of powdered metal. For usual applications its size varies from 0,5 mm to 3,2 mm. The distance between the contact tip and the electrode protrusion towards the work is called electrode extension and it affects the result of the welding process. The variation of this quantity affects the electrical resistance of the electrode producing remarkable changes of the current values in a constant voltage system. The current varies directly with wire feed speed but inversely with extension.

The shielding gas has the purpose to isolate the arc from the external atmosphere preventing the inclusion of unwanted substances or impurities in the welded pool and leading to smoother arc performance. It may often consist of carbon dioxide alone, carbon dioxide mixed with argon or carbon dioxide mixed with several gases.

The wide selection of consumable electrode sizes, shielding gas mixtures and travel speeds of the electrode along the groove allow to apply this technology to welding process of various ferrous and nonferrous metals of different thickness.

A.1.2 MANUAL METAL ARC WELDING TECHNOLOGY

Manual metal arc welding technology is one of the most known welding methods and is sometimes referred as stick welding. Electric arc is generated between the tip of a covered electrode and the base material as depicted in Figure A2.

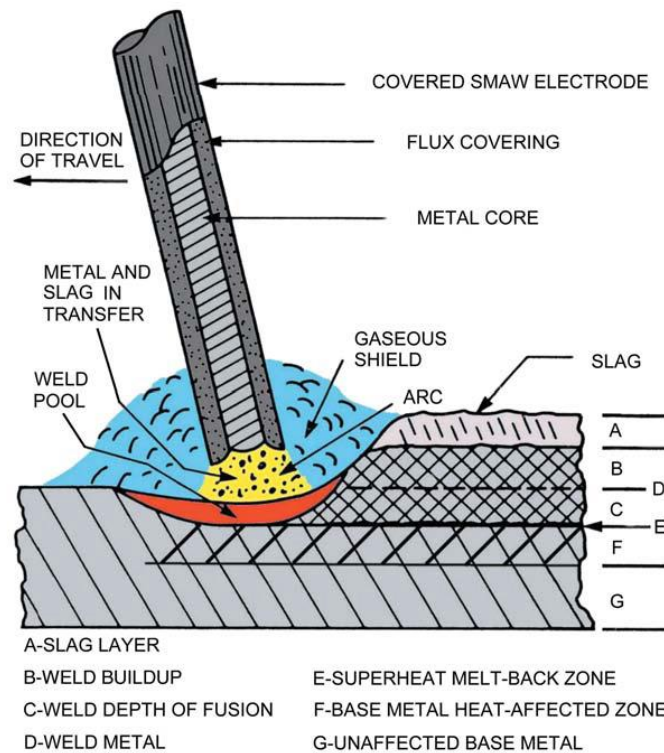


FIGURE A2: TYPICAL SETUP FOR MMA WELDING TECHNOLOGY [41]

The electrode on the final part opposite to the welding pool is clamped into an electrode holder, which is connected to the power source by a cable. Another cable connects the workpiece with the power source creating the electrical circuit. The arc is generated by touching the tip of the electrode on the workpiece and then withdraw it slightly.

The electrode consists of a metal core which is coated by mixture of silicate binders and powdered materials such as fluorides, carbonates, oxides, metal alloys and cellulose. The heat generated by the arc melts the parent material, the wire core as well as the coating. The purpose of this external layer is to release arc stabilizers, shielding vapours as well as metal and slag to protect, support, and insulate the hot weld metal. Typical electrodes are available in diameters ranging from 2 to 8 millimetres.

Manual metal arc welding technology advantage is the simplicity of the equipment necessary to perform the operation. The necessary components are a power source of adequate current rating and duty cycle, suitably sized electrical cables, an electrode holder, and a workpiece-lead clamp. Power source devices are usually easily portable and relatively not expensive make it possible the application of this technology to a wide range of uses. On the other hand, a clear disadvantage of MMA welding is its relatively low efficiency and high labour costs. This depends by the necessity to discard the electrode when consumed and to remove the slag from the weld after each pass.

A.1.3 SELF-SHIELDED FLUX CORED ARC WELDING TECHNOLOGY

Self-Shielded Flux Cored Arc Welding (SSAW or FCAW) is a welding technology like Gas Metal Arc Welding regarding power sources, wire feeders and welding guns. However, in this case during the welding process there is not an external shielding gas feed, but welding wire incorporates a core containing flux. The flux plays the same functions as the coating on the manual metal arc welding: it contains deoxidizers, scavengers, slag, and vapor-forming elements protecting the welding pool from external atmosphere. In Figure A3 it is depicted a schematic setup for SSA welding technology

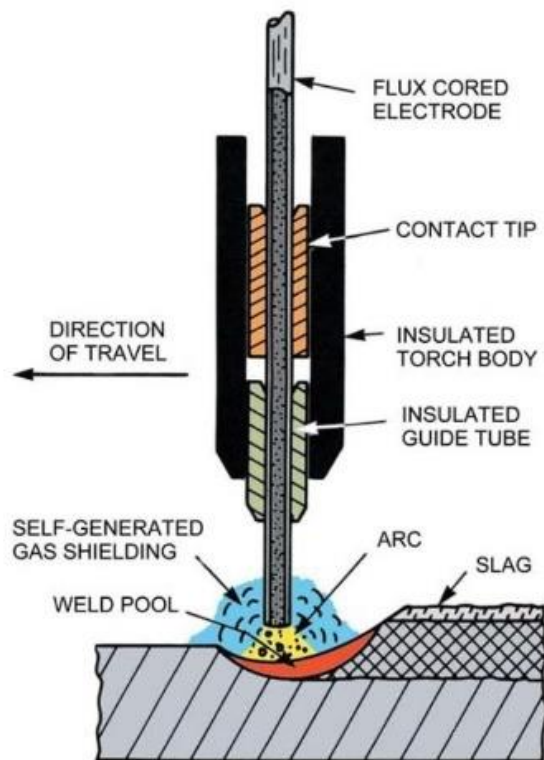


FIGURE A3: TYPICAL SETUP FOR SSA WELDING TECHNOLOGY [41]

A.1.4 LASER BEAM WELDING TECHNOLOGY

Laser beam welding (LBW) effects the fusion welding of materials with the heat supplied by a laser beam that impinges on the joint. The laser beam is generated from a concentrated beam of coherent, monochromatic light in the infrared or ultraviolet frequency portion of the electromagnetic radiation spectrum [41]. The beam is generated by a power source then directed by mirrors and finally focused with lenses (Figure A4) or with fibre-optic cables into a small spot on the workpiece.

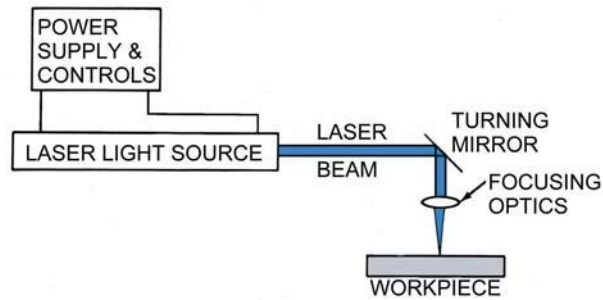


FIGURE A4: SCHEMATIC SETUP OF LASER BEAM WELDING TECHNOLOGY

The weld is formed as the intense laser light rapidly heats the material, typically in fractions of milliseconds. Laser welding requires large power density ranging from about $5 \cdot 10^4$ to 10^7 W/cm². This power can be provided by CO₂ gas laser (with a wavelength of the order of 10 μm) as well as solid state lasers such as Nd:YAG - rod, Yb:YAG - disk and Yb:glass - fibre (with wavelengths of the order of 1 μm). There are three types of welds, based on the power density contained within the focus spot size:

- conduction welding mode
- transition keyhole welding mode
- penetration/keyhole welding mode

For laser beam intensity below about 10^5 W/cm², the laser light is strongly reflected by the material and less than 30% of the beam energy is absorbed at the workpiece surface. This case, called conduction mode, results in shallow weld penetration. For higher intensities, approximately above 10^6 W/cm², the bonds between the atoms can be broken resulting in vaporization of the material. A large increase in vapour pressure causes a depression in the melted metal, forming a long and narrow cavity or keyhole: in this case the weld bead is much deeper than for conduction laser welding. The distinction between these three conditions is depicted in Figure A5, while a sketch of keyhole welding mode is presented in Figure A6.

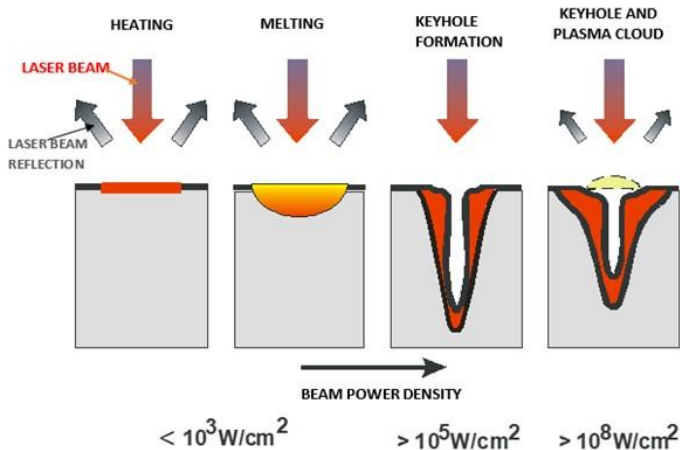


FIGURE A5: EFFECT OF LASER BEAM POWER DENSITY ON WORKPIECE [72]

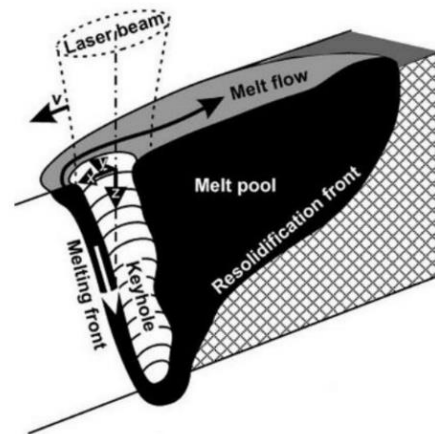


FIGURE A6: SKETCH OF LASER BEAM, KEYHOLE AND MELT POOL [73]

This technology has huge industrial potential, compared to conventional arc welding processes and the key factors are in particular:

- high quality and welding efficiency
- ease of automation and especially robotization
- production flexibility: the ability to simultaneously welding, surfacing, melting, heat treatment or cutting
- high melting depth of the laser welded joint
- narrow Heat Affected Zone (HAZ) on the workpiece
- almost zero level of residual stresses

Basic restrictions of laser welding technologies are instead:

- the high cost of laser apparatus and automatic or robotic stands
- required high precision of leading the laser beam focus along the welding track
- high accuracy and purity of the preparation of joints
- necessity to ensure high stability of the basic welding parameters

A.2 DEFECTS DETECTED IN THE PIPE SAMPLES

This section contains the list of the defects detected inside the butt-welded joints of the twelve pipe samples. For each of them, the list includes the exact position of the defects along the circumference and it is combined with the images of the correlated X-Ray films obtained from radiographic tests.

Defects Legend

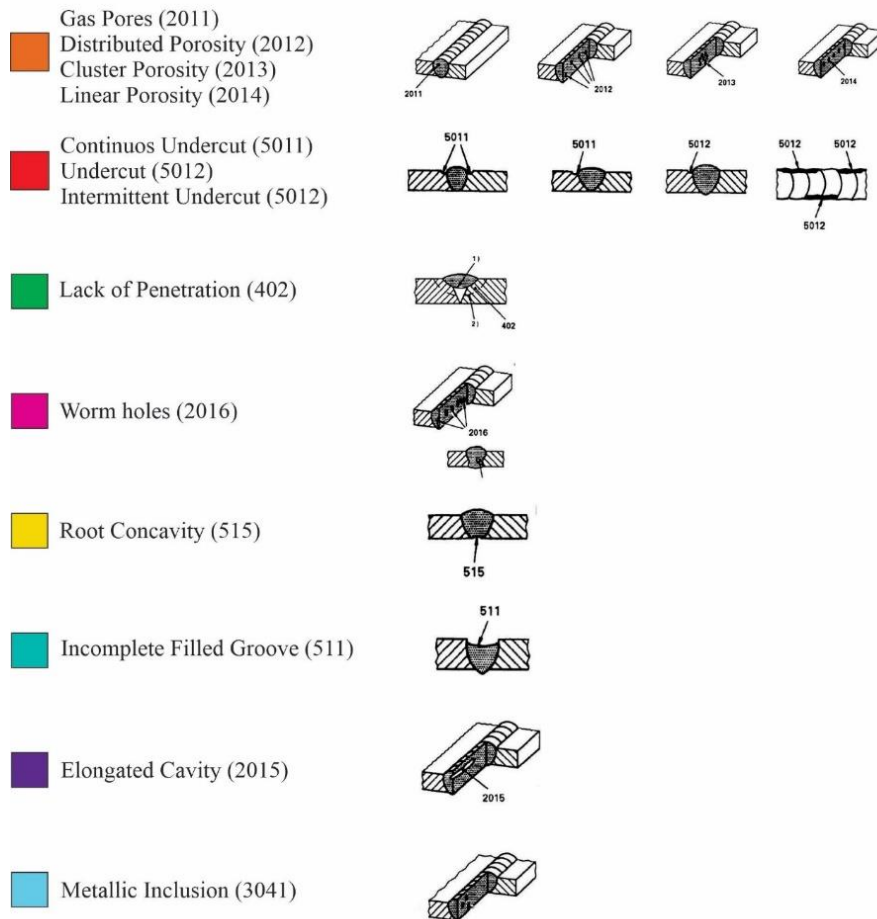


FIGURE A7: DEFECTS LEGEND FOR DEFECTS HIGHLIGHTED ON X-RAY FILMS

A.2.1 DEFECTS DETECTED IN GMA PIPE SAMPLES

Defect detected	Position along the circumference [cm]
Cluster Porosity (2013)	5
Linear Porosity (2014)	22
Lack of Penetration (402)	29
Root Concavity (515)	49
Worm hole (2016)	69
Lack of Penetration (402)	90
Lack of Penetration (402)	95
Lack of Penetration (402)	100

TABLE A1: LIST OF DEFECTS IN GMA1 PIPE SAMPLE

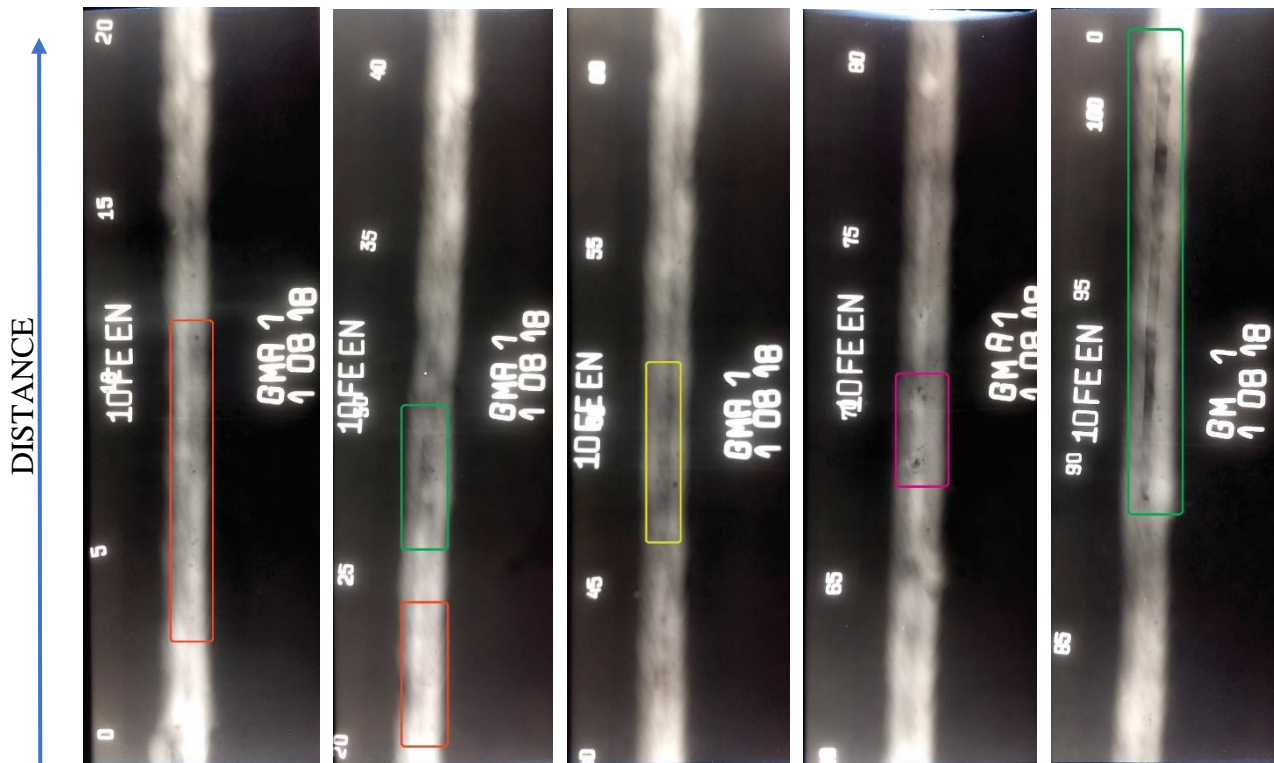


FIGURE A8: MAP OF THE DEFECTS IN GMA1 PIPE SAMPLE

Defect detected	Position along the circumference [cm]
Intermittent Undercut (5012) + Uniformly Distributed Porosity (2012)	3
Intermittent Undercut (5012) + Uniformly Distributed Porosity (2012)	9
Root Concavity (515)	14
Distributed Porosity (2012) + Worm holes (2016)	35
Distributed Porosity (2012) + Worm holes (2016)	44
Incomplete Filled Groove (511) + Gas Pores (2011)	51
Lack of Penetration (402) + Gas Pores (2011)	72
Lack of Penetration (402) + Gas Pores (2011)	78
Cluster Porosity (2013)	93

TABLE A2: LIST OF DEFECTS IN GMA2 PIPE SAMPLE

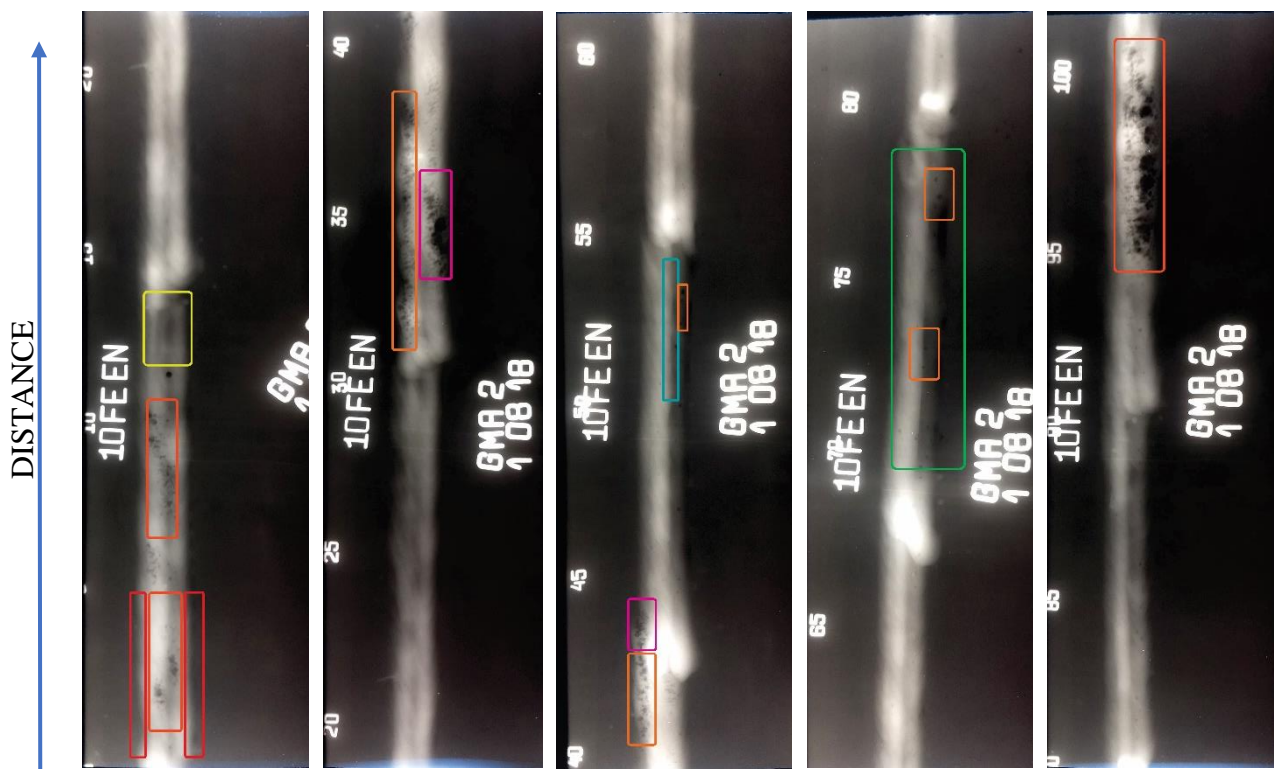


FIGURE A9: MAP OF THE DEFECTS IN GMA2 PIPE SAMPLE

Defect detected	Position along the circumference [cm]
Cluster Porosity (2013)	34
Lack of Penetration (402)	43
Lack of Penetration (402)	50
Lack of Penetration (402)	56
Lack of Penetration (402)	67
Cluster Porosity (2013) + Worm holes	78
Cluster Porosity (2013) + Worm holes	87
Lack of Penetration (402)	93

TABLE A3: LIST OF DEFECTS IN GMA3 PIPE SAMPLE

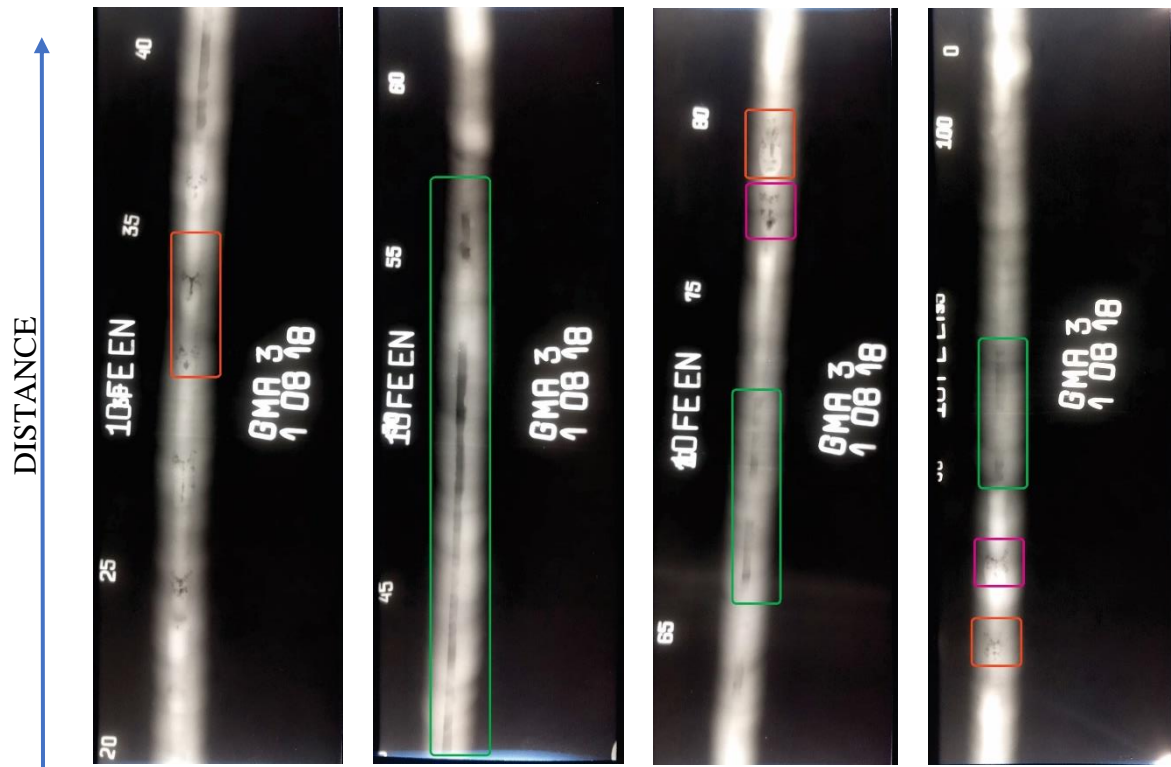


FIGURE A10: MAP OF THE DEFECTS IN GMA3 PIPE SAMPLE

Defect detected	Position along the circumference [cm]
Incomplete Filled Groove (511)	17
Continuous Undercut (5011)	45
Cluster Porosity (2013)	52
Worm holes (2016)	69
Incomplete Filled Groove + Cluster Porosity (2013)	81
Cluster Porosity (2013)	91
Cluster Porosity (2013)	98

TABLE A4: LIST OF DEFECTS IN GMA4 PIPE SAMPLE

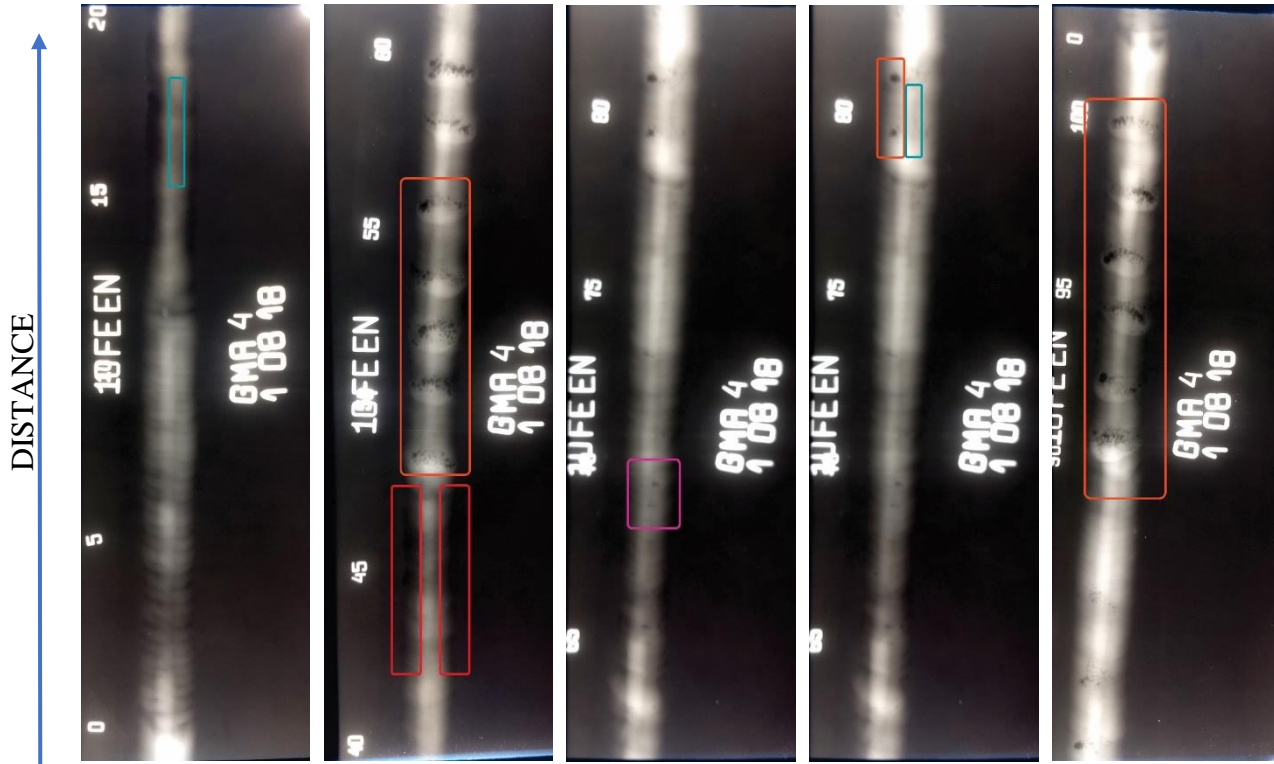


FIGURE A11: MAP OF THE DEFECTS IN GMA4 PIPE SAMPLE

A.2.2 DEFECTS DETECTED IN MMA PIPE SAMPLES

Defect detected	Position along the circumference [cm]
Intermittent Undercut (5012)	5
Lack of Penetration (402)	13
Lack of Penetration (402)	19
Lack of Penetration (402)	25
Lack of Penetration (402)	31
Lack of Penetration (402)	36
Elongated Cavity (2015)	45
Lack of Penetration (402)	56
Intermittent Undercut (5012) + Lack of Penetration (402)	65
Intermittent Undercut (5012) + Lack of Penetration (402)	72
Intermittent Undercut (5012) + Lack of Penetration (402)	77
Intermittent Undercut (5012) + Lack of Penetration (402)	85
Intermittent Undercut (5012) + Lack of Penetration (402)	92

TABLE A5: LIST OF DEFECTS IN MMA1 PIPE SAMPLE

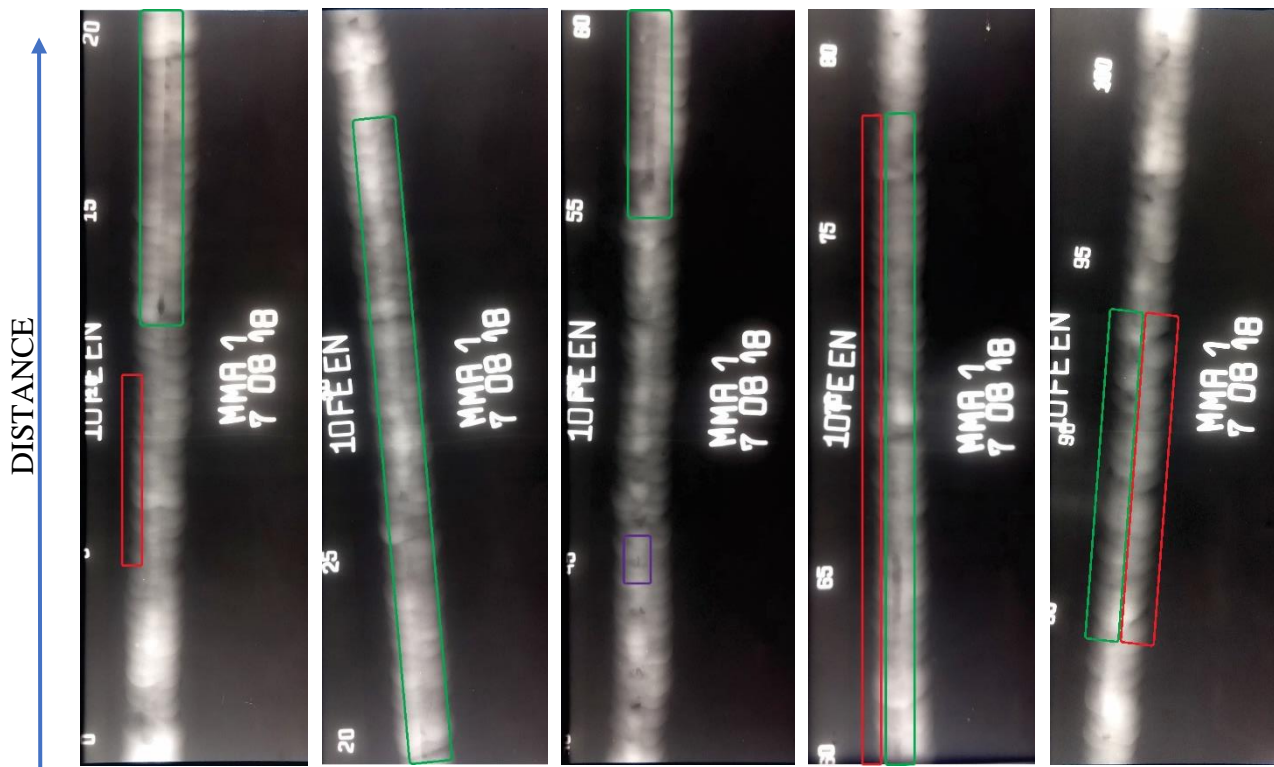


FIGURE A12: MAP OF THE DEFECTS IN MMA1 PIPE SAMPLE

Defect detected	Position along the circumference [cm]
Intermittent Undercut (5012)	6
Intermittent Undercut (5012) + Cluster Porosity (2013)	18
Metallic Inclusion (3041)	27
Undercut (5012) + Incomplete filled groove (511)	38
Intermittent Undercut (5012)	44
Intermittent Undercut (5012)	54
Intermittent Undercut (5012)	58
Intermittent Undercut (5012) + Cluster Porosity (2013)	89
Cluster Porosity (2013) + Worm holes (2016)	94
Cluster Porosity (2013) + Worm holes (2016)	99

TABLE A6: LIST OF DEFECTS IN MMA2 PIPE SAMPLE

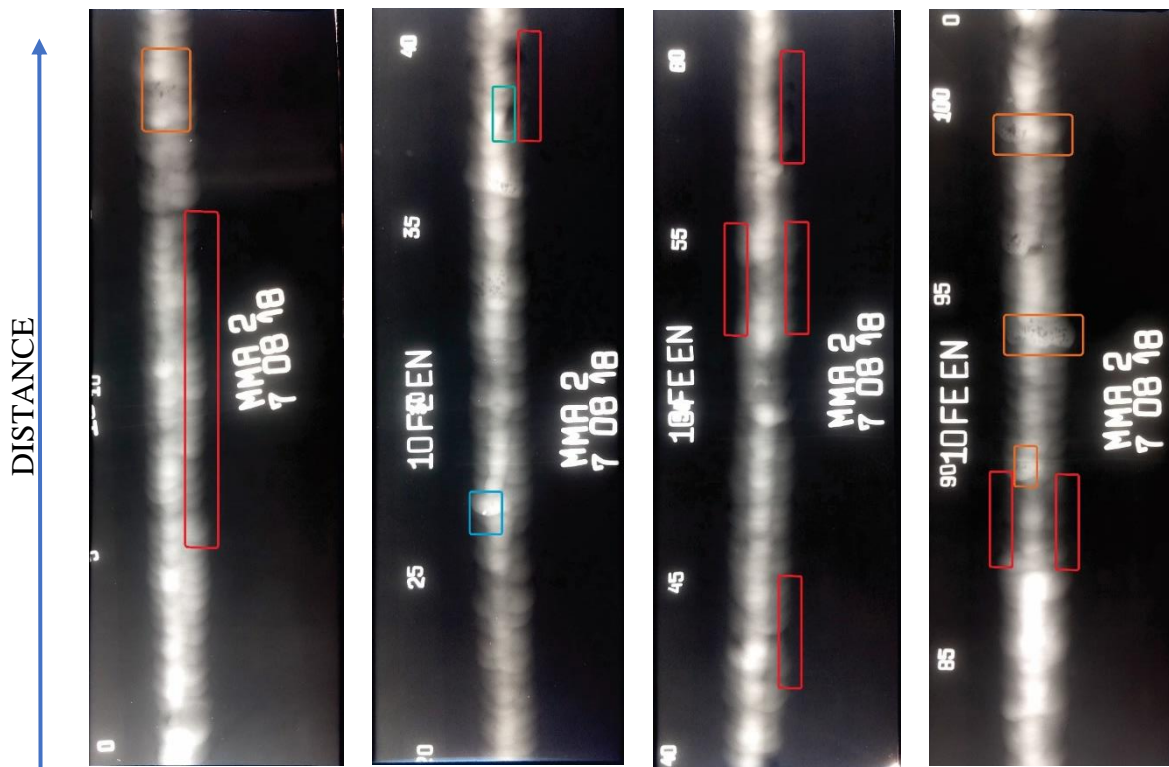


FIGURE A13: MAP OF THE DEFECTS IN MMA2 PIPE SAMPLE

Defect detected	Position along the circumference [cm]
Lack of Fusion (402)	4
Lack of Fusion (402)	10
Lack of Fusion (402)	16
Elongated Cavity (2015)	25
Worm-holes (2016) + Lack of Fusion (402)	40
Worm-holes (2016) + Lack of Fusion (402)	47
Lack of Fusion (402) + Undercut (5012)	57
Worm-holes (2016) + Lack of Fusion (402)	77
Lack of Fusion (402) – Root Concavity (515)	89

TABLE A7: LIST OF DEFECTS IN MMA3 PIPE SAMPLE

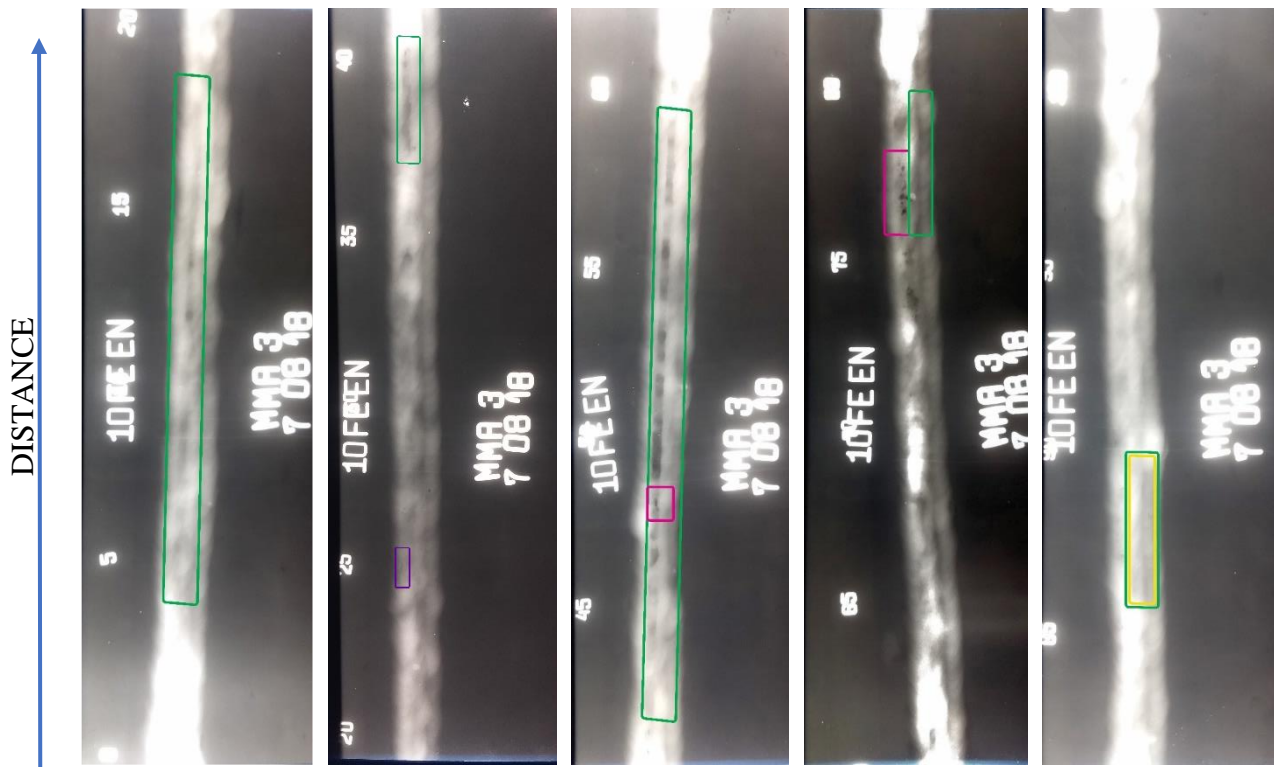


FIGURE A14: MAP OF THE DEFECTS IN MMA3 PIPE SAMPLE

Defect detected	Position along the circumference [cm]
Lack of Fusion Side Walls (4011)	14
Lack of Fusion Side Walls (4011)	19
Intermittent Undercut + Worm holes (2016)	25
Intermittent Undercut (5012)	40
Intermittent Undercut (5012)	48
Root Concavity (515)	56
Intermittent Undercut (5012)	67
Intermittent Undercut (5012)	77
Intermittent Undercut (5012) + Porosity	90
Worm holes (2016)	100

TABLE A8: LIST OF DEFECTS IN MMA4 PIPE SAMPLE

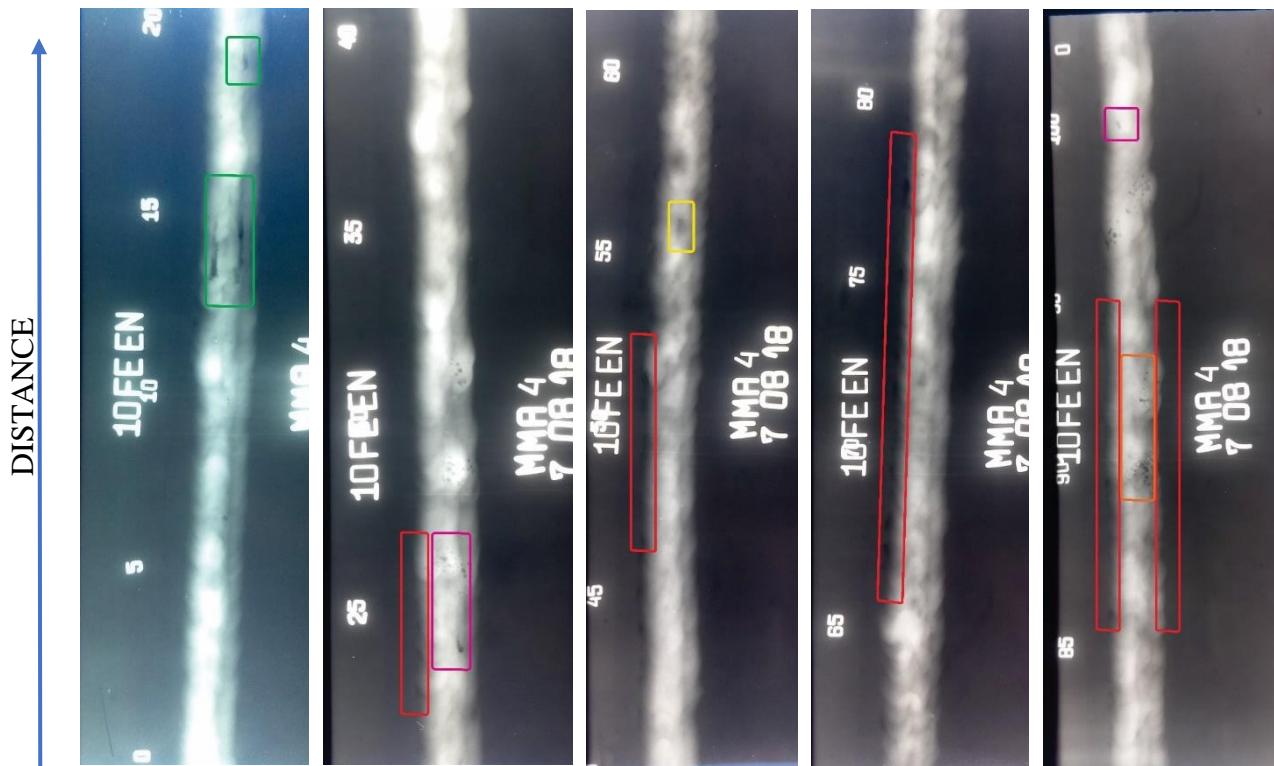


FIGURE A15: MAP OF THE DEFECTS IN MMA4 PIPE SAMPLE

A.2.3 DEFECTS DETECTED IN SSA PIPE SAMPLES

Defect detected	Position along the circumference [cm]
Worm-holes (2016)	8
Gas Pore (2011) + Intermittent Undercut (5012)	19
Gas Pore (2011)	26
Lack of Penetration (402)	36
Lack of Penetration (402) + Intermittent Undercut (5012)	45
Lack of Penetration (402)	57
Gas Pore (2011) + Cluster Porosity (2013) + Lack of Penetration (402)	64
Gas Pore (2011) + Cluster Porosity (2013)	76
Lack of Penetration (402) + Intermittent Undercut (5012)	86
Lack of Penetration (402) + Intermittent Undercut (5012)	96

TABLE A9: LIST OF DEFECTS IN SSA1 PIPE SAMPLE

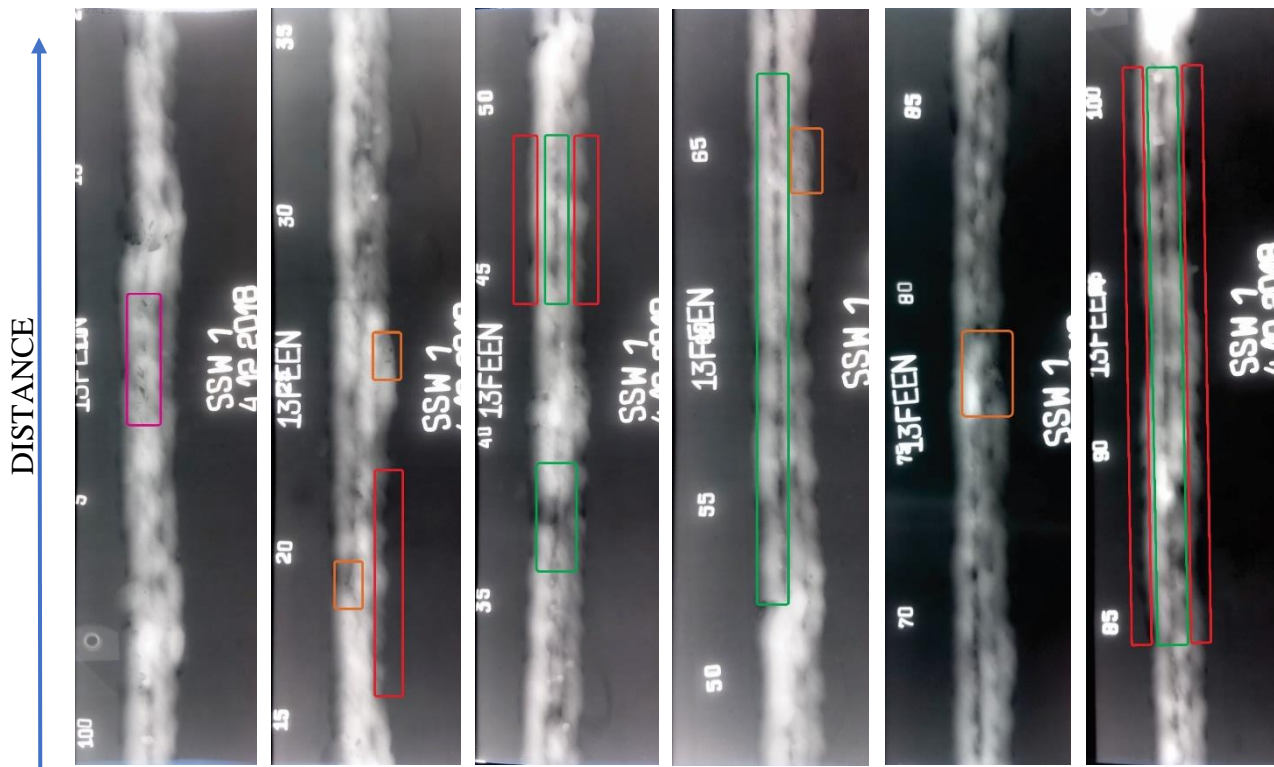


FIGURE A16: MAP OF THE DEFECTS IN SSA1 PIPE SAMPLE

Defect detected	Position along the circumference [cm]
Intermittent Undercut (5012) + Worm-hole (2016)	3
Incomplete Filled Groove (511) + Intermittent Undercut (5012) + Worm-holes (2016)	13
Elongated Cavity (2015) + Worm-holes (2016) + Gas Pore (2011)	23
Intermittent Undercut (5012) + Cluster Porosity (2013) + Gas Pore (2011)	49
Gas Pores (2011) + Worm-hole (2016)	60
Gas Pore (2011) + Worm-hole (2016)	86

TABLE A10: LIST OF DEFECTS IN MMA1 PIPE SAMPLE

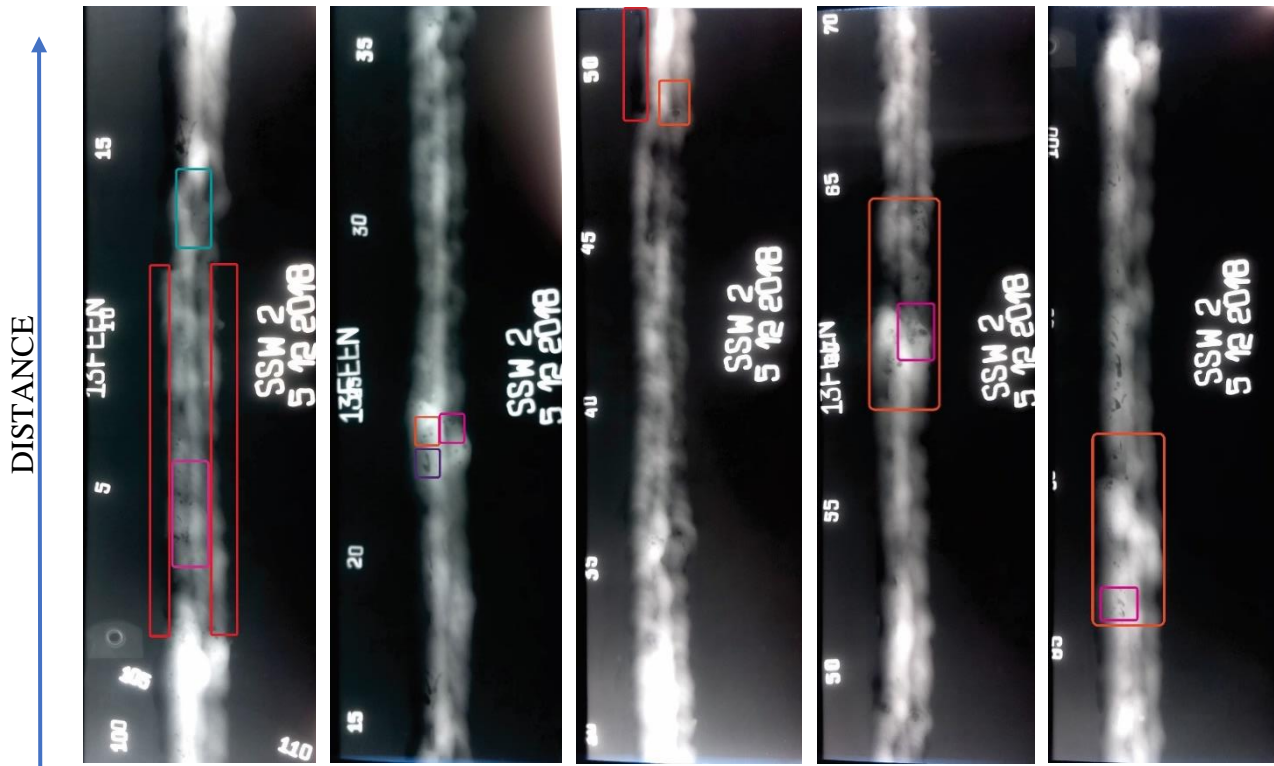


FIGURE A17: MAP OF THE DEFECTS IN SSA2 PIPE SAMPLE

Defect detected	Position along the circumference [cm]
Root Concavity (515)	43
Root Concavity (515)	56
Root Concavity (515) + Intermittent Undercut (5012)	76

TABLE A11: LIST OF DEFECTS IN SSA3 PIPE SAMPLE

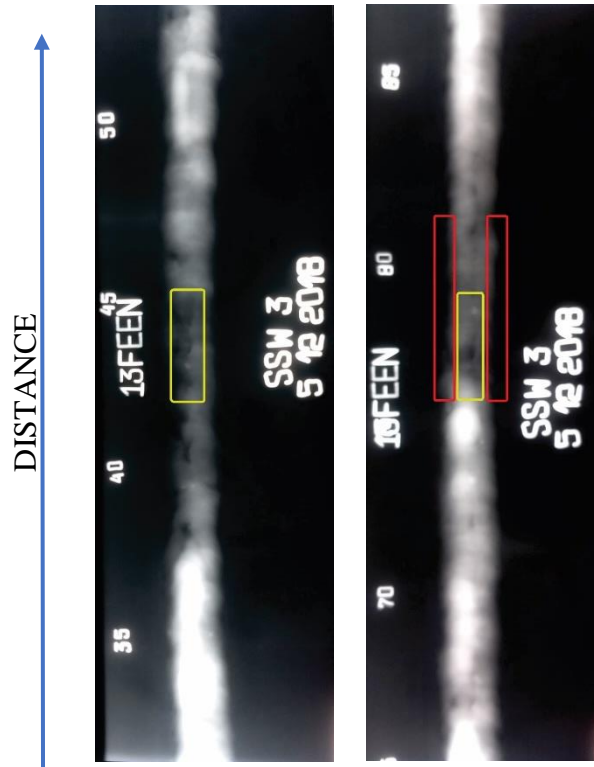


FIGURE A18: MAP OF THE DEFECTS IN SSA3 PIPE SAMPLE

Defect detected	Position along the circumference [cm]
Intermittent Undercut (5012)	12
Gas Pore (2011)	35
Intermittent Undercut (5012)	61

TABLE A12: LIST OF DEFECTS IN SSA4 PIPE SAMPLE

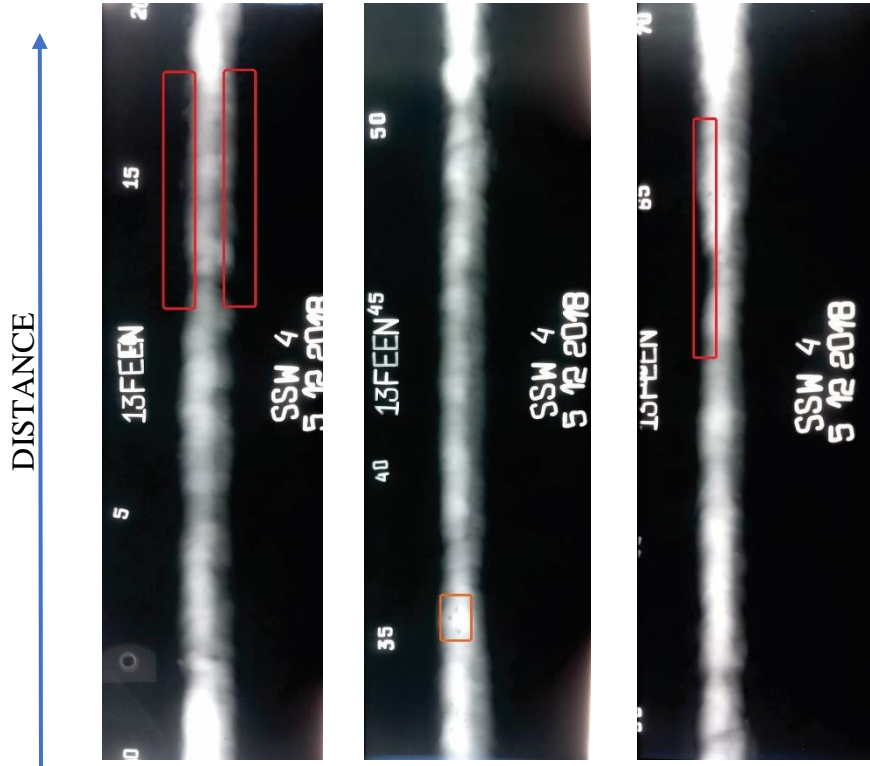
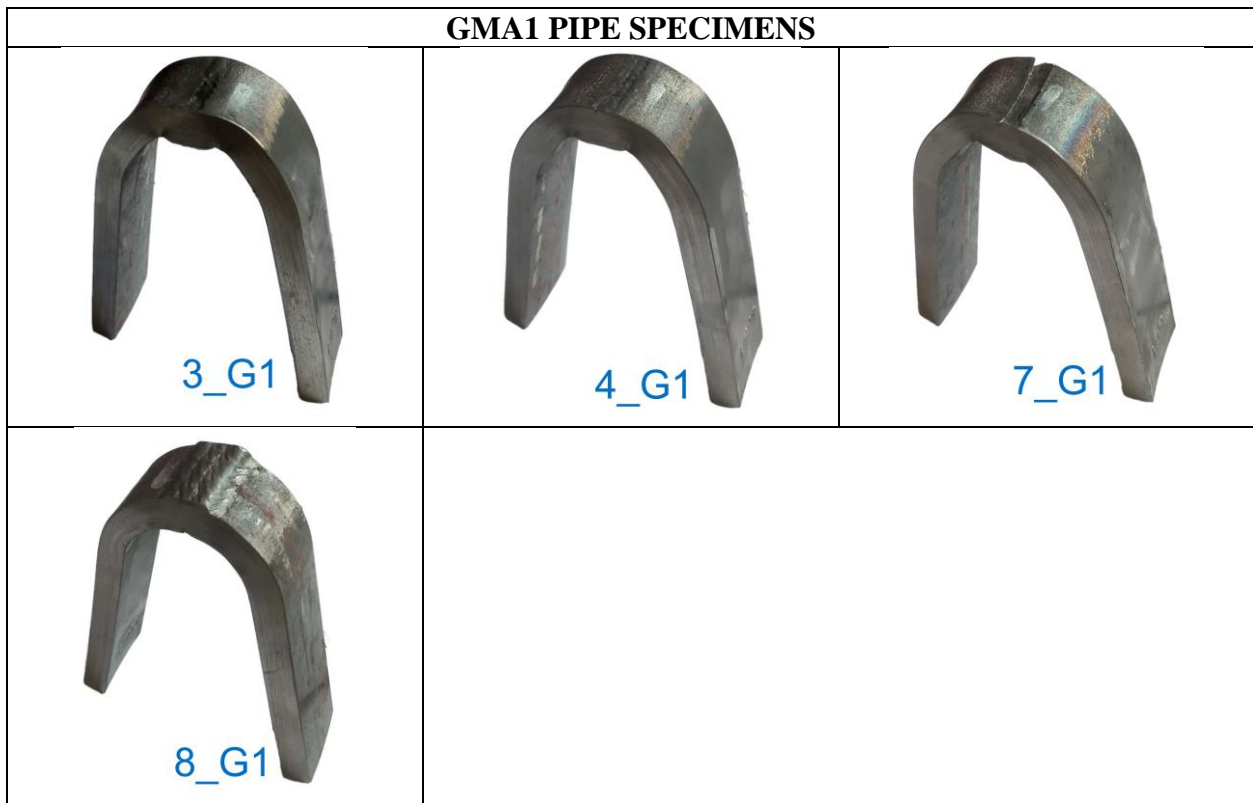


FIGURE A19: MAP OF THE DEFECTS IN SSA4 PIPE SAMPLE

A.3 DESTRUCTIVE TEST ON DEFECTIVE SAMPLES

A.3.1 BEND TEST





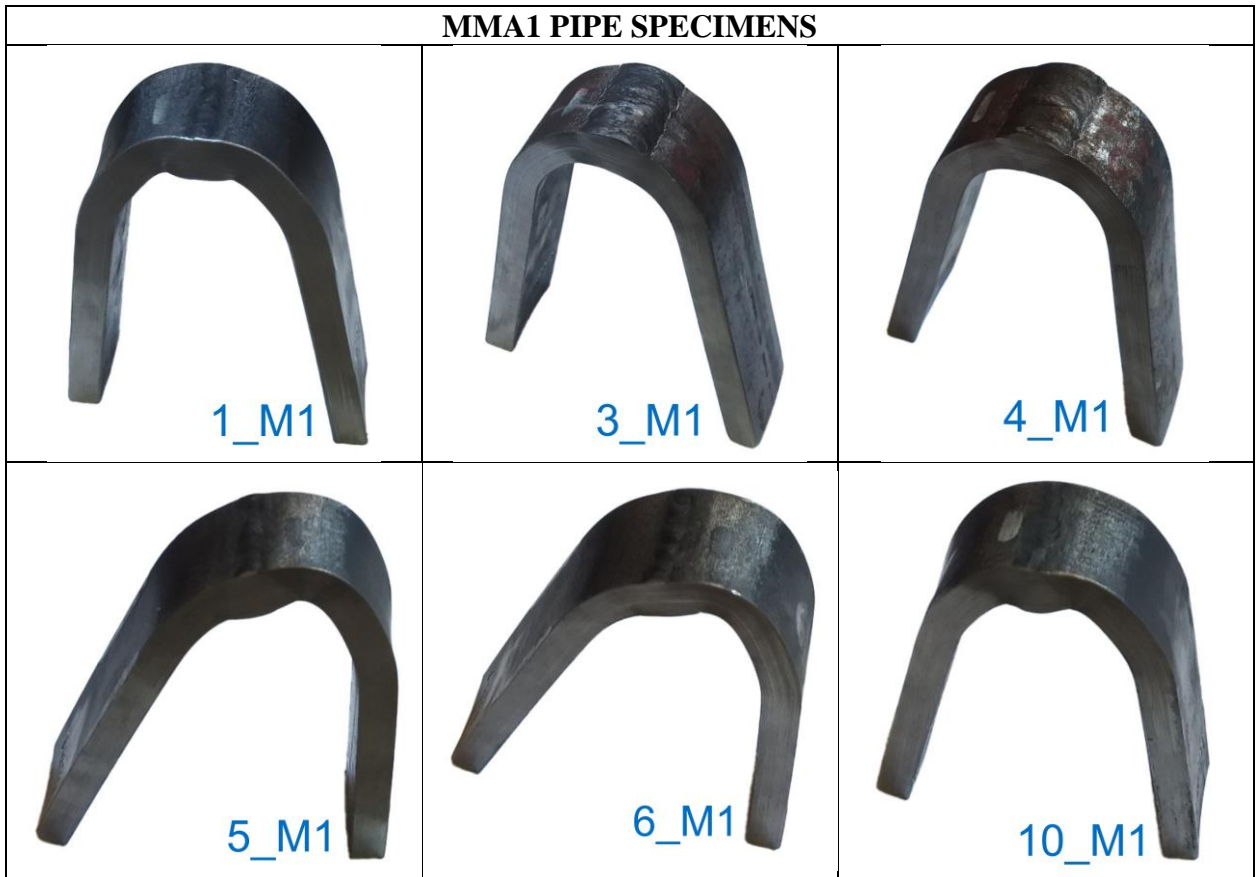
GMA3 PIPE SPECIMENS



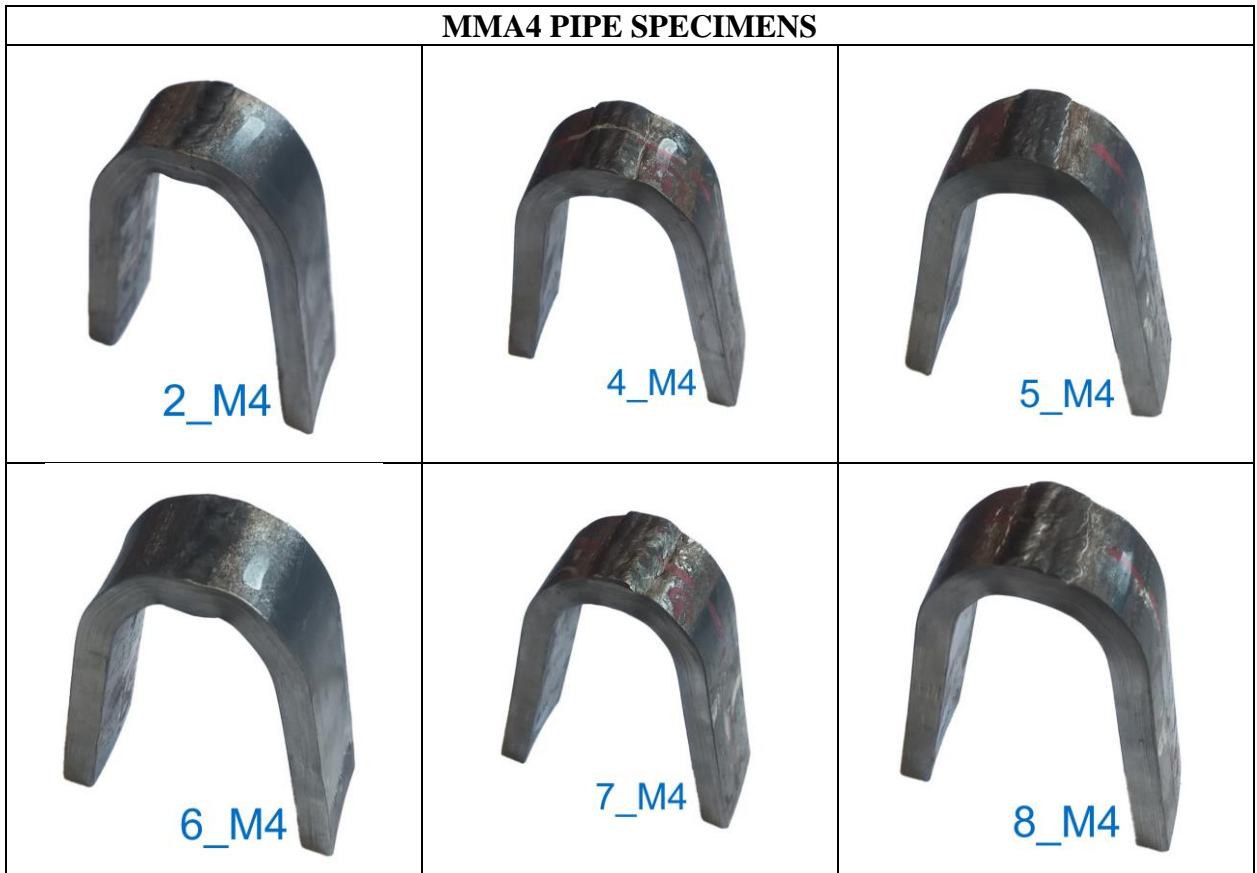
GMA4 PIPE SPECIMENS



MMA1 PIPE SPECIMENS







A.3.2 TENSILE TEST





GMA4 PIPE SPECIMENS



MMA1 PIPE SPECIMENS



MMA2 PIPE SPECIMENS

1_M2



3_M2



4_M2



5_M2



8_M2



9_M2



MMA3 PIPE SPECIMENS

1_M3



